Synthesis of Degradable Polymers for Biomedical Applications

Chairman:	Prof. Dr. Dirk Vanderzande
Promoter:	Prof. Dr. Tanja Junkers
Copromoter:	Prof. Dr. Anitha Ethirajan
Members of the Jury:	Prof. Dr. Bart Goderis, KU Leuven
	Dr. Hans Heuts, Eindhoven University of Technology
	Dr. Julien Nicolas, Université Paris-Sud
	Prof. Dr. Peter Adriaensens, Hasselt University
	Prof. Dr. Mieke Buntinx, Hasselt University

"Imagination is more important than knowledge. For knowledge is limited to all we now know and understand, while imagination embraces the entire world, and all there ever will be to know and understand."

- Albert Einstein -

TABLE OF CONTENTS

Chapter 1

Introduction

1.1 A history of polymers

The word polymer is derived from Greek words for '*Poly'* and '*Meros'* which literally translates into '*many parts*'. They are also commonly referred to as macromolecules which are defined by IUPAC as "a molecule of high relative molecular mass, the structure of which essentially comprises the multiple repetition of units derived, actually or conceptually, from molecules of low relative molecular mass."[1] The first account for a synthetically created polymer can be attributed to Leo Baekeland who, in 1907, created an insoluble material from the reaction of phenol and formaldehyde. This material was named Bakelite, after its discoverer, and was widely used in the early 1900's due it's good electrical- and thermal-insulating properties. At the time, this material was not yet known as a macromolecule, however this changed in the 1920's by Herman Staudinger who described the term 'macromolecule' by stating that large molecules with 1000 or more atoms, such as starch or cellulose, are actually build-up from smaller covalently linked repeating units.[2] Nowadays, polymers are part of our daily life with applications in bottles, car tires, paint, glue but also in medicine as drug carriers.

However, with the increased use of 'plastics', problems arose regarding the handling of the waste material. As these materials are made up of immensely long chains it takes nature thousands of years to break it down. With the increased concern for global warming, burning these materials is not a clean option either. More and more materials are therefore reused and recycled but not every material is suitable for that. (Bio)degradability therefore becomes a big part of polymer research. Biodegradability is making use of bacteria and other organisms to break

down the material. Introduction of degradable moieties suchs as esters or amides into large carbon chains improves the degradability.

1.2 Classification of polymers

There are various ways to categorize polymer classes. A common way is to look at the way the polymers are synthesized. In general, there are two pathways towards polymers being a step-growth and chain-growth mechanism. The difference of these methods can be attributed to the way the large chains are formed and the effect it has on the kinetics. The different mechanisms can be seen in Figure 1.1.

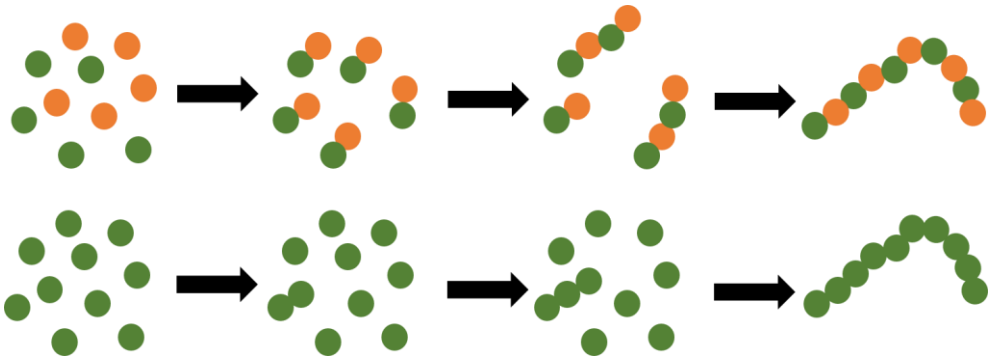

Figure 1.1 Different pathways towards polymer formation: Step-growth top reaction, chain-growth bottom reaction.

In the initial step of step-growth polymerization, monomers react with each other to form dimers. In the second step, these dimers then react with either monomer to form trimers or dimer to form tetramers. These steps are continued until one long chain is formed (Figure 1.1 top). For this type of polymerization, stoichiometry plays a key role and is the determining factor for the ultimate molecular weight as given in Equation 1.1a. Hence, molecular weight build-up is

slow in early stages as shown in Figure 1.2 (green). The resulting molecular weight distribution (MWD) is based on the cumulative molecular weights.

Equation 1.1 Dependence of degree of polymerization (DP_n) *for*:

$DP_n = \frac{1+r_0}{1+r_0-2r_0p}$ $with\ r_0 = \frac{n_{A,0}}{n_{B,0}}$ a) Step-growth polymerization

with monomer conversion (p) and mol of monomer A and B ($n_{a,o}$ and $n_{b,0}$)

$DP_n = \frac{k_p}{(2f \cdot k_d)^{0.5} \cdot k_t^{0.5}} \cdot [I]^{-0.5} \cdot [M]$ b) chain-growth polymerization

with k_p, k_d and k_t being the rate coefficients for respectively propagation, dissociation and termination, f being the initiator efficiency and [I] and [M] being the initiator and monomer concentration. The equation is only valid for thermally decomposing initiators.

$DP_n = \frac{[M]_0-[M]_t}{[I]}$ c) living polymerization

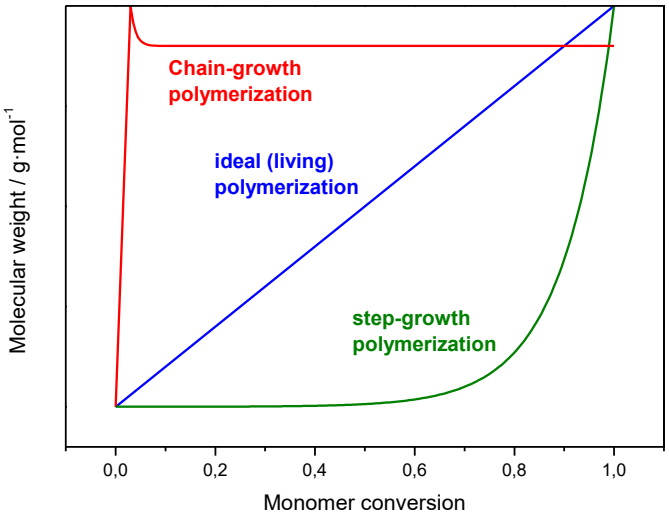

Figure 1.2 Comparison of dependence of molecular weight on monomer conversion for step-growth (green), chain-growth (red) polymerization. In addition, the dependence for ideal (living) conditions (blue) is given.

In addition, with some reactions a condensate is formed which needs to be removed simultaneously to avoid the formation of an equilibrium. Examples of this pathway are the synthesis of polyesters, polyamides and polyurethanes.

In a chain growth mechanism, external initiators are necessary to start the reaction. In the first step the initiator reacts with a monomer unit (initiation). In the second step, this monomer unit (with attached initiator) then reacts with a second monomer unit. Further steps add new units to this growing chain (propagation) until all monomer is consumed (Figure 1.1 bottom). In the final step, the radical can undergo termination reaction such as disproportionation and/or recombination.

Here, the ultimate molecular weight is not dependent on the stoichiometry but rather by rate of initiation, propagation and termination (Equation 1.1b). Thus, the molecular weight increases instantly to reach ultimate molecular weight within a matter of seconds as shown in Figure 1.2 (red). Therefore, contrary to the equation for step-growth polymerization, the resulting MWD is determined by instantaneous molecular weights. This equation, however, is only valid for thermally decomposing initiators.

Different types of initiator species can be used such as cations, anions or radicals leading to typical polymers such as polyethylene, polypropylene and polycaprolactone. Nowadays, most polymers are made using chain growth polymerization due to its very fast reaction rate – able to reach almost full conversion in a matter of seconds leading to molecular weights in excess of 1 million dalton – its wide applicability and its readily available reagents.

1.3 Free radical polymerization

Free radical polymerization has rapidly become one of the most popular polymerization techniques in industry. A major part of polymer production uses free radical polymerization to produce typical polymer such as polystyrene and polyethylene.

Free radical polymerization is a statistical process which involves usually 4 steps as shown in Figure 1.3.[3-4] An external source (typically an azo- or peroxide containing component) is necessary to start the process. Decomposition of the initiator to from radicals can happen via several ways (most commonly temperature or light). In the initiation step, the radicals react with available monomer. This addition of monomer is then repeated through the propagation phase until termination occurs which can happen by either recombination of two chains or by disproportionation (giving one proton-terminated chain and one chain containing a C=C double bond). In addition to termination, the radicals may also be transferred from one chain to either solvent, monomer or another by a chain transfer process whereby one polymer stops growing and a new propagating point is formed on another chain. This process can lead to all kinds of different side-reactions such as branching and ring-closing. When this transfer happens intramolecularly, it is commonly referred to as backbiting.

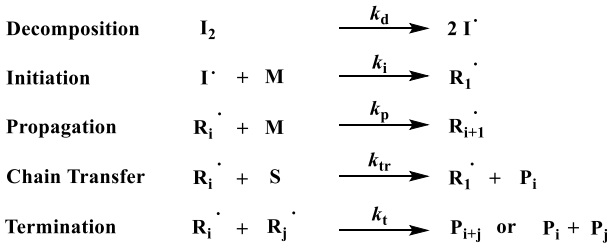

Figure 1.3 overview of the radical polymerization process.

Due to the statistical nature of the process, these polymers have typically a broad range of different lengths where values for polydispersity between 2 and 20 are common.

1.4 Architecture of (co)polymers

Polymers can come in different shapes and sizes depending on the conditions used which has a substantial impact on the properties of the final product. An overview of common polymer structures is given in Figure 1.4. However, polymers rarely consist of only one kind of monomer. Adding one (or more) monomers to the mix may improve physical or thermal properties for the final material. Depending on which monomers are selected, the final copolymer structure may differ which ultimately leads to a difference in properties of the final material. The outcome is strongly dependent on the miscibility and interaction between the monomers. An overview of possible copolymer structures is also given in Figure 1.4. In addition, polymers are also widely employed in dispersions as i.e. paint. Just as with traditional copolymers, the choice of copolymer composition has a strong influence of the particle structure affecting the ultimate properties of the dispersion whereby i.e. a block copolymer structure can lead to phase separation in the particle forming a Janus type particle while a graft copolymer may lead to phase separation to form a core-shell structure. These and other examples are given in the 3rd column in Figure 1.4.

Nowadays an increasing amount of research is application driven. The necessary materials have to meet certain specifications and typically have to be designed for the respective purpose. Traditional free-radical polymerization techniques lack the necessary 'control' over the kinetics due to the statistical and random nature of the radicals involved.

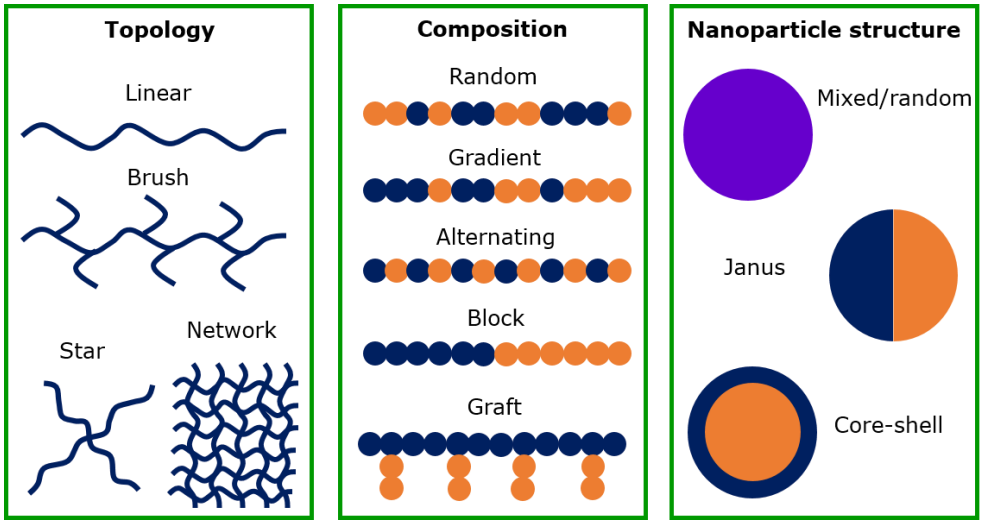

Figure 1.4 Overview of complex (co)polymer architectures.

1.5 Controlled radical polymerization

To overcome this issue, a lot of research was performed to solve this lack of control by looking for ways to allow for steady chain growth and to limit the amount of side- and termination-reactions. Products of this research are the so-called controlled radical polymerization techniques (CRP) and include popular reactions such as atom transfer radical polymerization (ATRP), nitroxide mediated polymerization (NMP) and reversible addition fragmentation/transfer (RAFT) polymerization which will be discussed in more detail.

1.5.1 Atom transfer radical polymerization

ATRP was developed in the mid 1990's and is based on the atom transfer radical addition reaction whereby alkenes are reacted with a halogen compound in the presence of a transition metal complex to form a new carbon-carbon bond. Two separate research groups simultaneously reported the use of ATRP in radical polymerization. In the work by Sawamoto et al, a ruthenium(III) catalyst was

used while the group of Matyjaszewski chose a copper(II) species as catalyst.[5-7] Both groups found that during the polymerization a linear increase in molecular weight was observed in time leading to polymers with narrow polydispersities (Đ < 1.5). While both groups showed similar results, it was the system of Matyjaszwewski that gained widespread attention and is still the most used system to date owing to its readily available components and its ease of application.

The reason for the effective control over the radical polymerization process lies in its mechanism as shown in Figure 1.5.

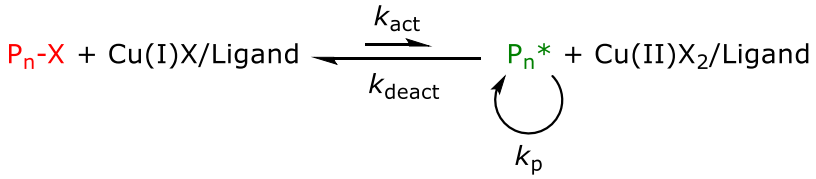

Figure 1.5 Schematic representation for the ATRP mechanism.

In the process, a halogen containing initiator is chosen (typically bromide or chloride) and a copper catalytic system (including a ligand for solubilization purposes) is added. Thanks to the inherent redox process, the copper(I) species will undergo oxidation by displacing the halogen from the initiator to form a copper(II) species along with a radical. The initiator is now in the active state and can enter propagation in the presence of monomer. However, the process is reversible whereby the copper(II) species is reduced back to copper(I) by transferring the halogen back to the now growing polymer chain making it inactive. The key to control is the significantly higher rate of deactivation with respect to the activation rate, keeping the growing chain in the dormant or inactive state for the majority of time. As a consequence, the concentration of radicals is

kept very low limiting the occurrence of side- and termination-reactions. A major benefit is that the halogen group is maintained on the polymer even after consumption of monomer. This way the chain can be extended further upon monomer addition which is not possible in any free radical process.

Though this process has remained a popular technique, efforts were made to the reduce the amount copper as unwanted impurity when aiming for biomedical applications. This lead to the development of activators (re)generated by electron transfer A(R)GET polymerization whereby a reducing agent is added to generate the copper(I) species in-situ from copper(II) species.[8-10] This drastically reduces the necessary amount of copper(I) in the polymerization. Another way to reduce the amount of copper(I) in the system is the addition of supplementary radicals to the polymerization by use of free-radical initiators. These added radicals assist in reducing copper(II) back to copper(I) due to the high deactivation rate. This process is therefore called initiators for continuous activator regeneration (ICAR) ATRP.[11-12]

Despite being a versatile tool for the polymerization of several different monomers, the ATRP process lacks the applicability to perform reactions in polar solvents and at ambient conditions while maintaining control. This issue spiked the development of single-electron transfer living radical polymerization (SET-LRP) whereby a copper(0) species is used to generate active copper(I) (Figure 1.6).[13] By using the more reactive copper(0) the amount of copper catalyst can be significantly reduced leading to polymers with higher purity and end group fidelity.

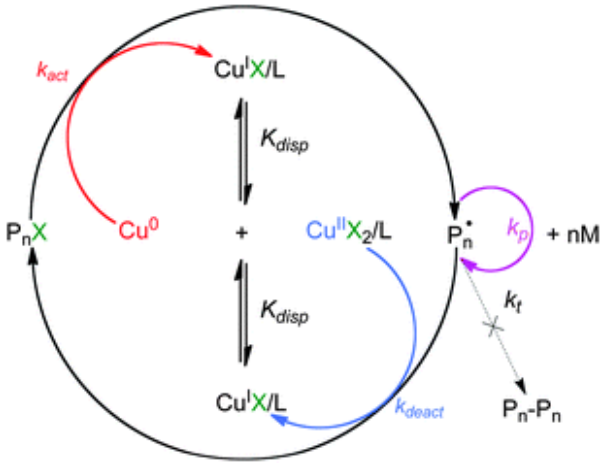

Figure 1.6 Schematic overview for the catalytic cycle involved in the single electron transfer living radical polymerization process.[14]

In SET-LRP, activation happens when copper(0) undergoes electron transfer from the alkyl halide initiator or halide terminated polymer (P_nX) to form copper (I) and a radical to which propagation can now happen. The active copper(I) readily disproportionates back to the *activator* copper(0) and the *deactivator* copper(II) driven by the ligand and polar solvents. The copper(II) species will react with the radical terminated polymer chain to form a deactivated halide terminated polymer chain and copper(I) which again readily disproportionates to copper(0) and copper(II). This self-regulation of in-situ generation of active and deactive species is crucial to SET-LRP polymerization and differs from traditional ATRP.

Recent research focuses on light induced ATRP in both batch as well as flow chemistry.[15-17]

1.5.2 Nitroxide mediated polymerization

Nitroxide mediated polymerization has been around for a long time: with the original patent dating back to 1986.[18] It is derived from the concept that

alkoxyamines reversibly produce a radical and a nitroxide at high temperatures as shown in Figure 1.7. In presence of monomer, propagation occurs at the radical R until deactivation happens whereby the nitroxide recombines with the growing polymer chain. Just as with ATRP, the deactivation rate is much higher than the rate of activation, leaving the growing polymer in a dormant state for the majority of time.

A major advantage over ATRP is the fact that this method is completely metal-free making it much more suitable for the preparation of polymers for biomedical purposes, making NMP a popular method for preparing tailor made polymers in this field.

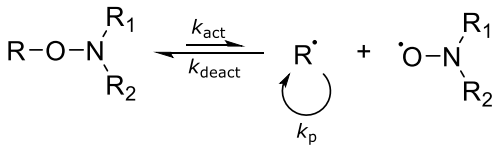

Figure 1.7 schematic representation of the NMP mechanism.[19]

1.5.3 Reversible activation fragmentation/ transfer polymerization

The last CRP technique to be discussed here is possibly one of the most used at the moment namely reversible addition fragmentation/transfer (RAFT) polymerization. It's origin can be traced back to the use of so-called iniferter (*ini*tiator-trans*fer* agent-*ter*minator) polymerization to control the chain length of polymers under free radical conditions by an addition and fragmentation mechanism developed by Otsu *et al*.[20-22] An iniferter is defined as a molecule which can decompose into radicals to initiate chain growth. This reversible procedure

formed the basis for the discovery of the RAFT process by CSIRO in 1998.[23] In their research a dithioester was used to allow reversible activation/deactivation to take place. They also showed that the RAFT-agent can be designed to accommodate the reactivity of different monomers by introducing a leaving group (R) and a radical stabilizing group (Z). These can be chosen to allow better stabilization or fragmentation to happen. As it is still a free-radical based process using traditional radical initiators, an adapted polymerization scheme was proposed for the RAFT-process (Figure 1.8).

Polymerization is started by decomposition of the free-radical initiator followed by the addition of monomer units to the radical. From here on, the growing chain may enter in what is known as the pre-equilibrium phase where the radical of the growing chain reacts with S=C double bond to form in intermediate form. There are now two options for beta scission: releasing the growing chain (P_m) or liberate the leaving group R. By choosing an appropriate leaving group, the beta scission can be driven towards the generation of new formed chains. In case of the latter option, the growing chain is now dormant (and is now called macroRAFT-agent) while the R group can reinitiate to form a new growing chain (P_n). When all R-groups are re-initiated, the process enters the main equilibrium. Herein, growing chain P_n can now react with the macroRAFT-agent and form a similar intermediate as the pre-equilibrium.

Just as before, there are two options for beta scission: releasing either P_n or P_m to allow further propagation while the respective other chain remains in the dormant state.

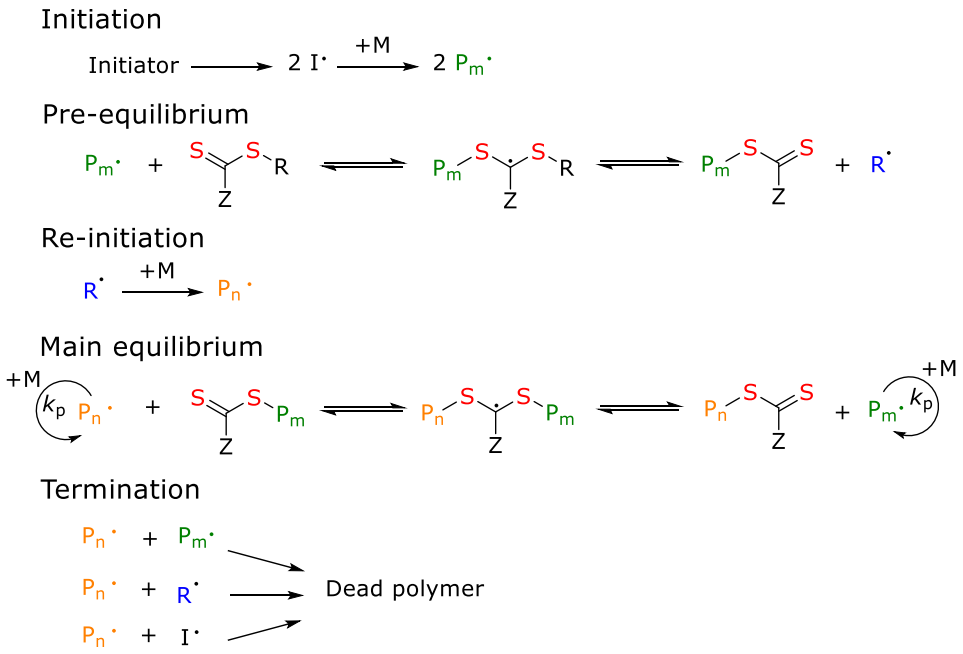

Figure 1.8 Schematic representation of the RAFT polymerization process.[24]

Due to the nature of the underlying free-radical process, termination can occur due to the constant presence of radical species. This is totally different from other controlled radical polymerization techniques whereby the concentration of radicals is kept very low due to the deactivation of active species. However, thanks to the reversible character of the RAFT process, further extension of the RAFT-polymers upon addition of monomer can be achieved.

A major advantage of RAFT polymerization is its flexibility towards almost all monomer species. This is due to the fact that the RAFT-agent can be designed by changing the leaving group R and stabilizing group Z to meet requirements for the specific system. Typical structures include dithiobenzoates and trithiocarbonates for monomers such as (meth)acrylates and styrene. These types of RAFT-agent however have limited compatibility with less activated monomers

such as vinyl acetate or vinyl amides. This lead to the simultaneous development of the MADIX (macromolecular design via interchange of xanthates) process by S. Zard in 1997.[25] MADIX follows a similar process as RAFT, but thanks to the design of the xanthate – using a Z-group with lower stabilizing capability – the radical is more reactive, improving the addition to electron deficient double bonds of vinylesters and vinylamides.

A major advantage of RAFT/MADIX over other CRP techniques is the easy implementation in already established free radical procedures without the need for excessive optimatization. In addition, it's metal-free conditions also gives it an advantage in preparing polymers for biomedical applications. As a consequence, it is possibly the preferred CRP technique for many cases.

1.6 Radical ring-opening polymerization

The problem, however, with polymers stemming from radical polymerization is a lack in degradability. This inhibits the use of these polymers in applications where degradability plays an important role such as many environmentally friendly applications and drug delivery purposes. For these applications, typically polyesters and polyamides are used due to the readily hydrolysable ester (both acidic as well as basic) and amide (only acidic) bonds in the main chain. However, as already mentioned in the start of this chapter, synthesis of these materials usually requires elaborate procedures under stringent conditions. Unification of these two worlds would be an advantageous situation where degradable polymers are prepared using the wide variety of radical polymerization techniques.

In the late 1970s, Bailey et al. performed research on the effect of radicals on ring-like structures called cyclic ketene acetals (CKAs). They expected these

structures to undergo vinyl addition to form a traditional vinyl polymer. However, they were surprised when they found that the resulting polymer also contained polyester parts. They realized that some form of ring-opening reaction must take place on CKAs when exposed to radicals. They proposed a mechanism for this ring-opening reaction and while still under small debate it is commonly accepted as the radical ring-opening reaction of CKAs (Figure 1.9).[26] For the first time it was possible to prepare polyesters using radical polymerization. With his group, he continued research through the 1980s focusing on different CKA structures as well as the ability to copolymerize CKAs with traditional vinyl monomers such as styrene and methyl methacrylate.[27-34]

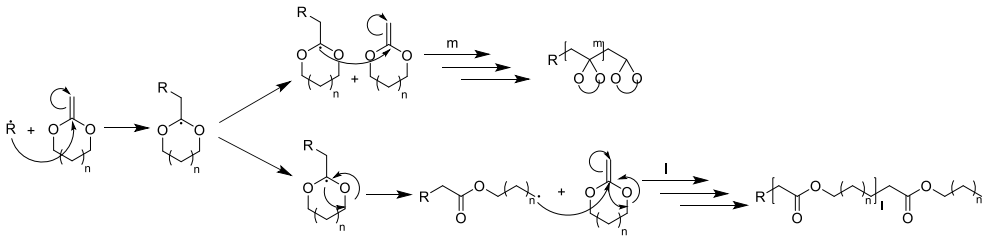

Figure 1.9 General mechanism for the reactions involved in the radical ring-opening polymerization of cyclic ketene acetals.

Unfortunately, this work did not result into immediate continuation of research in this field. This was partially due to the lack of interest and drive for degradable polymer materials but mostly due to the sometimes tedious synthesis of the CKAs.

1.6.1 Synthesis of cyclic ketene acetals

In the early reports by Bailey et al, the same synthetic procedure was applied for the synthesis of different CKA structures. This procedure involves two steps a transacetalization followed by a dehydrohalogenation as shown in Figure 1.10.[27-29]

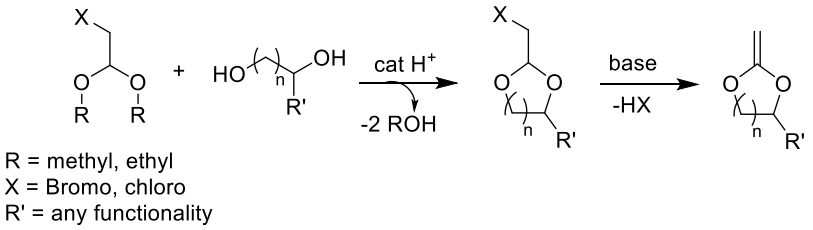

Figure 1.10 General synthesis procedure for the preparation of cyclic ketene acetals.

The first step, the transacetalization reaction, is an acid catalyzed reaction between a haloaldehyde dialkyl acetal and a diol whereby a condensate of alcohol is removed simultaneously to increase product yield. For the halogen X, typically chloride or bromide are chosen whereby the latter is the better leaving group in the follow-up reaction. While the R-group can basically by any alkyl chain, methyl or ethyl groups are preferred to thanks the low boiling points of their respective alcohols to allow for easier removal. The ring-size is determined by the diol leading to 1,3-dioxolanes in the case of 1,2-ethandiol, 1,3-dioxanes in the case of 1,3-propandiol or 1,3-dioxepanes in the case of 1,4-butanediol.[27]

The second step, the dehydrohalogenation, is typically performed by using a strong base at high temperatures to remove the halogen towards the formation of a C=C double bond. Early work showed that, although technically any base can be used (i.e. potassium hydroxide), a bulky base such as potassium *tertiary*-butoxide (KOtBu) generally leads to higher yields.[27] In more recent work, a phase transfer catalyst is used to make it possible to perform this reaction at much lower temperatures to avoid side-product formation and increase the yield even more. However, this works better for bromide substituted pre-CKAs since the C-Cl bond is too strong.[35-37]. While this pathway allows for the synthesis of a whole range of

different CKAs, only a handful of structures have been favored through the years. The most important factor is the capability to exhibit quantitative ring-opening. Due to the increased ring-strain, 5- or 7-membered rings are most suitable, while 6-membered rings are too stable to undergo ring-opening. With this in mind, only a few CKAs have been investigated in the last years, mostly thanks to the ease of synthesis, well-known behavior and the ability to allow quantitative ring-opening under mild conditions. The three most popular CKAs are 2-methylene-1,3-dioxepane (MDO), 5,6-benzo-2-methylene-1,3-dioxepane (BMDO) and 2-methylene-4-phenyl-1,3-dioxolane (MDPL), of which the structures are given in Figure 1.11.

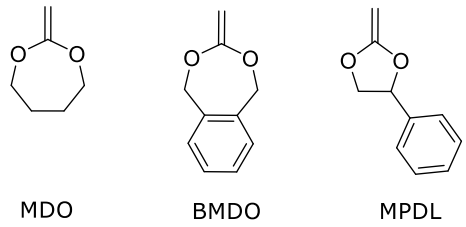

Figure 1.11 CKA structures for 2-methylene-1,3-dioxepane (MDO), 5,6-benzo-2-methylene-1,3-dioxepane (BMDO) and 2-methylene-4-phenyl-1,3-dioxolane (MDPL).

In the next paragraphs, the development of these monomers will be discussed in more detail.

1.6.2 2-methylene-1,3-dioxepane

MDO is probably the most studied CKA in literature. This is likely to the fact that - being an isomer of ε-caprolactone – polymerization leads to polycaprolactone. It was among the first CKAs studied by Bailey et al in the 1980s and has lately been expanded to the preparation of copolymers of PCL and a variety of different

comonomers. Through the years, copolymers of MDO with styrene[33, 38-39], MMA[27, 40-41], dimethyl aminoethyl methacrylate (DMAEMA)[42-43] and vinyl acetate (VAc)[27, 44-46] have been studied in terms of their copolymerization behavior resulting in valuable insights in the reactivity of the monomers in question. In most cases a significantly higher reactivity was observed leading to polymers with a higher content of the respective comonomer.

With these new insights and the emergence of controlled radical polymerization techniques, more research groups are now using RROP for the preparation of tailor-made degradable polymers. The first occurrence of using RROP in combination with some form of a controlled behavior was reported by Wei *et al.* in 1996.[47] In their work, they make use of 2,2,6,6-tetramethyl-1-piperidinyloxy (TEMPO) to successfully control the free radical polymerization of MDO leading to low dispersity polymers. The living nature of these polymers was also proven by the successful chain extension. Despite this evidence, people continued to use free-radical polymerization of MDO which mainly focused on studying the copolymerization with all kinds of different vinyl monomers.[38-45, 48-59] Therefore, this research was expanded by the combined effort of J. Nicolas and Y. Guillaneuf, where a full NMP process was used in the (co)polymerization of several different CKAs by switching TEMPO for the more effective *N*-*tert*-butyl-*N*-(1-diethylphosphono-2,2-dimethylpropyl) nitroxide (SG1) to successfully prepare polymers as well as copolymers with predictable molecular weights and low dispersities.[60-61] Other research groups also reported on the use of RAFT/MADIX [46, 62] and ATRP [63] to successfully control the radical ring-opening polymerization of CKAs.

Post-functionalization also starts playing a more dominant role when going for a certain application. In recent years, people have reported on the use of epoxides[64-65], azlactones[66] and crosslinking[62] as methods of making functionalized MDO based materials. With the rise of click-chemistry, this was further expanded by using the copper catalyzed azide-alkyne click reaction[42,56] or thiol-ene chemistry[46, 59]. With this toolbox, several attempts have been reported were a combination of CKAs and specific vinyl monomers has led to functioning applications predominantly in the biomedical field such as drug delivery systems[42, 58-59, 67], tissue engineering[45] but also biocompatible adhesives[65] and will likely expand in the future.

1.6.3 5,6-benzo-2-methylene-1,3-dioxepane

Similar to MDO, 5,6-benzo-2-methylene-1,3-dioxepane (BMDO) is one of the most studied CKAs incorporating the effective ring-opening of the 7-membered ring with an added phenyl-ring for increased ring-strain and radical stability.[28] Soon after the discovery of RROP of MDO, Bailey et al investigated different ways to improve the amount of ring-opening, which lead him to the use of BMDO. In this early work the copolymerization with several vinyl monomers was studied. With respect to MDO copolymerization, a higher polymerization temperature (120°C w.r.t 90°C) was necessary to allow decent BMDO conversions in a similar time range. This is mostly caused by the high melting point of BMDO (which is 92°C) whereas MDO is a liquid at ambient conditions. Even though, this research showed promising results, it was not until 2000 that new research involving BMDO was reported where Yuan and coworkers continued Bailey's work with the introduction of ATRP to the (co)polymerization of BMDO.[68] Their work nicely showed the synthesis of BMDO homopolymers with dispersity values between 1.1 and 1.4 at

different temperatures. This principle was expanded to the use of other CKAs but more importantly to the block-copolymerization of BMDO and other vinyl monomers to further prove the controlled/living character of these polymers.[69-70] Meanwhile, other research groups expanded on this development to investigate their own preferred combination of BMDO and comonomers.[71-78] Efforts were made to clarify the copolymerization behavior in terms of reactivity for BMDO towards the respective monomers. Similar observations were reported for MDO, whereby higher reactivities are reported for any vinyl monomer with respect to BMDO, leading to copolymers with a slightly higher content of the monomer in question.

Besides the use of ATRP to control the (co)polymerization, there are also report on the successful use of RAFT[79-84] and NMP[60-61, 85-86] to prepare (co)polymers with defined molecular weights and low polydispersities. This use of these techniques resulted in an increased number of reports on (possible) application of these materials for drug delivery purposes.[84, 87-89] Through these studies it was found that these polymers – including side and degradation products – are non-cytotoxic and that in-vitro degradation occurs readily in a range of different cell-lines. Even though the number of reports is limited in comparison to MDO, the use of BMDO could increase in the future thanks to the easy handling, easy copolymerization with a wide range of different monomers and the compatibility with several different CRP techniques.

1.6.4 2-methylene-4-phenyl-1,3-dioxolane

The last CKA to discuss is 2-methylene-4-phenyl-1,3-dioxolane (MPDL), one of the most recent discoveries in the field of radical ring-opening polymerizations. Although its first use dates back to the work of W.J. Bailey, it has recently gained

a lot of attention due to its ability to copolymerize with styrene (an ability which BMDO and MDO lack), thanks to similarity of the propagating radical of MPDL with respect to styrene.[29] However, MPDL contains a 5-membered ring rather than a 7-membered ring in the case of (B)MDO, and tends to polymerize in the presence of any cation resulting in a drastically reduced shelf life and the need for multiple purification steps in order to reach a pure product. While this can be counteracted with the addition of a small amount (2 wt% typically) of a base, this is most of the time undesired. Still, this has only been a limiting factor for a few researchers to use MPDL in their studies towards degradable polymers.

After the initial report of the (co)polymerization of MPDL and different vinyl monomers in the 1980s, the research was continued in the early 2000s with the work of Pan et al, who reported on the use of ATRP for the synthesis MPDL homopolymers with defined size and low dispersities.[90] In similar work as performed for BMDO, they nicely showed the controlled behavior expressed by the ATRP mechanism resulting in polymers with a dispersity in range of 1.2 to 1.5 depending on the temperature.

Even though these results were promising, it took another decade for researchers to further investigate the usability of MPDL. This time it was work by Nicolas et al. who, instead of ATRP, used their expertise in NMP to develop a novel route towards the synthesis of degradable materials with controllable properties around MPDL. [61, 91-92] In their work, they performed comparative studies with regards to MDO, BMDO and MPDL testing which CKA was best suited for the preparation of copolymers consisting of oligo(ethylene glycol) methyl ether methacrylate and acrylonitrile. MPDl proved to be best suitable for this specific task further showing the controlled behavior and the non-cytotoxic behavior of the polymers and its

respective degradation products. These results nicely show that MPDL is very much a strong contender as a CKA for the preparation of degradable polymers with defined properties.

1.7 Aim and outline of research

The aim of this thesis is to synthesize degradable nanoparticles for use in biomedical applications. Herein, a combination of radical ring-opening polymerization and miniemulsion was explored. An important step is to get a clear idea of the behavior involved in i.e. the (co)opolymerization and degradation in order to improve the controllability of various aspects such as molecular weight, composition and functionality.

In chapter 2, the copolymerization behavior of BMDO and MMA is studied by calculating the reactivity ratios based on the Mayo-Lewis approach. In a first attempt, copolymers of MMA and BMDO were synthesized using a RAFT-procedure to control the molecular weight build-up for linear as well as 4-arm star structure. As a final test, the hydrolytic degradability of both RAFT copolymer architectures was tested.

Chapter 3 focuses on expanding and optimizing the procedure used in Chapter 2, to determine the copolymerization parameters in a fast and accurate manner using online infrared spectra as a tool. Employing a model system based on MPDL several different comonomer classes was tested. Furthermore, an attempt was made to use RAFT as a method to prepare copolymers of MPDL and several comonomers with defined composition and size.

Important for the development of drug delivery systems is the ability for post functionalization of polymers to allow the attachment of biomolecules for the recognition of proteins/enzymes in the human body. In chapter 4, the use of click chemistry in the form of the copper catalyzed azide alkyn 1,3-dipolar cycloaddition was introduced via the copolymerization of MDO and propargyl acrylate. In

addition, a novel way of producing functionalized degradable polymers is presented by means of an alkyne functionalized CKA.

In chapter 5 the preparation of degradable nanoparticles is presented by using a combination of RROP and miniemulsion. Two different pathways are presented whereby the order of RROP and miniemulsion is tested.

Furthermore, a collection of all relevant synthetic procedures is combined in Chapter 6. Finally, a summary and outlook of the research performed in this thesis is given in Chapter 7.

1.8 References

1. Wilkinson, A. D. M. a. A., Glossary of basic terms in polymer science (IUPAC Recommendations 1996). *Compendium of Chemical Terminology, 2nd ed. (the "Gold Book")* **1996,** (2), 2289.
2. Staudinger, H., Über die Konstitution des Kautschuks (6. Mitteilung). *Berichte der deutschen chemischen Gesellschaft (A and B Series)* **1924,** *57* (7), 1203-1208.
3. Odian, G., Radical Chain Polymerization. In *Principles of Polymerization*, John Wiley & Sons, Inc.: 2004; pp 198-349.
4. Barner-Kowollik, C.; Vana, P.; Davis, T. P., The Kinetics of Free-Radical Polymerization. In *Handbook of Radical Polymerization*, John Wiley & Sons, Inc.: 2002; pp 187-261.
5. Kato, M.; Kamigaito, M.; Sawamoto, M.; Higashimura, T., Polymerization of Methyl Methacrylate with the Carbon Tetrachloride/Dichlorotris-(triphenylphosphine)ruthenium(II)/Methylaluminum Bis(2,6-di-tert-butylphenoxide) Initiating System: Possibility of Living Radical Polymerization. *Macromolecules* **1995,** *28* (5), 1721-1723.
6. Wang, J.-S.; Matyjaszewski, K., Controlled/"living" radical polymerization. atom transfer radical polymerization in the presence of transition-metal complexes. *Journal of the American Chemical Society* **1995,** *117* (20), 5614-5615.
7. Wang, J.-S.; Matyjaszewski, K., Controlled/"Living" Radical Polymerization. Halogen Atom Transfer Radical Polymerization Promoted by a Cu(I)/Cu(II) Redox Process. *Macromolecules* **1995,** *28* (23), 7901-7910.
8. Jakubowski, W.; Matyjaszewski, K., Activator Generated by Electron Transfer for Atom Transfer Radical Polymerization. *Macromolecules* **2005,** *38* (10), 4139-4146.
9. Min, K.; Gao, H.; Matyjaszewski, K., Preparation of Homopolymers and Block Copolymers in Miniemulsion by ATRP Using Activators Generated by Electron Transfer (AGET). *Journal of the American Chemical Society* **2005,** *127* (11), 3825-3830.
10. Jakubowski, W.; Matyjaszewski, K., Activators Regenerated by Electron Transfer for Atom-Transfer Radical Polymerization of (Meth)acrylates and Related Block Copolymers. *Angewandte Chemie International Edition* **2006,** *45* (27), 4482-4486.
11. Dong, H.; Tang, W.; Matyjaszewski, K., Well-Defined High-Molecular-Weight Polyacrylonitrile via Activators Regenerated by Electron Transfer ATRP. *Macromolecules* **2007,** *40* (9), 2974-2977.
12. Mueller, L.; Jakubowski, W.; Tang, W.; Matyjaszewski, K., Successful Chain Extension of Polyacrylate and Polystyrene Macroinitiators with Methacrylates in an ARGET and ICAR ATRP. *Macromolecules* **2007,** *40* (18), 6464-6472.

13. Percec, V.; Guliashvili, T.; Ladislaw, J. S.; Wistrand, A.; Stjerndahl, A.; Sienkowska, M. J.; Monteiro, M. J.; Sahoo, S., Ultrafast Synthesis of Ultrahigh Molar Mass Polymers by Metal-Catalyzed Living Radical Polymerization of Acrylates, Methacrylates, and Vinyl Chloride Mediated by SET at 25 °C. *Journal of the American Chemical Society* **2006,** *128* (43), 14156-14165.
14. Levere, M. E.; Nguyen, N. H.; Leng, X.; Percec, V., Visualization of the crucial step in SET-LRP. *Polymer Chemistry* **2013,** *4* (5), 1635-1647.
15. Mosnáček, J.; Ilčíková, M., Photochemically Mediated Atom Transfer Radical Polymerization of Methyl Methacrylate Using ppm Amounts of Catalyst. *Macromolecules* **2012,** *45* (15), 5859-5865.
16. Anastasaki, A.; Nikolaou, V.; Zhang, Q.; Burns, J.; Samanta, S. R.; Waldron, C.; Haddleton, A. J.; McHale, R.; Fox, D.; Percec, V.; Wilson, P.; Haddleton, D. M., Copper(II)/Tertiary Amine Synergy in Photoinduced Living Radical Polymerization: Accelerated Synthesis of ω-Functional and α,ω-Heterofunctional Poly(acrylates). *Journal of the American Chemical Society* **2014,** *136* (3), 1141-1149.
17. Pan, X.; Tasdelen, M. A.; Laun, J.; Junkers, T.; Yagci, Y.; Matyjaszewski, K., Photomediated controlled radical polymerization. *Progress in Polymer Science* **2016,** *62*, 73-125.
18. Solomon, D. H.; Rizzardo, E.; Cacioli, P., Polymerization process and polymers produced thereby. Google Patents: 1986.
19. Nicolas, J.; Guillaneuf, Y.; Lefay, C.; Bertin, D.; Gigmes, D.; Charleux, B., Nitroxide-mediated polymerization. *Progress in Polymer Science* **2013,** *38* (1), 63-235.
20. Otsu, T., Iniferter concept and living radical polymerization. *Journal of Polymer Science Part A: Polymer Chemistry* **2000,** *38* (12), 2121-2136.
21. Otsu, T.; Matsunaga, T.; Doi, T.; Matsumoto, A., Features of living radical polymerization of vinyl monomers in homogeneous system using N,N-diethyldithiocarbamate derivatives as photoiniferters. *European Polymer Journal* **1995,** *31* (1), 67-78.
22. Otsu, T.; Yoshida, M.; Tazaki, T., A model for living radical polymerization. *Die Makromolekulare Chemie, Rapid Communications* **1982,** *3* (2), 133-140.
23. Chiefari, J.; Chong, Y. K.; Ercole, F.; Krstina, J.; Jeffery, J.; Le, T. P. T.; Mayadunne, R. T. A.; Meijs, G. F.; Moad, C. L.; Moad, G.; Rizzardo, E.; Thang, S. H., Living Free-Radical Polymerization by Reversible Addition−Fragmentation Chain Transfer: The RAFT Process. *Macromolecules* **1998,** *31* (16), 5559-5562.
24. Moad, G.; Rizzardo, E.; Thang, S. H., Living Radical Polymerization by the RAFT Process. *Australian Journal of Chemistry* **2005,** *58* (6), 379-410.
25. Zard, S. Z., On the Trail of Xanthates: Some New Chemistry from an Old Functional Group. *Angewandte Chemie International Edition in English* **1997,** *36* (7), 672-685.

26. Bailey, W. J.; Chen, P. Y.; Chiao, W.-B.; Endo, T.; Sidney, L.; Yamamoto, N.; Yamazaki, N.; Yonezawa, K., Free-Radical Ring-Opening Polymerization. In *Contemporary Topics in Polymer Science: Volume 3*, Shen, M., Ed. Springer US: Boston, MA, 1979; pp 29-53.
27. Bailey, W. J.; Ni, Z.; Wu, S.-R., Synthesis of poly-ϵ-caprolactone via a free radical mechanism. Free radical ring-opening polymerization of 2-methylene-1,3-dioxepane. *Journal of Polymer Science: Polymer Chemistry Edition* **1982,** *20* (11), 3021-3030.
28. Bailey, W. J.; Ni, Z.; Wu, S. R., Free radical ring-opening polymerization of 4,7-dimethyl-2-methylene-1,3-dioxepane and 5,6-benzo-2-methylene-1,3-dioxepane. *Macromolecules* **1982,** *15* (3), 711-714.
29. Bailey, W. J.; Wu, S.-R.; Ni, Z., Synthesis and free radical ring-opening polymerization of 2-methylene-4-phenyl-1,3-dioxolane. *Die Makromolekulare Chemie* **1982,** *183* (8), 1913-1920.
30. Bailey William, J.; Gapud, B.; Lin, Y.-N.; Ni, Z.; Wu, S.-R., Free-Radical Ring-Opening Polymerization. In *Reactive Oligomers*, American Chemical Society: 1985; Vol. 282, pp 147-159.
31. Endo, T.; Yako, N.; Azuma, K.; Nate, K., Ring-opening polymerization of 2-methylene-4-phenyl-1,3-dioxolane. *Die Makromolekulare Chemie* **1985,** *186* (8), 1543-1548.
32. Bailey, W. J.; Chen, P. Y.; Chen, S.-C.; Chiao, W.-B.; Endo, T.; Gapud, B.; Kuruganti, V.; Lin, Y.-N.; Ni, Z.; Pan, C.-Y.; Shaffer, S. E.; Sidney, L.; Wu, S.-R.; Yamamoto, N.; Yamazaki, N.; Yonezawa, K.; Zhou, L.-L., Free radical ring-opening polymerization and its use to make biodegradable polymers and functionally terminated oligomers. *Makromolekulare Chemie. Macromolecular Symposia* **1986,** *6* (1), 81-100.
33. Bailey, J.; Chou, J. L.; Feng, P. Z.; Kuruganti, V.; Zhou, L. L., Recent advances in free radical ring-opening polymerization. *Acta Polymerica* **1988,** *39* (7), 335-341.
34. Bailey William, J.; Kuruganti Vijaya, K.; Angle Jay, S., Biodegradable Polymers Produced by Free-Radical Ring-Opening Polymerization. In *Agricultural and Synthetic Polymers*, American Chemical Society: 1990; Vol. 433, pp 149-160.
35. Barry, J.; Bram, G.; Decodts, G.; Loupy, A.; Pigeon, P.; Sansoulet, J., Solid-liquid phase-transfer catalysis reactions without solvent; very mild conditions for .beta.-eliminations. *The Journal of Organic Chemistry* **1984,** *49* (6), 1138-1140.
36. Zheng, Q.-H.; Su, J., Solid-Liquid Phase Transfer Catalytic Method for the Preparation of Acyclic and Cylic and Cyclic Ketene Acetals. *Synthetic Communications* **1999,** *29* (20), 3467-3476.
37. Tran, J.; Guegain, E.; Ibrahim, N.; Harrisson, S.; Nicolas, J., Efficient synthesis of 2-methylene-4-phenyl-1,3-dioxolane, a cyclic ketene acetal for

controlling the NMP of methyl methacrylate and conferring tunable degradability. *Polym. Chem.* **2016,** *7* (26), 4427-4435.
38. Morris, L. M.; Davis, T. P.; Chaplin, R. P., An assessment of the copolymerization reaction between styrene and 2-methylene-1,3-dioxepane. *Polymer* **2000,** *42* (2), 495-500.
39. Xu, J.; Liu, Z.-L.; Zhuo, R.-X., Synthesis and biodegradability evaluation of 2-methylene-1,3-dioxepane and styrene copolymers. *Journal of Applied Polymer Science* **2007,** *103* (2), 1146-1151.
40. Roberts, G. E.; Coote, M. L.; Heuts, J. P. A.; Morris, L. M.; Davis, T. P., Radical Ring-Opening Copolymerization of 2-Methylene-1,3-Dioxepane and Methyl Methacrylate: Experiments Originally Designed To Probe the Origin of the Penultimate Unit Effect. *Macromolecules* **1999,** *32* (5), 1332-1340.
41. Agarwal, S., Microstructural characterisation and properties evaluation of poly (methyl methacrylate-co-ester)s. *Polymer Journal* **2007,** *39* (2), 163-174.
42. Maji, S.; Mitschang, F.; Chen, L.; Jin, Q.; Wang, Y.; Agarwal, S., Functional Poly(Dimethyl Aminoethyl Methacrylate) by Combination of Radical Ring-Opening Polymerization and Click Chemistry for Biomedical Applications. *Macromol. Chem. Phys.* **2012,** *213* (16), 1643-1654.
43. Zhang, Y.; Aigner, A.; Agarwal, S., Degradable and Biocompatible Poly(N,N-dimethylaminoethyl Methacrylate-co-caprolactone)s as DNA Transfection Agents. *Macromol. Biosci.* **2013,** *13* (9), 1267-1275.
44. Agarwal, S.; Kumar, R.; Kissel, T.; Reul, R., Synthesis of Degradable Materials Based on Caprolactone and Vinyl Acetate Units Using Radical Chemistry. *Polym. J* **2009,** *41* (8), 650-660.
45. Undin, J.; Illanes, T.; Finne-Wistrand, A.; Albertsson, A.-C., Random introduction of degradable linkages into functional vinyl polymers by radical ring-opening polymerization, tailored for soft tissue engineering. *Polym. Chem.* **2012,** *3* (5), 1260-1266.
46. Bell, C. A.; Hedir, G. G.; O'Reilly, R. K.; Dove, A. P., Controlling the synthesis of degradable vinyl polymers by xanthate-mediated polymerization. *Polym. Chem.* **2015,** *6* (42), 7447-7454.
47. Wei, Y.; Connors, E. J.; Jia, X.; Wang, B., First Example of Free Radical Ring-Opening Polymerization with Some Characteristics of a Living Polymerization. *Chemistry of Materials* **1996,** *8* (3), 604-606.
48. Fukuzawa, S.-I.; Yamaishi, Y.; Furuya, H.; Terao, K.; Iwasaki, F., Effective transformation of aldoximes to nitriles by dehydration with 2-methylene-1,3-dioxepane in the presence of a Lewis acid catalyst. *Tetrahedron Lett.* **1997,** *38* (41), 7203-7206.
49. Jin, S.; Gonsalves, K. E., A study of the mechanism of the free-radical ring-opening polymerization of 2-methylene-1,3-dioxepane. *Macromolecules* **1997,** *30* (10), 3104-3106.

50. Jin, S.; Gonsalves, K. E., Synthesis and Characterization of Functionalized Poly(ε-caprolactone) Copolymers by Free-Radical Polymerization. *Macromolecules* **1998,** *31* (4), 1010-1015.
51. Wei, Y.; Connors, E. J.; Jia, X.; Wang, C., Controlled free radical ring-opening polymerization and chain extension of the "living" polymer. *J. Polym. Sci., Part A: Polym. Chem.* **1998,** *36* (5), 761-771.
52. Sun, L. F.; Zhuo, R. X.; Liu, Z. L., Synthesis and enzymatic degradation of 2-methylene-1,3-dioxepane and methyl acrylate copolymers. *J. Polym. Sci., Part A: Polym. Chem.* **2003,** *41* (18), 2898-2904.
53. Kwon, S.; Lee, K.; Bae, W.; Kim, H., Precipitation polymerization of 2-methylene-1,3-dioxepane in supercritical carbon dioxide. *Polym. J. (Tokyo, Jpn.)* **2008,** *40* (4), 332-338.
54. Seema, A.; Liqun, R., Polycaprolactone-Based Novel Degradable Ionomers by Radical Ring-Opening Polymerization of 2-Methylene-1,3-dioxepane. *Macromolecules* **2009,** *42* (5), 1574-1579.
55. Agarwal, S.; Speyerer, C., Degradable blends of semi-crystalline and amorphous branched poly(caprolactone): Effect of microstructure on blend properties. *Polymer* **2010,** *51* (5), 1024-1032.
56. Maji, S.; Zheng, M.; Agarwal, S., Functional Degradable Polymers via Radical Ring-Opening Polymerization and Click Chemistry. *Macromolecular Chemistry and Physics* **2011,** *212* (23), 2573-2582.
57. Guo, J.-w.; Ma, Q.; Cui, Y.-h.; Liu, S.; Peng, J.-p., Synthesis and characterization of biodegradable copolymers as non-phosphorous detergent builders. *Gaofenzi Xuebao* **2012,** (9), 958-964.
58. Jin, Q.; Maji, S.; Agarwal, S., Novel amphiphilic, biodegradable, biocompatible, cross-linkable copolymers: synthesis, characterization and drug delivery applications. *Polym. Chem.* **2012,** *3* (10), 2785-2793.
59. Cai, T.; Chen, Y.; Wang, Y.; Wang, H.; Liu, X.; Jin, Q.; Agarwal, S.; Ji, J., Functional 2-methylene-1,3-dioxepane terpolymer: a versatile platform to construct biodegradable polymeric prodrugs for intracellular drug delivery. *Polym. Chem.* **2014,** *5* (13), 4061-4068.
60. Delplace, V.; Tardy, A.; Harrisson, S.; Mura, S.; Gigmes, D.; Guillaneuf, Y.; Nicolas, J., Degradable and Comb-Like PEG-Based Copolymers by Nitroxide-Mediated Radical Ring-Opening Polymerization. *Biomacromolecules* **2013,** *14* (10), 3769-3779.
61. Delplace, V.; Harrisson, S.; Tardy, A.; Gigmes, D.; Guillaneuf, Y.; Nicolas, J., Nitroxide-Mediated Radical Ring-Opening Copolymerization: Chain-End Investigation and Block Copolymer Synthesis. *Macromolecular Rapid Communications* **2014,** *35* (4), 484-491.

62. Hedir, G. G.; Bell, C. A.; Ieong, N. S.; Chapman, E.; Collins, I. R.; O'Reilly, R. K.; Dove, A. P., Functional Degradable Polymers by Xanthate-Mediated Polymerization. *Macromolecules* **2014,** *47* (9), 2847-2852.
63. Agarwal, S., Microstructural Characterisation and Properties Evaluation of Poly (methyl methacrylate-co-ester)s. *Polym. J* **2006,** *39* (2), 163-174.
64. Undin, J.; Finne-Wistrand, A.; Albertsson, A.-C., Copolymerization of 2-Methylene-1,3-dioxepane and Glycidyl Methacrylate, a Well-Defined and Efficient Process for Achieving Functionalized Polyesters for Covalent Binding of Bioactive Molecules. *Biomacromolecules* **2013,** *14* (6), 2095-2102.
65. Shi, Y.; Zhou, P.; Jérôme, V.; Freitag, R.; Agarwal, S., Enzymatically Degradable Polyester-Based Adhesives. *ACS Biomaterials Science & Engineering* **2015**.
66. Carter, M. C. D.; Jennings, J.; Appadoo, V.; Lynn, D. M., Synthesis and Characterization of Backbone Degradable Azlactone-Functionalized Polymers. *Macromolecules (Washington, DC, U. S.)* **2016,** *49* (15), 5514-5526.
67. Asoh, T.-A.; Nakajima, T.; Matsuyama, T.; Kikuchi, A., Surface-Functionalized Biodegradable Nanoparticles Consisting of Amphiphilic Graft Polymers Prepared by Radical Copolymerization of 2-Methylene-1,3-Dioxepane and Macromonomers. *Langmuir* **2015,** *31* (24), 6879-6885.
68. Yuan, J.-Y.; Pan, C.-Y.; Tang, B. Z., "Living" Free Radical Ring-Opening Polymerization of 5,6-Benzo-2-methylene-1,3-dioxepane Using the Atom Transfer Radical Polymerization Method. *Macromolecules* **2000,** *34* (2), 211-214.
69. Yuan, J. Y.; Pan, C. Y., Block copolymerization of 5,6-benzo-2-methylene-1,3-dioxepane with conventional vinyl monomers by ATRP method. *European Polymer Journal* **2002,** *38* (8), 1565-1571.
70. Yuan, J.-y.; Pan, C.-y., The effects of monomer structure of cyclic ketene acetals on the behavior of controlled radical ring-opening polymerization. *Chin. J. Polym. Sci.* **2002,** *20* (1), 9-14.
71. Wickel, H.; Agarwal, S., Synthesis and Characterization of Copolymers of 5,6-Benzo-2-methylene-1,3-dioxepane and Styrene. *Macromolecules* **2003,** *36* (16), 6152-6159.
72. Wickel, H.; Agarwal, S.; Greiner, A., Homopolymers and Random Copolymers of 5,6-Benzo-2-methylene-1,3-dioxepane and Methyl Methacrylate: Structural Characterization Using 1D and 2D NMR. *Macromolecules* **2003,** *36* (7), 2397-2403.
73. Huang, J.; Gil, R.; Matyjaszewski, K., Synthesis and characterization of copolymers of 5,6-benzo-2-methylene-1,3-dioxepane and n-butyl acrylate. *Polymer* **2005,** *46* (25), 11698-11706.
74. Huang, J.; Gil, R.; Matyjaszewski, K., Atom transfer radical copolymerization of 5,6-benzo-2-methylene-1,3-dioxepane and n-butyl acrylate. *Polym. Prepr. (Am. Chem. Soc., Div. Polym. Chem.)* **2005,** *46* (2), 150-151.

75. Agarwal, S., Radical Ring Opening and Vinyl Copolymerization of 2,3,4,5,6-pentafluorostyrene with 5,6-Benzo-2-methylene-1,3-dioxepane: Synthesis and Structural Characterization Using 1D and 2D NMR Techniques. *Journal of Polymer Research* **2006,** *13* (5), 403-412.
76. Ren, L.; Agarwal, S., Synthesis, characterization, and properties evaluation of poly[(N-isopropylacrylamide)-co-ester]s. *Macromol. Chem. Phys.* **2007,** *208* (3), 245-253.
77. Ren, L.; Speyerer, C.; Agarwal, S., Free-Radical Copolymerization Behavior of 5,6-Benzo-2-methylene-1,3-dioxepane and Methacrylic Acid via the in Situ Generation of 3-Methyl-1,5-dihydrobenzo[e][1,3]dioxepin-3-yl Methacrylate and 2-(Acetoxymethyl)benzyl Methacrylate. *Macromolecules* **2007,** *40* (22), 7834-7841.
78. Agarwal, S.; Ren, L., Unexpected new route to free radical copolymerisation of 5,6-benzo-2-methylene-1,3-dioxepane with methacrylic acid as proved by 1D and 2D NMR techniques. *Polym. Prepr. (Am. Chem. Soc., Div. Polym. Chem.)* **2008,** *49* (1), 743-744.
79. He, T.; Zou, Y.-F.; Pan, C.-Y., Controlled/“Living” Radical Ring-Opening Polymerization of 5,6-Benzo-2-Methylene-1,3-Dioxepane Based on Reversible Addition-Fragmentation Chain Transfer Mechanism. *Polymer Journal* **2002,** *34* (3), 138-138.
80. Siegwart, D. J.; Bencherif, S. A.; Srinivasan, A.; Hollinger, J. O.; Matyjaszewski, K., Synthesis, characterization, and in vitro cell culture viability of degradable poly(N-isopropylacrylamide-co-5,6-benzo-2-methylene-1,3-dioxepane)-based polymers and crosslinked gels. *Journal of Biomedical Materials Research Part A* **2008,** *87A* (2), 345-358.
81. d'Ayala, G. G.; Malinconico, M.; Laurienzo, P.; Tardy, A.; Guillaneuf, Y.; Lansalot, M.; D'Agosto, F.; Charleux, B., RAFT/MADIX Copolymerization of Vinyl Acetate and 5,6-Benzo-2-methylene-1,3-dioxepane. *Journal of Polymer Science Part a-Polymer Chemistry* **2014,** *52* (1), 104-111.
82. Kobben, S.; Ethirajan, A.; Junkers, T., Synthesis of degradable poly(methyl methacrylate) star polymers via RAFT copolymerization with cyclic ketene acetals. *Journal of Polymer Science Part A: Polymer Chemistry* **2014,** *52* (11), 1633-1641.
83. Decker, C. G.; Maynard, H. D., Degradable PEGylated protein conjugates utilizing RAFT polymerization. *Eur. Polym. J.* **2015,** *65*, 305-312.
84. Ganda, S.; Jiang, Y.; Thomas, D. S.; Eliezar, J.; Stenzel, M. H., Biodegradable Glycopolymeric Micelles Obtained by RAFT-controlled Radical Ring-Opening Polymerization. *Macromolecules (Washington, DC, U. S.)* **2016,** *49* (11), 4136-4146.
85. Tardy, A.; Delplace, V.; Siri, D.; Lefay, C.; Harrisson, S.; Pereira, B. d. F. A.; Charles, L.; Gigmes, D.; Nicolas, J.; Guillaneuf, Y., Scope and limitations of the

nitroxide-mediated radical ring-opening polymerization of cyclic ketene acetals. *Polym. Chem.* **2013,** *4* (17), 4776-4787.
86. Albergaria Pereira, B. d. F.; Tardy, A.; Monnier, V.; Guillaneuf, Y.; Gigmes, D.; Charles, L., Elucidation of a side reaction occurring during nitroxide-mediated polymerization of cyclic ketene acetals by tandem mass spectrometric end-group analysis of aliphatic polyesters. *Rapid Commun. Mass Spectrom.* **2015,** *29* (23), 2302-2308.
87. Xiao, N.; Liang, H.; Lu, J., Degradable and biocompatible aldehyde-functionalized glycopolymer conjugated with doxorubicin via acid-labile Schiff base linkage for pH-triggered drug release. *Soft Matter* **2011,** *7* (22), 10834-10840.
88. Siebert, J. M.; Baumann, D.; Zeller, A.; Mailänder, V.; Landfester, K., Synthesis of Polyester Nanoparticles in Miniemulsion Obtained by Radical Ring-Opening of BMDO and Their Potential as Biodegradable Drug Carriers. *Macromolecular Bioscience* **2012,** *12* (2), 165-175.
89. Zhang, Y.; Chu, D.; Zheng, M.; Kissel, T.; Agarwal, S., Biocompatible and degradable poly(2-hydroxyethyl methacrylate) based polymers for biomedical applications. *Polymer Chemistry* **2012,** *3* (10), 2752-2759.
90. Pan, C.-Y.; Lou, X.-D., "Living" free radical ring-opening polymerization of 2-methylene-4-phenyl-1,3-dioxolane by atom transfer radical polymerization. *Macromolecular Chemistry and Physics* **2000,** *201* (11), 1115-1120.
91. Tardy, A.; Delplace, V.; Siri, D.; Lefay, C.; Harrisson, S.; de Fatima Albergaria Pereira, B.; Charles, L.; Gigmes, D.; Nicolas, J.; Guillaneuf, Y., Scope and limitations of the nitroxide-mediated radical ring-opening polymerization of cyclic ketene acetals. *Polymer Chemistry* **2013,** *4* (17), 4776-4787.
92. Delplace, V.; Guegain, E.; Harrisson, S.; Gigmes, D.; Guillaneuf, Y.; Nicolas, J., A ring to rule them all: a cyclic ketene acetal comonomer controls the nitroxide-mediated polymerization of methacrylates and confers tunable degradability. *Chemical Communications* **2015,** *51* (64), 12847-12850.

Chapter 2

Synthesis of Degradable Poly(Methyl Methacrylate) Star Polymers via RAFT Copolymerization with Cyclic Ketene Acetals

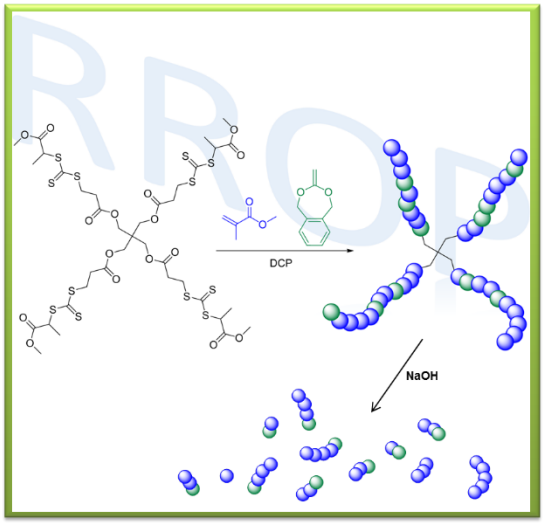

Kobben, S.; Ethirajan, A.; Junkers, T., *J. Polym. Sci. Part A: Polym. Chem.* **2014,** *52* , 1633-1641

2.1 Abstract

Copolymerization of the cyclic ketene acetal 5,6-benzo-2-methylene-1,3-dioxepane (BMDO) with methyl methacrylate (MMA) is studied with respect to its copolymerization parameters and the suitability to control BMDO/MMA copolymerizations via the reversible addition-fragmentation chain transfer (RAFT) polymerization technique to obtain linear and 4-arm star polymers. BMDO shows disparate copolymerization behavior with MMA and r_1 = 0.33 ± 0.06 and r_2 = 6.0 ± 0.8 have been determined for polymerization at 110 °C in anisole from fitting copolymer composition *vs.* comonomer feed data to the Lewis-Mayo equation. Copolymerization of the two monomers is successful in RAFT polymerization employing a trithiocarbonate control agent. As desired, polymers contain only little amount of polyester units stemming from BMDO units. Preliminary degradation experiment show that the polymer degrades slowly, but steadily in aqueous 1 M NaOH dispersion. Within ten days, the polymers are broken down to low molecular weight segments from an initial number-average molecular weight of M_n = 6000 g·mol^{-1}. Star (co)polymerization with an erythritol-based tetra-functional RAFT agent following the Z-group approach proceeds efficiently and polymers with a number-average molecular weight of M_n = 10 000 g·mol^{-1} are readily obtained that degrade in similar manner as the linear copolymer counterparts.

2.2 Introduction

The polymerization of cyclic ketene acetals (CKAs) to obtain polyesters via a radical ring-opening polymerization (RROP) process has first been described in the seventies of the last century.[1] While in principle being a highly interesting process, RROP did not gain much interest and remained largely unused for a long time, mostly due to the seemingly better accessibility of polyesters from either step-growth polymerization or the ring opening polymerization of lactones.[2-3] However, in recent years RROP has seen a revival and a considerable amount of studies have been published on polyester materials stemming from this process.[3-7] This resurrection is mostly due to two factors, (i) being the availability of controlled radical polymerization (CRP) methods[8-10] that allow (in combination with CKAs) for the simple design of mixed polyester/polyvinyl (block) copolymers with controlled structure, functionality and defined dispersity and (ii) the general possibility to produce statistical copolymers of CKAs with conventional vinyl monomers that allow for the synthesis of materials that feature the degradability of the polyester component.[11]

Especially the second feature is highly attractive for the design of materials for a broad range of applications. The possibility to synthesize materials that consist primarily of a conventional vinyl monomer in which polyester units are randomly located along the backbone of the chains is highly attractive. Such material will feature (bio)degradability of the polyester compound, but retain – as long as the CKA content is kept low – essentially the physical properties of the vinyl polymer. Degradable polystyrene or poly(meth)acrylates are in this manner accessible and deeper exploration of these copolymerizations has the potential to shape the

future of such materials since degradability becomes increasingly important for specialties as well as bulk materials.

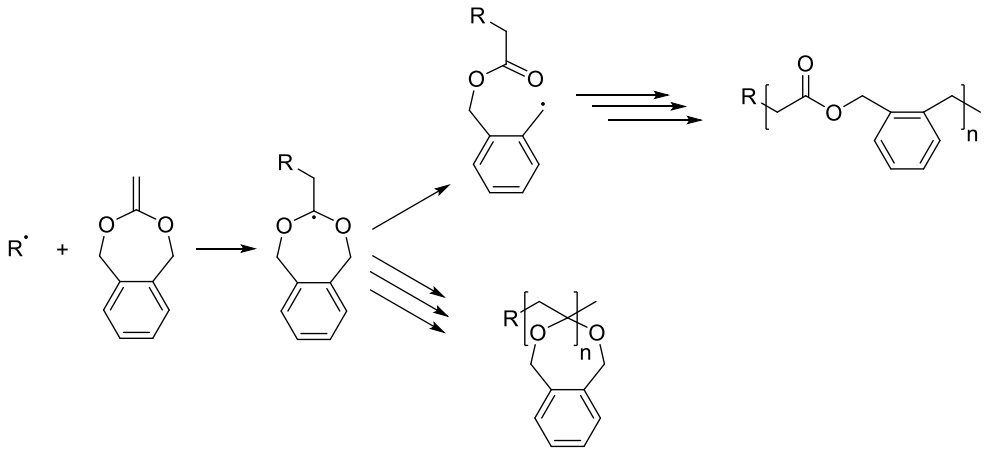

Figure 2.1 Simplified reaction mechanism for CKA polymerization leading to ring opening polymerization as well as to ring-retaining structures. Note that also a combination of both mechanisms may occur.

CKAs polymerize radically via a two-step process, see Figure 2.1. First, an intermediate radical is formed by addition of a propagating radical to the monomer, which is ideally followed by ring opening via β-scission, yielding a primary radical. Polymerizations in which most monomer units have been ring-opened (in contrast to units where propagation occurred directly via the initially formed intermediate radical, see lower part of the scheme), are usually only observed at high reaction temperatures, which is unsurprising since β-scission reactions are typically associated with high activation energies.[12-13] High reaction temperatures pose no direct problem for polymerization and are even favorable due to the overall relatively slow propagation rates of CKAs. Difficult with respect to controlled polymerization is though that the propagating ring-opened species is of primary nature, which renders reversible deactivation reactions difficult.

Indeed, when reviewing literature, almost random patterns are observed with respect to which CRP method is able to control the polymerization of a certain CKA.[4]

Addition of a comonomer has in the past proven to be beneficial for controlling CKA polymerizations. By employing a comonomer, control over the polymerization may be achieved by solely controlling propagating chains with a comonomer terminus. Yet, CKAs do not copolymerize easily and polymerizations may be interrupted if the control-agent CKA-chain terminus adduct is too stable.

In this chapter we have focused on the copolymerization of 5,6-benzo-2-methylene-1,3-dioxepane (BMDO) with methyl methacrylate (MMA). To gain control over the polymerizations, reversible addition-fragmentation chain transfer polymerization (RAFT) has been chosen. The copolymerization of BMDO and methacrylates has been described before[14-16] and the overall suitability of RAFT to control BMDO homopolymerization is also known.[17] The exact combination of both has, however, not yet been described. In order to reach a precision design of complex (meth)acrylates that feature biodegradable units, a closer kinetic understanding of the copolymerization and the possibility to control it via CRP methods – or more specifically via RAFT – is required. Thus, an in-depth kinetic study was performed on the copolymerization behavior of BMDO with MMA to set the fundament for further synthetic studies. With this kinetic knowledge at hand, the work was expanded to RAFT polymerizations and the synthesis of four-arm star RAFT polymers that are essentially made of MMA, but that feature (bio)degradability. First degradation results for the synthesized polymers are presented in the last section of this chapter.

2.3 Results and Discussion

2.3.1 Monomer synthesis

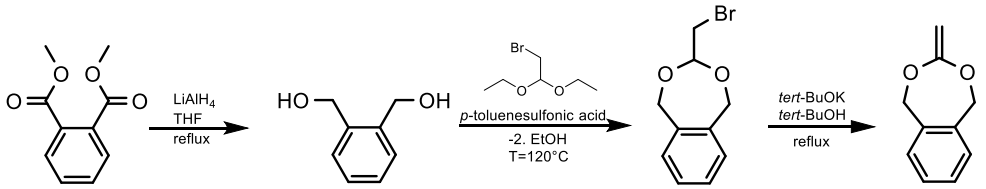

Figure 2.2 Synthesis route to 5,6-benzo-2-methylene-1,3-dioxepane (BMDO).

The CKAs required to perform RROP are only of very limited commercial availability. The monomer 5,6-benzo-2-methylene-1,3-dioxepane (BMDO) was thus synthesized using the method described by Wickel et al. as given in Figure 2.2.[18] The synthesis of the monomer is straightforward and only minor adaptations of the literature protocols were required (see Paragraph 6.2 for details). Handling of BMDO on the contrary – which is not often described in literature – has proven to be somewhat challenging due to the tendency to undergo hydrolysis under atmospheric conditions. Upon contact with traces of water, the double bond is lost by H_2O addition and subsequent ring-opening, which yields the side-product 2-(hydroxymethyl)benzyl acetate.[19] The ^{1}H-NMR spectra for BMDO and its degradation product (measured in deuterated chloroform) are given in Figure 2.3. NMR analysis clearly shows that the described degradation takes place rapidly, which can also be easily observed by the naked eye, as the degradation product 2-(hydroxymethyl)benzyl acetate is a liquid while BMDO is solid. Once BMDO is dissolved in its degradation product, it is nearly impossible to recover BMDO from the solution. In consequence, for the present study the monomer was stored under inert atmosphere at a temperature of −20 °C.

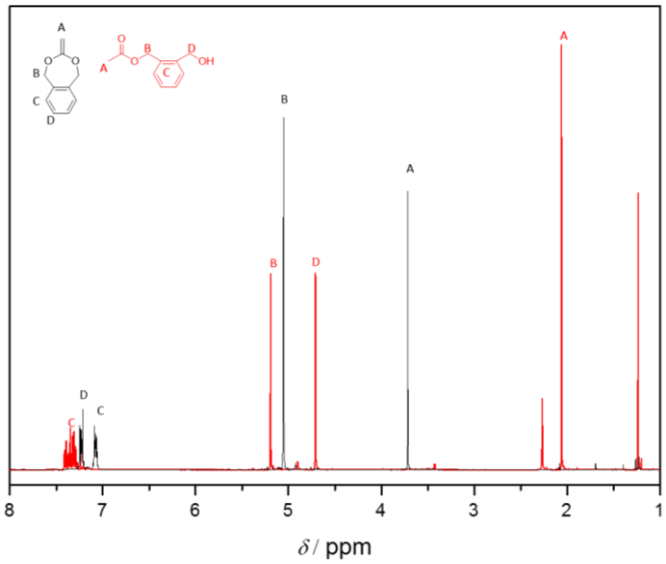

Figure 2.3 ^{1}H-NMR spectrum (measured in deuterated chloroform) of BMDO and its hydrolysis degradation product that is formed upon exposure of the monomer to air.

2.3.2 Copolymerization of BMDO with MMA

To investigate BMDO polymerization, MMA was chosen as a comonomer. Early work by Bailey et al. showed that BMDO homopolymerization is rather slow (43% conversion in 15h at T=120°C) but that the polymer contained 100 % ester-groups and that ring retention does not play a significant role.[20] Wickel et al. first reported on the BMDO/MMA comonomer combination in 2003.[16] In their work, they used ATRP to obtain copolymers with defined copolymer composition and via an in-depth 2D NMR study, they determined the copolymerization reactivity ratios.

To avoid interference of the CRP technique on the copolymerization kinetics, we opted herein to determine the reactivity ratios for the BMDO/MMA polymerization under uncontrolled radical polymerization conditions. Monomer mixtures were

therefore dissolved in anisole using dicumyl peroxide as initiator. The polymerizations were carried out under inert conditions at a temperature T = 110 °C to facilitate reasonable reaction speeds. At lower T, polymerizations become unpractically slow. A typical ^{1}H-NMR for poly(BMDO-*r*-MMA) (measured in deuterated chloroform) is shown in Figure 2.4.

In the insert to Figure 2.4 the structure of the copolymer is depicted. All individual peaks in the spectrum can be assigned to BMDO and MMA typical signals or residual solvent. The strong resonance around 2 and 5 ppm stem from moieties that are formed after stopping the polymerization by exposing the reaction to air, by which residual BMDO is hydrolyzed immediately.

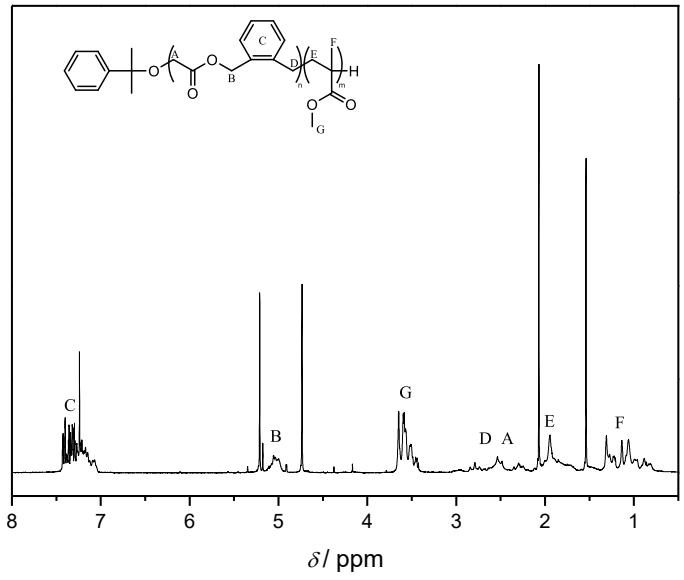

Figure 2.4 ^{1}H-NMR spectrum (measured in deuterated chloroform) and peak assignments for the copolymer of BMDO and MMA, with a monomer ratio in the feed of [BMDO]:[MMA] 70:30.

Agarwal and coworkers reported for BMDO/MMA reactivity ratios of r_1 = 0.53 and r_2 = 1.96.[16]

Whereby

$$r_1 = \frac{k_{p,BMDO-BMDO}}{k_{p,BMDO-MMA}} \quad \text{and} \quad r_2 = \frac{k_{p,MMA-MMA}}{k_{p,MMA-BMDO}}$$

and $k_{p,BMDO\text{-}BMDO}$ and $k_{p,MMA\text{-}MMA}$ denote the respective homopropagation rate coefficients and $k_{p,BMDO\text{-}MMA}$ and $k_{p,MMA\text{-}BMDO}$ denote the crosspropagation rate coefficients. Unfortunately, in their study they used for their analysis polymer composition data from polymers obtained at varying and partially higher monomer conversions (no exact conversion data was reported). In systems where r_1 and r_2 are significantly differing unity, composition drift occurs during polymerization, consequently changing the composition of the copolymer with proceeding polymerization. For a reliable determination of *r* values, it is thus mandatory to determine copolymerization parameters from samples that were taken at low monomer conversion before composition drift has occurred to significant extent.

First, the change in monomer composition with polymerization and monomer concentrations is investigated via in-line polymerization monitoring with an IR-probe. In this manner, time-resolved monomer concentrations can be followed, which allows for a first assessment of copolymerization behavior and also allows determining the optimal point in time to stop polymerizations for copolymer composition determination. A series of reactions were analyzed where the monomer concentration in the feed was changed, but where the conversion of BMDO was kept low in order to avoid larger composition drifts. An overview over

these reactions with respect to feed composition, apparent molecular weight obtained, BMDO conversion and reaction time is given in Table 2.1.

Table 2.1 Overview of the results for (co)polymerization of BMDO and MMA in anisole with c_{DCP} = 0.4 mol·L^{-1} at T = 110°C under variation of feed concentrations.

[BMDO]: [MMA]	M_n / 10^4 **g·mol^{-1}**	M_w / 10^4 **g·mol^{-1}**	**Đ**	x_{BMDO} **/ %**	x_{MMA} **/ %**	***t*** **/ min**
100:0	0.28	0.69	2.42	41	-	3120
90:10	0.32	0.71	2.25	13	89	155
80:20	0.75	1.41	1.88	7.6	84	54
70:30	0.99	1.77	1.78	4.1	85	34
60:40	1.47	2.85	1.94	5.6	77	55
50:50	1.57	3.32	2.11	5.5	76	46
40:60	1.81	3.63	2.01	3.2	81	43
30:70	2.02	4.11	2.03	5.2	85	36
20:80	2.29	4.60	2.01	5.6	85	35
10:90	3.14	6.26	1.99	0.8	92	19
0:100	2.16	6.17	2.86	-	95	259

For all data given in Table 1 a certain error in M_n, M_w and $Đ$ needs to be taken into account, since no precise copolymerization Mark-Houwink parameters are available and the numbers have been obtained using pure pMMA parameters. Regardless, a slight increase in average molecular weights with increasing MMA content is observed, which is probably caused by a faster overall propagation rate at higher MMA feed concentrations. Also, with higher MMA contents in the feed, the reaction time to reach significant conversion of BMDO decreases significantly.

This is a first indication that BMDO reacts faster with MMA than with itself and that already addition of small amounts of MMA can increase the overall reaction rate significantly.

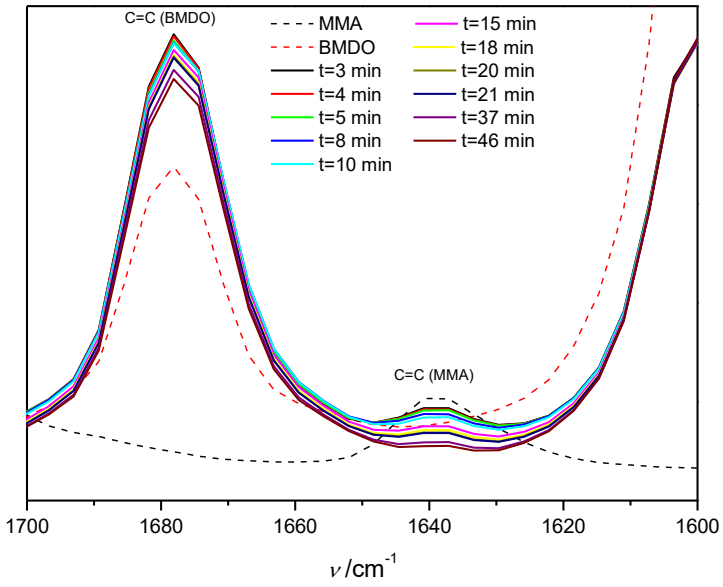

Figure 2.5 IR-spectra for the free-radical copolymerization of BMDO and MMA at a BMDO:MMA composition of 50:50 and T = 110 °C in anisole. IR-spectra were recorded in-situ after given time intervals as indicated. The dashed lines represent the pure monomers.

To explore the copolymerization behavior further, the IR-data is analyzed in more detail. A series of spectra taken at different reaction times is depicted in Figure 2.5. Only the wavelength region of interest is depicted, that is the stretching vibration of the C=C double bonds. Due to the different monomer structures, the signals for the C=C vibration for BMDO and MMA, respectively, are nicely separated and can be analyzed without the need for band deconvolution. As a comparison to the copolymerization monomer mixtures, also the spectra of pure MMA and BMDO are included in the figure as dashed lines.

The absorption intensity of BMDO is much more pronounced compared to MMA. It should be noted that Figure 2.5 depicts spectra from a polymerization with equal monomer starting concentration. Nevertheless, absolute intensities are irrelevant and conversions are directly calculated from the relative loss of intensity of the individual vibration bands. First investigation of the spectra directly reveals that the signal associated to MMA depletes at a much faster rate than the BMDO signal, indicating that MMA propagates much quicker in the copolymerization than BMDO, explaining the average molecular weight increase with increasing MMA content as speculated above. In order to sustain this observation, absolute monomer concentrations (and thus conversions) were calculated from the half-height area under the peaks. In conjunction with the known initial concentration for BMDO and MMA, the concentration traces in Figure 2.6 can be constructed. To facilitate an easy comparison, the data from the reaction with a monomer ratio BMDO:MMA of 50:50 was used.

As already qualitatively assessed, it can be immediately observed that the consumption of MMA happens at a much faster rate than BMDO, indicating a considerable composition drift. As seen from the third trace in the figure, a shift in composition from 1:1 to 1:4 after roughly 45 hours is observed. While this obviously results in polymer chains that consist of significantly more MMA compared to BMDO, this also means that the composition of monomer units in the polymer product will largely differ when product is compared from early stages of the polymerization with late stages of polymerization. From a certain point on, all MMA will be consumed and BMDO homopolymer will start to form. While this obviously results in polymer chains that consist of significantly more MMA compared to BMDO, this also means that the composition of monomer units in the

polymer product will largely differ when product is compared from early stages of the polymerization with later stages of polymerization.

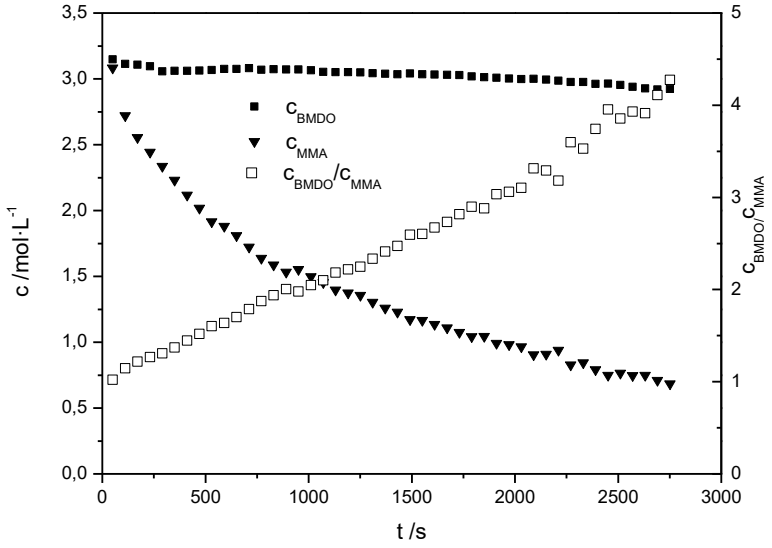

Figure 2.6 Monomer concentration versus time plot for both BMDO (squares) and MMA (triangles) as obtained from integration of the IR bands depicted in Figure 3. The change in the ratio of BMDO over MMA concentration is additionally indicated.

This phenomenon is even better visualized by looking at the change if composition in time (Figure 2.7). It is immediately obvious that the fraction of BMDO in the feed is increasing over time whereas the fraction of MMA decreases. The composition drift information allows in principle for assessment of reactivity ratios. To simplify the procedure, we have, however, opted to calculate the *r* values (following the terminal model)[21-22] from the monomer feed and polymer composition as determined from NMR (see spectrum described above).[5, 14, 16, 23-25] Thereby, r_1 and r_2 are determined from fitting the Mayo-Lewis equation

(Equation 2.1) to the monomer feed (f_{MMA} and f_{BMDO}) *vs.* copolymer composition data (F_{MMA}) obtained from polymerizations at different feed concentrations.

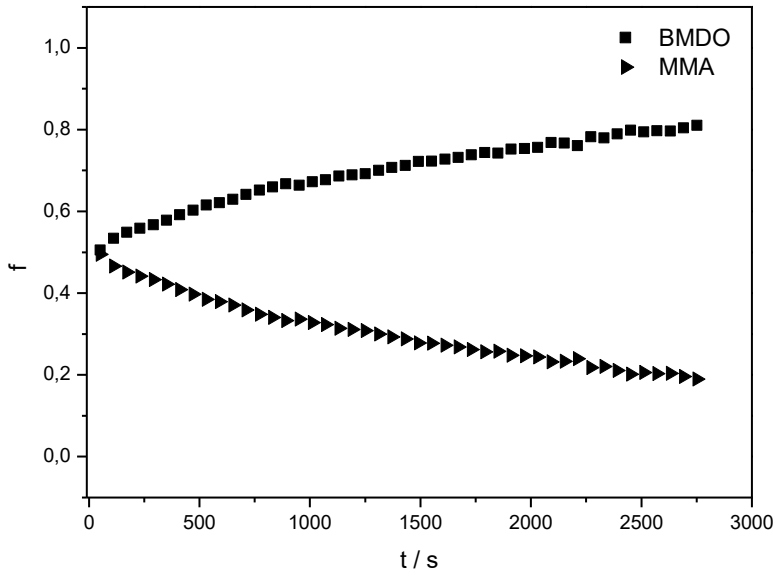

Figure 2.7 evolution of the composition with time for a sample containing a 0.5:0.5 starting composition.

Equation 2.1

$$F_{MMA} = \frac{r_2 f_{MMA}^2 + f_{MMA} f_{BMDO}}{r_2 f_{MMA}^2 + 2 f_{MMA} f_{BMDO} + r_1 f_{BMDO}^2}$$

Generally, using the terminal model is not without problems. Often, this model allows for a good representation of copolymer composition data, but yields erroneous results when trying to predict kinetic coefficients. To describe composition and kinetics concomitantly, the explicit penultimate model should be used. Since the aim in this study was, however, to only analyze (and predict) copolymer compositions, the simpler model was applied.

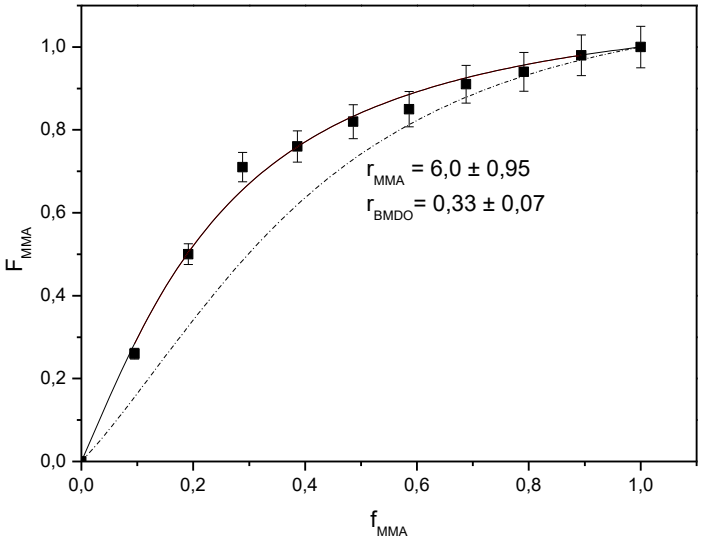

Figure 2.8 Polymer composition as a function of comonomer feed composition for copolymerizations of BMDO and MMA. The monomer feed concentration ratio is given by *f* (with respect to MMA) and the copolymer composition ratio is given by *F* (with respect to MMA). The curve displays the best fit of the data to the Mayo-Lewis equation (Equation 1). The error bars are based on experiment errors whereas the error values for the r-values are based on the fit only. The dashed line represents a simulated curved based on the reactivity ratios obtained via the Skeist equation.

Using the data from the experiments given in Table 2.1 the so-called Mayo-Lewis plot can be constructed as is shown in Figure 2.8. In this graph the feed composition is plotted versus the composition in the polymer, all with respect to MMA. To calculate the composition of the formed polymer, ^{1}H-NMR spectra were measured for all polymer samples (as exemplified in Figure 2.4). By integration of the MMA characteristic peaks (3H, 3.4-3.6 ppm) and of BMDO typical ones (2H, 4.9-5.1 ppm), the composition is directly obtained. In an ideal situation where both monomers are equally reactive, a straight line would be observed in the Mayo-Lewis plot. Any deviation from this ideal behavior (either positive or

negative) directly indicates different reactivities for either of the monomers. Due to the composition drift that is associated with such behavior, significantly higher amounts of one monomer (here BMDO) will be built in at higher conversions, and erroneous reactivity ratios would in such case inevitably be obtained.

From the data in Figure 2.8, the reactivity ratios are determined by fitting the data to Equation 2.1. This results in a reactivity ratio for BMDO of r_1 = 0.33 ± 0.07 and r_2 = 6.0 ± 0.98 for MMA, respectively, which nicely fits with the expected range for the reactivity ratios ($r_1 << 1 << r_2$).

Using alternative evaluation methods, for example by fitting an integrated version of the Mayo-Lewis equation (so called Skeist-equation, Equation 2.2) to the composition drift data shown in Figure 2.6, yields comparable values, even though with some deviation.

Equation 2.2

$$1 - \frac{M}{M_0} = 1 - \left[\frac{f_1}{f_{1,0}}\right]^{\alpha} \left[\frac{f_2}{f_{2,0}}\right]^{\beta} \left[\frac{f_{1,0} - \delta}{f_1 - \delta}\right]^{\gamma}$$

$$\alpha = \frac{r_2}{1 - r_2}, \beta = \frac{r_1}{1 - r_1}, \gamma = \frac{1 - r_1 r_2}{(1 - r_1)(1 - r_2)}, \delta = \frac{1 - r_2}{2 - r_1 - r_2}$$

We opted herein, however, for the fitting procedure as given in Figure 2.8 since this approach is statistically more robust on the basis of the available data. Even though a copolymerization with such vastly different reactivity ratios would normally be considered to be very unideal, good materials with respect to (bio)degradability can still be obtained. For degradation, high amounts of polyester units are not required since a high molecular weight BMDO/MMA copolymer can still decompose into smaller fractions of oligo-MMA. In fact, to retain good material properties it may even be desirable to maintain low polyester contents.

As noted above, Wickel et al. had earlier already attempted to determine the reactivity ratios for BMDO and MMA, with the main difference being that the polymerizations were performed under ATRP conditions.[16]

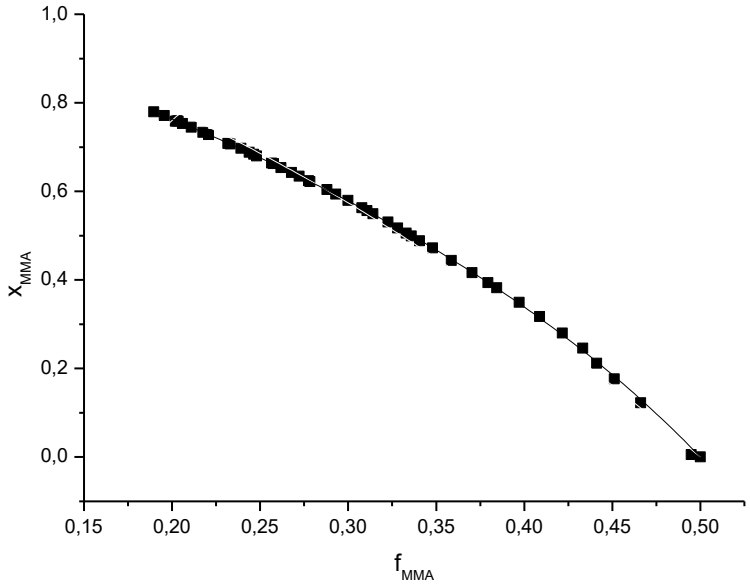

Figure 2.9 Evaluation of the concentration data given in Figure 2.6 via the Skeist method resulting in r_1 = 0.7 and r_2 = 3.88.

In this paper, the Kelen-Tüdõs method was used to linearize the Mayo-Lewis equation, which yielded a reactivity ratios r_1 = 0.51 and r_2 = 1.96. These values differ quite significantly from the values determined herein. Even though it cannot be excluded, the ATRP mechanism should not have too much influence on the reactivity ratios – assuming that the activation/deactivation equilibrium state is similar for both macroradical termini. However, as discussed above, conversion has a large influence on the result. Although Wickel et al. did not report any numbers for monomer conversion, it is expected that polymers with high or at

least considerable conversion were used. Thus, in fact copolymers with a composition gradient were obtained and F_{BMDO} was overestimated, leading to increased r_1 and decreased r_2 exactly as is observed in here. Another important factor to consider is the difference in temperature: in the work by Wickel et al. the polymerization is performed at T=120°C whereas a polymerization of T=90°C is used in this study. Since temperature has a significant influence at the polymerization rate at can lead to very different reactivity ratios.

2.3.3 Synthesis of (co)polymers of BMDO and MMA under RAFT polymerization conditions.

After the analysis of the uncontrolled radical copolymerization of BMDO/MMA, we proceeded to the synthetic aim of the study and thus to employ RAFT polymerization for production of well-defined BMDO copolymers with defined molecular weight. For what follows, we assume that the copolymerization parameters as determined above are also valid in the RAFT polymerization. After some initial tests with several available RAFT-agent structures, the trithiocarbonate methyl-2-(((octylthio)-carbonothioyl)thio)propanoate (RA-1) has proven to be the most efficient RAFT agent for the preparation of copolymers with decent polydispersities. Reasonable control is achieved and a clear shift of molecular weight distributions is seen with increasing monomer conversion (see 2.10). Interestingly, the employed RAFT agent is not suited for MMA homopolymerization and a certain amount of BMDO is required to achieve low polydispersities. Thus, it can be concluded that the BMDO termini interact well in the RAFT equilibrium and feature favorable kinetics.

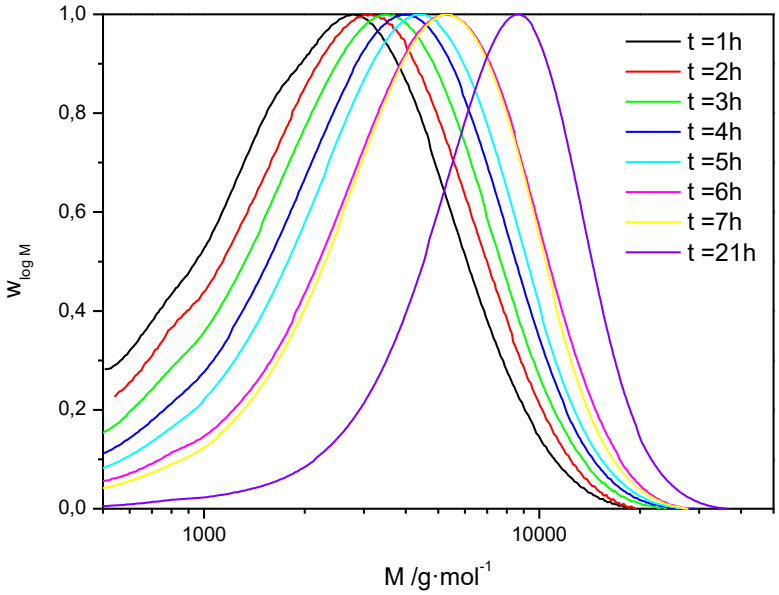

Figure 2.10 Evolution of molecular weight distributions with time for a RAFT copolymerization of BMDO and MMA (conditions: DCP:RA-1:BMDO:MMA 0.1:1:50:50 at T=100°C). Samples were taken after given time intervals and the molecular weight was determined by SEC in THF using pMMA Mark-Houwink parameters.

The molecular weight distributions display initially small low-molecular weight tailing, which disappears with proceeding polymerization. Also, it should be noted that the molecular weight distributions are cut off on the low molecular weight side. BMDO (or its degradation product, respectively) can after reaction not be fully removed from the product, hence always a small molecular weight fraction is left in the elugrams. For BMDO:MMA:RA-1 = 1:1:0.01 in anisole and a polymerization temperature of 110 °C, a shift of number average molecular weights from M_n = 1.8 x10^3 g·mol^{-1} after 1 hour to M_n = 5.8 x10^3 g·mol^{-1} after 21 hours is observed. Dispersities of all samples remained below 1.5, which for a CKA copolymerization may be regarded as satisfactory. Equal amounts of BMDO

and MMA are used in the polymerization, thus around 80 % of MMA is expected to be found in the copolymer (see Figure 2.8), whereby the BMDO content should continuously increase with proceeding polymerization.

2.3.4 Degradation test of poly(MMA-*r*-BMDO)

To test whether the obtained polymers indeed display the expected degradation behavior, the polymer was dissolved in a minimal amount of THF and was mixed with 5 ml of 1M NaOH solution. The result of the degradation experiment is shown in Figure 2.11).

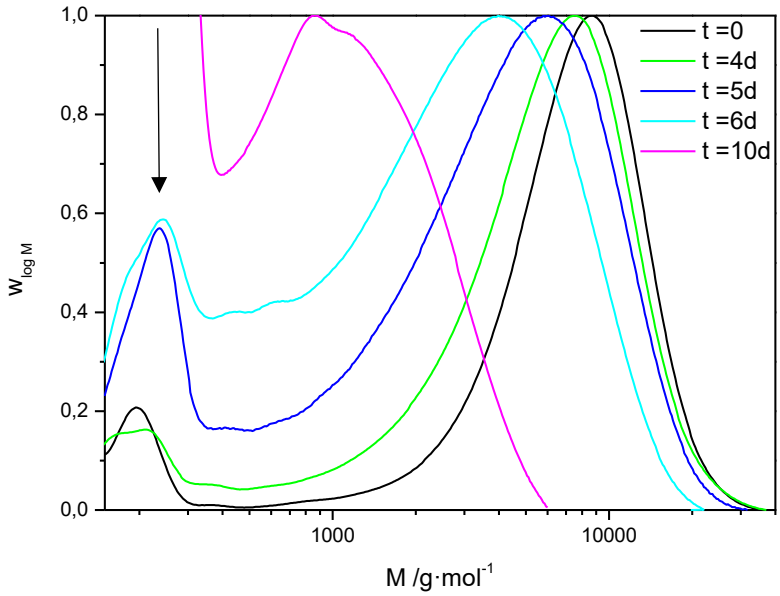

Figure 2.11 Evolution of molecular weight distributions for the degradation of the BMDO/MMA copolymer prepared via the RAFT polymerization technique.

Degradation of these polymers does not happen at a fast rate, as even after several days, polymer distributions are clearly observable. As poly(MMA-*r*-BMDO) is not water soluble, no fast degradation should be expected since only the outer sphere of the polymer aggregates in the resulting dispersion are in contact with

the base. However, a clear continuous shift is observed from high to low molecular weight, indicating that the material breaks down over time into smaller segments.

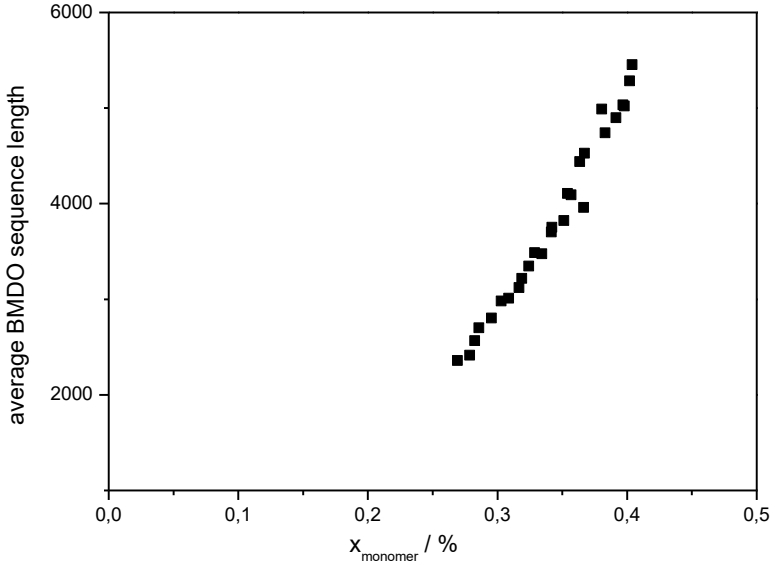

Figure 2.12 average BMDO sequence length versus total monomer conversion (x_{mon}).

Apart from the decrease in overall molecular weight, another interesting observation is the increase in a small molecular weight peak (indicated by the arrow in the figure), which can most likely be attributed to degradation product of BMDO segments or to additional de-esterification of the methyl esters. Experiments were stopped after 10 days when sufficient breakdown of material was observed. It should, however, be noted that further decrease in molecular weight could be achieved at longer degradation times.

2.3.5 4-arm star synthesis of poly(MMA-*r*-BMDO) via RAFT polymerization

The above degradation experiments proved that the synthesis of RAFT polymers from BMDO/MMA mixtures was successful. To increase complexity, we thus

proceeded to the original goal of the study, the synthesis of RAFT star polymers. Star polymers find applications in many areas due to their unique properties with respect to hydrodynamic radius and viscosity. Among other, star polymers are interesting materials for drug delivery purposes, an area where (bio) degradability of the materials could display a large additional value.

Using the above conditions from the linear RAFT synthesis, an attempt was made to synthesize well-defined four-arm star copolymers. For the synthesis of star polymers using RAFT, two approaches may in principle be chosen: the Z- and R-star synthesis approach. The difference lies in how the individual arms grow: with the R-star approach the chains grow from a central core and the controlling RAFT end-group is always located at the end of each arm. In the Z-star approach, the core connects the trithiocarbonate moieties via the stabilizing Z-group and growth of the chains occurs in solution while being detached from the core. Thus, formation of linear polymer is a possible side reaction. While linear polymers may not significantly occur in the R-approach, this specific methodology might lead to star-star coupling. Nevertheless, both approaches have been shown to yield satisfactory star polymers.[26] Because star coupling has usually a much higher impact on material properties than presence of small amounts of linear material that can be more easily removed, the Z-star approach was in here favored (see Figure 2.13 for the structure of the control agent). To reach this aim, a tetra-functional trithiocarbonate was synthesized according to the procedure as published by Boschmann et al.[27] (see Figure 2.13).

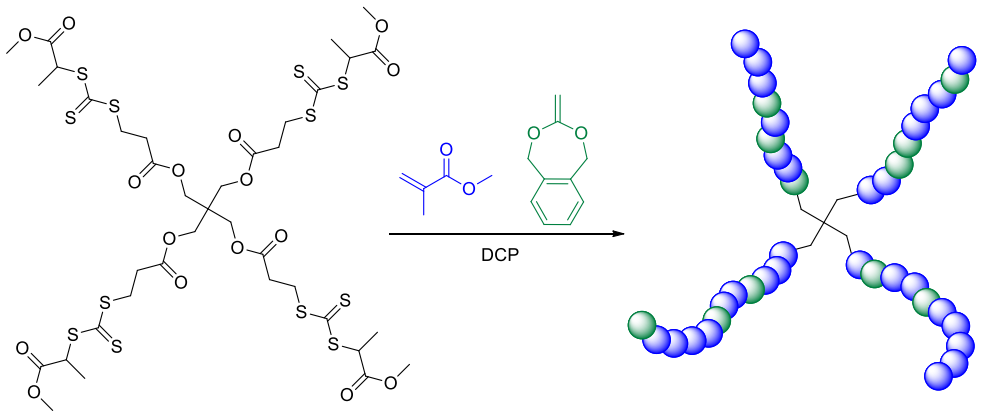

Figure 2.13 Reaction scheme for the copolymerization of BMDO and MMA using the four-arm functional RAFT-agent RA-4.

The conditions from the linear polymerization could be directly implemented without the need for extensive re-optimization. The only difference between the linear and the star polymerization was a four times higher concentration of initiator due to the fact that the chain can polymerize at four sites per RAFT core molecule. The RAFT:initiator ratio was thus kept constant and also the polymerization temperature remained unchanged (T = 100°C). Also, a steady increase in molecular weight is observed with increasing reaction time and monomer conversion. The evolution of molecular weight distributions is shown in Figure 2.14. Initially, the polymerization rate is slightly lowered and a shoulder is seen in the distribution taken at 2 h reaction time stemming from the initial RAFT-agent. This indicates that the polymerization has not yet fully left the pre-equilibrium phase and not all arms have started chain growth.

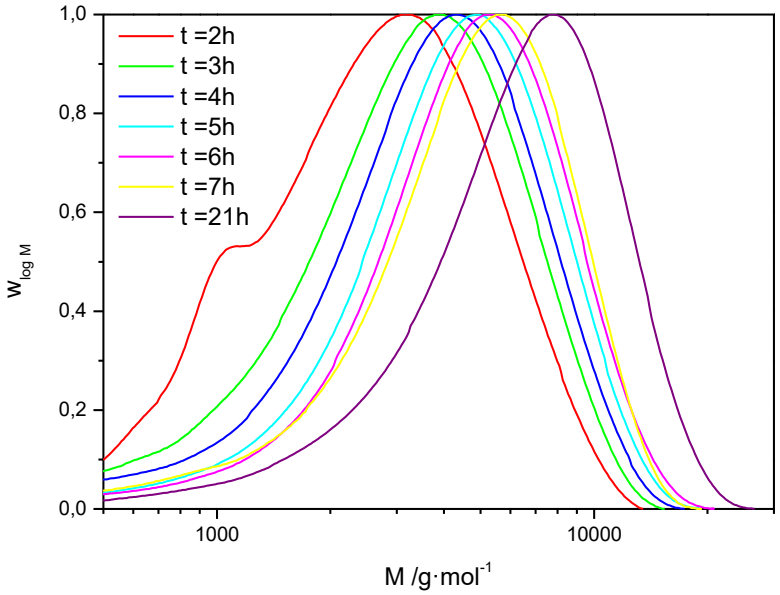

Figure 2.14 Evolution of molecular weight distributions with time for the RAFT star-copolymerization of BMDO and MMA (conditions: [DCP]:[RA-4]:[BMDO]:[MMA] 0.25:1:50:50 at T=100°C). Samples were taken after given time intervals and the molecular weight was determined by SEC in THF based on pMMA Mark-Houwink parameters.

After this initial delay, the polymerization speeds up and proceeds even faster than its linear analogue, which may be explained by the overall higher initiator concentration in this polymerization. In terms of molecular weights, a deviation is observed in comparison with the linear analogue. Star polymers are associated with significantly smaller hydrodynamic radii when compared to their linear counterparts at same molecular weight. Radke et al. determined a factor of 1.42 to apply to results obtained from linear standard calibration SEC to correct for these changes.[28] In Figure 2.15, the evolution of M_n (for the star polymers

corrected by the factor of 1.42) is given for both linear and star copolymers of BMDO/MMA.

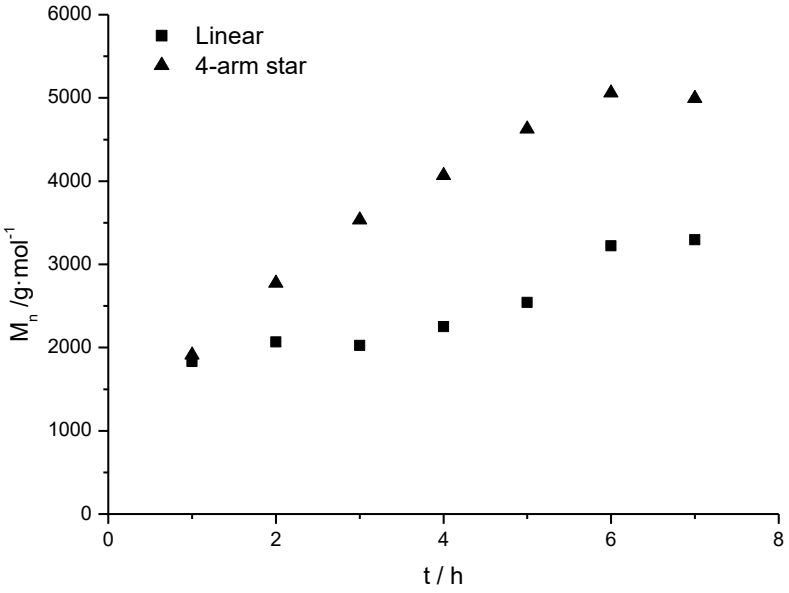

Figure 2.15 Number average molecular weight as a function of time in the linear RAFT copolymerization compared to the 4-arm star synthesis. Squares mark M_n from the linear polymerization, triangles denote star polymers.

For both polymerizations, a steady increase in molecular weight is observed with time, whereby the fast growth of the star RAFT polymer is observed, which is again easily explained by the four times higher overall trithiocarbonate concentration in case of the star polymerization.

Like with the linear polymer, also here it was checked whether a polyester copolymer was formed via a degradation experiment. The result from such test (under equal conditions compared to the linear counterpart, see Figure 2.11) is shown in Figure 2.15. The low molecular weight peak present in all samples stems

from hydrolyzed BMDO. Over time, additional peaks are observed stemming from degradation products formed through degradation of the copolymer.

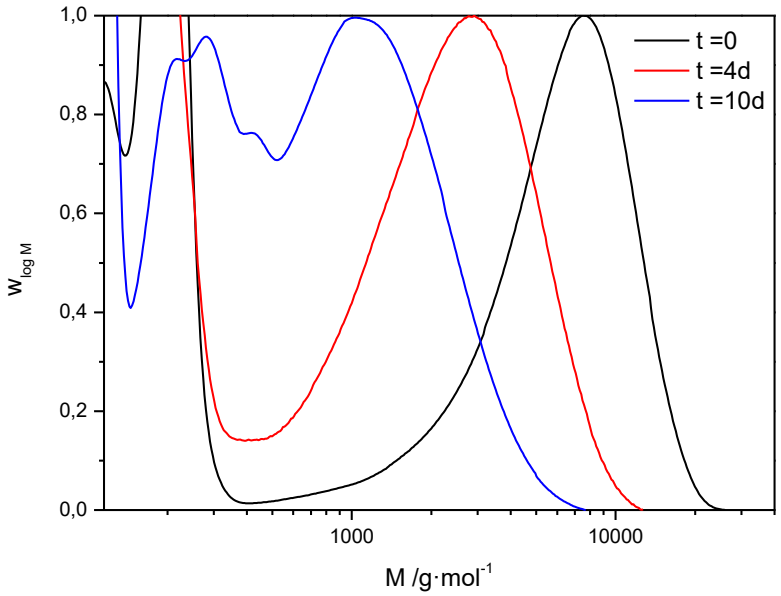

Figure 2.17 Molecular weight distributions for the degradation of the RAFT-star copolymers of BMDO and MMA in 1 molar aqueous NaOH.

At first, the degradation seems to occur faster as compared to the linear polymer, since a significant shift is observed after already four days, a timespan where only little change had been observed for the linear chains. However, since the core of the RAFT agent is erythritol based, also at this point ester hydrolysis may occur. It may thus be postulated that first the core is degraded, which is followed by main chain degradation. In fact, when comparing the (topology corrected) peak molecular weights, then a decrease from initial 10 900 g·mol^{-1} to 2700 g·mol^{-1} (without star topology correction) after the fourth day is observed, which is in very good agreement to this hypothesis. It should hereby be noted though that not the erythritol core part itself must be necessarily degraded first. Due to the

composition drift, more BMDO will be found close to the core compared to the corona of the star. Thus, cleavage of the arms could also happen via BMDO-ester degradation close to the core. Regardless, only after longer times further backbone degradation is then observed and after ten days, polymer segments of similar size as in the linear copolymers are found. Such double-degradation behavior is highly interesting as it may allow for example in drug delivery applications to work with two individual degradation speeds and thus release rates. However, at this point it must be noted that the above described mechanism is a pure hypothesis and further experiments would be required to proof its validity.

2.4 Conclusion

Copolymerization of a CKA, namely BMDO, with methyl methacrylate, is a viable pathway to obtain polymers that consist primarily of methacrylate units and thus resemble the physical properties of the methacrylate, but that are at the same time degradable via hydrolysis of main chain polyester bonds formed in radical ring opening polymerization steps. BMDO shows disparate copolymerization behavior with MMA. r_1 = 0.33 ± 0.06 and r_2 = 6.0 ± 0.8 have been determined from polymer samples taken at low BMDO conversion and a polymerization temperature of 110 °C via fitting of the Lewis-Mayo equation to the copolymer composition data. Copolymerization of the two monomers is successful also in RAFT polymerization employing a trithiocarbonate control agent. Preliminary degradation experiments show that the polymer degrades slowly, but steadily in aqueous 1 M NaOH dispersion and after ten days, the polymers are broken down to segments of roughly 1000 g·mol^{-1}. Similar results are obtained for four-arm star polymers, likewise obtained via the RAFT polymerization mechanism following the Z-group approach with an erythritol-based tetra-functional RAFT agent. Star polymerization proceeds efficiently and copolymers are readily obtained. Degradation proceeds on a similar time scale as for the linear copolymer counterparts, however, an initial fast breakdown of material is observed, which may be attributed to faster hydrolysis of the star core.

2.5 References

1. Bailey, W. J.; Chen, P. Y.; Chiao, W.-B.; Endo, T.; Sidney, L.; Yamamoto, N.; Yamazaki, N.; Yonezawa, K., Free-Radical Ring-Opening Polymerization. In *Contemporary Topics in Polymer Science: Volume 3*, Shen, M., Ed. Springer US: Boston, MA, 1979; pp 29-53.
2. Albertsson, A.-C.; Varma, I., Aliphatic Polyesters: Synthesis, Properties and Applications. In *Degradable Aliphatic Polyesters*, Springer Berlin Heidelberg: 2002; Vol. 157, pp 1-40.
3. Höcker, H.; Keul, H., Ring-Opening Polymerization and ring-closing depolymerization. *Advanced Materials* **1994,** *6* (1), 21-36.
4. Agarwal, S., Chemistry, chances and limitations of the radical ring-opening polymerization of cyclic ketene acetals for the synthesis of degradable polyesters. *Polymer Chemistry* **2010,** *1* (7), 953-964.
5. Tardy, A.; Delplace, V.; Siri, D.; Lefay, C.; Harrisson, S.; de Fatima Albergaria Pereira, B.; Charles, L.; Gigmes, D.; Nicolas, J.; Guillaneuf, Y., Scope and Limitations of the Nitroxide-Mediated Radical Ring Opening Polymerization of Cyclic Ketene Acetals. *Polymer Chemistry* **2013**.
6. Undin, J.; Finne-Wistrand, A.; Albertsson, A.-C., Copolymerization of 2-Methylene-1,3-dioxepane and Glycidyl Methacrylate, a Well-Defined and Efficient Process for Achieving Functionalized Polyesters for Covalent Binding of Bioactive Molecules. *Biomacromolecules* **2013,** *14* (6), 2095-2102.
7. Siebert, J. M.; Baumann, D.; Zeller, A.; Mailänder, V.; Landfester, K., Synthesis of Polyester Nanoparticles in Miniemulsion Obtained by Radical Ring-Opening of BMDO and Their Potential as Biodegradable Drug Carriers. *Macromolecular Bioscience* **2012,** *12* (2), 165-175.
8. Moad, G.; Rizzardo, E.; Thang, S. H., Living Radical Polymerization by the RAFT Process. *Australian Journal of Chemistry* **2005,** *58* (6), 379-410.
9. Matyjaszewski, K.; Xia, J., Atom Transfer Radical Polymerization. *Chemical Reviews* **2001,** *101* (9), 2921-2990.
10. Nicolas, J.; Guillaneuf, Y.; Lefay, C.; Bertin, D.; Gigmes, D.; Charleux, B., Nitroxide-mediated polymerization. *Progress in Polymer Science* **2013,** *38* (1), 63-235.
11. Okada, M., Chemical syntheses of biodegradable polymers. *Progress in Polymer Science* **2002,** *27* (1), 87-133.
12. Barner-Kowollik, C.; Junkers, T., Kinetic and mechanistic similarities between reversible addition fragmentation chain transfer intermediate and acrylate midchain radicals. *Journal of Polymer Science Part A: Polymer Chemistry* **2011,** *49* (5), 1293-1297.
13. Matyjaszewski, K.; Davis, T. P., Future Outlook and Perspectives. In *Handbook of Radical Polymerization*, John Wiley & Sons, Inc.: 2002; pp 895-900.

14. Delplace, V.; Tardy, A.; Harrisson, S.; Mura, S.; Gigmes, D.; Guillaneuf, Y.; Nicolas, J., Degradable and Comb-Like PEG-Based Copolymers by Nitroxide-Mediated Radical Ring-Opening Polymerization. *Biomacromolecules* **2013,** *14* (10), 3769-3779.
15. Delplace, V.; Harrisson, S.; Tardy, A.; Gigmes, D.; Guillaneuf, Y.; Nicolas, J., Nitroxide-Mediated Radical Ring-Opening Copolymerization: Chain-End Investigation and Block Copolymer Synthesis. *Macromolecular Rapid Communications* **2014,** *35* (4), 484-491.
16. Wickel, H.; Agarwal, S.; Greiner, A., Homopolymers and Random Copolymers of 5,6-Benzo-2-methylene-1,3-dioxepane and Methyl Methacrylate: Structural Characterization Using 1D and 2D NMR. *Macromolecules* **2003,** *36* (7), 2397-2403.
17. He, T.; Zou, Y.-F.; Pan, C.-Y., Controlled/“Living” Radical Ring-Opening Polymerization of 5,6-Benzo-2-Methylene-1,3-Dioxepane Based on Reversible Addition-Fragmentation Chain Transfer Mechanism. *Polymer Journal* **2002,** *34* (3), 138-138.
18. Wickel, H.; Agarwal, S., Synthesis and Characterization of Copolymers of 5,6-Benzo-2-methylene-1,3-dioxepane and Styrene. *Macromolecules* **2003,** *36* (16), 6152-6159.
19. Agarwal, S.; Kumar, R.; Kissel, T.; Reul, R., Synthesis of Degradable Materials Based on Caprolactone and Vinyl Acetate Units Using Radical Chemistry. *Polym. J* **2009,** *41* (8), 650-660.
20. Bailey, W. J.; Ni, Z.; Wu, S. R., Free radical ring-opening polymerization of 4,7-dimethyl-2-methylene-1,3-dioxepane and 5,6-benzo-2-methylene-1,3-dioxepane. *Macromolecules* **1982,** *15* (3), 711-714.
21. Fukuda, T.; Kubo, K.; Ma, Y.-D., Kinetics of free radical copolymerization. *Progress in Polymer Science* **1992,** *17* (5), 875-916.
22. Coote, M. L.; Davis, T. P., The mechanism of the propagation step in free-radical copolymerisation. *Progress in Polymer Science* **1999,** *24* (9), 1217-1251.
23. Agarwal, S., Radical Ring Opening and Vinyl Copolymerization of 2,3,4,5,6-pentafluorostyrene with 5,6-Benzo-2-methylene-1,3-dioxepane: Synthesis and Structural Characterization Using 1D and 2D NMR Techniques. *Journal of Polymer Research* **2006,** *13* (5), 403-412.
24. Undin, J.; Illanes, T.; Finne-Wistrand, A.; Albertsson, A.-C., Random introduction of degradable linkages into functional vinyl polymers by radical ring-opening polymerization, tailored for soft tissue engineering. *Polym. Chem.* **2012,** *3* (5), 1260-1266.
25. Huang, J.; Gil, R.; Matyjaszewski, K., Synthesis and characterization of copolymers of 5,6-benzo-2-methylene-1,3-dioxepane and n-butyl acrylate. *Polymer* **2005,** *46* (25), 11698-11706.

26. Chaffey-Millar, H.; Stenzel, M. H.; Davis, T. P.; Coote, M. L.; Barner-Kowollik, C., Design Criteria for Star Polymer Formation Processes via Living Free Radical Polymerization. *Macromolecules* **2006,** *39* (19), 6406-6419.
27. Boschmann, D.; Edam, R.; Schoenmakers, P. J.; Vana, P., Z-RAFT star polymerization of styrene: Comprehensive characterization using size-exclusion chromatography. *Polymer* **2008,** *49* (24), 5199-5208.
28. Gerber, J.; Radke, W.; Wittmann, G., Simulation of GPC-Distribution Coefficients of Linear and Star-Shaped Molecules in Spherical Pores: Comparison of Simulation and Experiment. *International Journal of Polymer Analysis and Characterization* **2004,** *9* (1-3), 39-52.

Chapter 3

Copolymerization evaluation of 2-methylene-4-phenyl-1,3-dioxolane and various vinyl monomers.

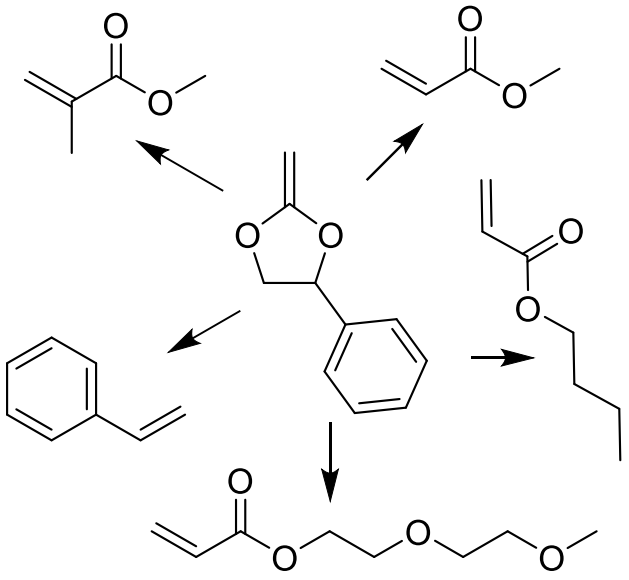

3.1 Abstract

Free radical copolymerization of 2-methylene-4-phenyl-1,3-dioxolane (MPDL) is studied in the presence of several comonomers with regards to the reactivity ratios. An optimized approach is developed by combining the Skeist-formula with online IR experiments. By using this method, it is possible to determine reactivity ratios for any given combination of monomers within a day. In this report this was shown for MPDL in combination with common monomers such as methyl methacrylate (MMA), butyl acrylate (BA), styrene and diethylene glycol monomethylether acrylate (DEGA) by comparing literature values (if present) with the calculated values. In all cases the values are in the following range $r_{MPDL} < 1 < r_{mon}$ leading to a mixture of homopolymers and copolymers. This research was taken a step further by introducing the RAFT-method in order to control the molecular weight and aim for optimal polymer design. Hence, copolymers of MPDL and styrene, MMA, BA, and N-isopropyl acrylamide (NiPAM) are successfully prepared showing low molecular weights in combination with decent polydispersities between 1 and 1.5. Further research on the BA and MPDL system also showed that control was maintained (and even improved) with different feed ratios.

3.2 Introduction

In recent years, (bio)degradation of polymers is becoming increasingly popular owing to the development of more environmentally friendly materials but also thanks to major developments in the biomedical field. Especially for the latter case, it is off the upmost importance to be able to control the size, composition and architecture of polymers. Thanks to the extensive research in the field of controlled polymerization techniques such as RAFT[1], NMP[2] and ATRP[3] we are already able to control size and architecture.

With respect to degradability, polyesters have proven to be a suitable candidate with polymers such as *poly*(lactic acid) or *poly*lactones. However, due to the way they are commonly prepared - via either polycondensation or via anionic or enzymatic ring-opening polymerization - it is impossible to combine these materials with traditional vinyl polymers like polystyrene or poly(methyl methacrylate). With the discovery and development of radical ring-opening polymerization (RROP) of cyclic ketene acetals (CKAs) in the early 1980s this was now possible[4-7]. Since its discovery, several combinations of CKAs and monomers have been explored but only in the last couple of years has more research started to focus on studying the behavior of the copolymerization.[8-14] An important parameter for these studies are the so-called reactivity ratios defined as follows:

$$r_1 = \frac{k_{p,1-1}}{k_{p,1-2}} \text{ and } r_2 = \frac{k_{p,2-2}}{k_{p,2-1}}$$

Where $k_{p,1\text{-}1}$ and $k_{p,2\text{-}2}$ denote the respective homopropagation rate coefficients and $k_{p,1\text{-}2}$ and $k_{p,2\text{-}1}$ denote the crosspropagation rate coefficients. In literature various methods can be found to determine these parameters. In essence, there

are two ways to evaluate the copolymerization behavior by looking at either the terminal end or the combination of the terminal and penultimate atom on a growing chain. In both cases evaluation happens on the composition of the feed/copolymer and the kinetics of the copolymerization.[15-18] In addition, conversion plays an important role, whereby composition drift – the change in feed composition with conversion due to different reactivities of the respective monomers - can lead to erroneous values for reactivity ratios. While both methods are in theory the same, in practice the terminal model is preferred owing to the elaborate calculations and modelling involved in determining reactivity ratios. Thus, even though the penultimate model typically yield parameters with higher accuracy, the terminal model is much more suitable for screening different systems in a short amount of time. Aiming for low monomer conversions should make sure that the effect of composition drift is circumvented.

Most available methods using the terminal model are derived from the Mayo-Lewis equation (Equation 3.1), which describes the relation between the feed composition *f* and the copolymer composition *F*:[19]

Equation 3.1

$$F_2 = \frac{r_2 f_2^{\,2} + f_2 f_1}{r_2 f_2^{\,2} + 2 f_2 f_1 + r_1 f_1^{\,2}}$$

The simplest method is a direct fit of the Mayo-Lewis equation to data obtained by screening mixtures of the desired monomers in different ratios and examining the composition of the formed copolymer with i.e. ^{1}H-NMR or FT-IR. From the obtained data, the reactivity ratios can be determined by fitting the Mayo-Lewis equation where the ratios's are given as fit parameters. This method was already explained in detail in Chapter 2.[8]

Besides, the direct fitting of the Mayo-Lewis equation the data can be rearranged in several ways to facilitate linearization of the Mayo-Lewis equation whereby the values can be determined graphically. This was first reported by Fineman and Ross[20] who defined the parameters G and H based on the values for *f* and *F* to rearrange the Mayo-Lewis equation to the following form:

Equation 3.2

$G = Hr_1 - r_2$ with $G = \frac{f_1(2F_1-1)}{(1-f_1)F_1}$ and $H = \left[\frac{{f_1}^2(1-F_1)}{(1-f_1)^2F_1}\right]$

The reactivity ratios can be easily determined by plotting composition data and performing a linear fit. The slope of the fit will then give r_1 and the intersection with the x-axis has the value $-r_2$. However, Kelen and Tudos discovered that this model is biased towards very high and low conversions leading to erroneous values. The suggested an adapted version of the Fineman-Ross method by introducing a factor averaging the difference between the highest and lowest values for *F*. This lead to a redefined version of the Fineman-Ross equation:

Equation 3.3

$\eta = \left[r_1 + \frac{r_2}{\alpha}\right]\mu - \frac{r_2}{\alpha}$ with $\eta = \frac{G}{\alpha+H}$, $\mu = \frac{H}{\alpha+H}$ and $\alpha = \sqrt{H_{min}H_{max}}$

The values can be found through the slope and x-axis intersection of a linear fit of the modified Fineman-Ross equation. The Kelen-Tudos is by far the most popular method of determining reactivity ratios in the field of RROP. Several papers have already been published in this area with various combinations of CKAs and vinyl monomers.[12-14, 21-26] For the majority of calculations the reactivity ratios for both the CKAs as well as comonomers belong to the same range with the value

for CKAs being below 1 while the comonomers typically give a value for *r* well above 1.

The problem with all these methods however is that in order to calculate the reactivity ratios, several experiments need to be performed in parallel while making sure that conversion are kept low. Since the information about copolymers in RROP is limited studying the copolymerization behavior is always a necessity. It would be very beneficial if this could be performed in a limited amount of time which allows for easier and faster screening. In this chapter, an optimized method is explained and tested building on the existing Skeist equation:

Equation 3.4

$$1-\frac{M}{M_0}=1-\left[\frac{f_1}{f_{1,0}}\right]^{\alpha}\left[\frac{f_2}{f_{2,0}}\right]^{\beta}\left[\frac{f_{1,0}-\delta}{f_1-\delta}\right]^{\gamma} \quad \text{with } \alpha=\frac{r_2}{1-r_2},\ \beta=\frac{r_1}{1-r_1},\ \gamma=\frac{1-r_1r_2}{(1-r_1)(1-r_2)},\ \delta=\frac{1-r_2}{2-r_1-r_2}$$

In chapter 2, we already described the use of this method to calculate reactivity ratios and showed that this can be performed in a single experiment. In this chapter this method is further expanded to the copolymerization of the CKA 2-methylene-4-phenyl-1,3-dioxolane (MPDL) with several common monomers. Based on this data, a first attempt is made to use RAFT polymerization to synthesize copolymers with defined composition and size.

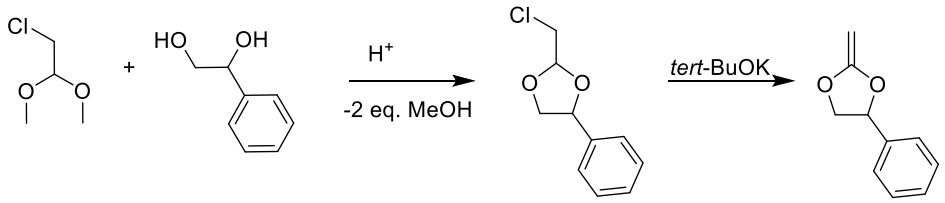

Figure 3.1 schematic representation for the synthesis of 2-methylene-4-phenyl-1,3-dioxolane (MPDL).

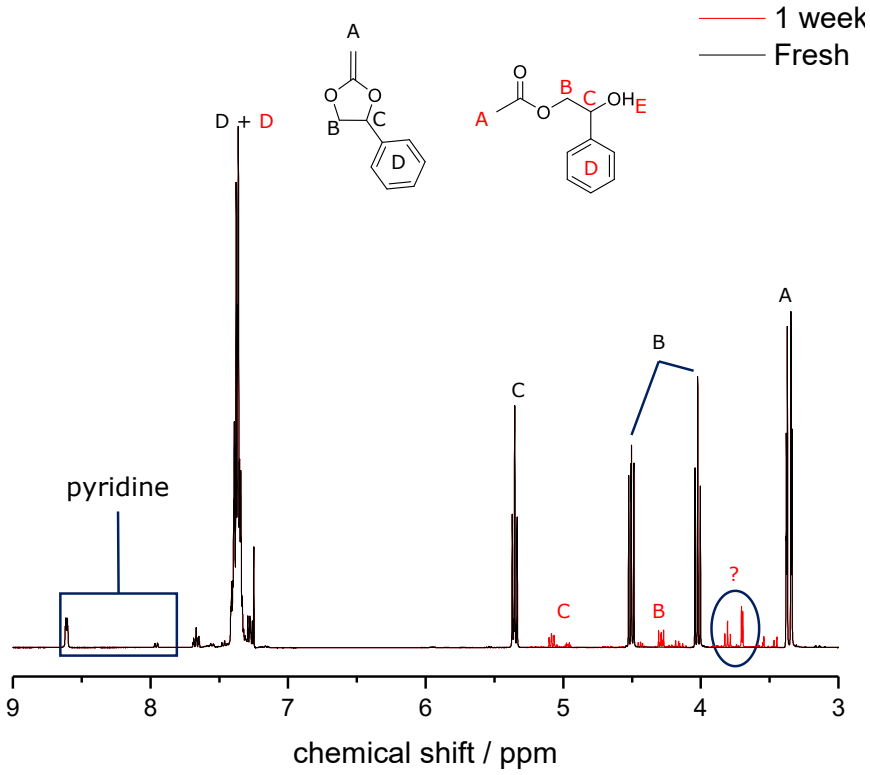

Figure 3.2 ^{1}H-NMR spectrum for 2-methylene-4-phenyl-1,3-dioxolane both freshly distilled (shown in black) as well as after standing for standing for 1 week (shown in red) (measure in deuterated chloroform). The peaks are assigned according to the structures shown in the insert; MPDL in black letters and hydrolysis product in red letters.

3.3 Results and discussion

In this chapter, the results regarding the copolymer of MPDL with various comonomers will be discussed starting with the synthesis of MPDL.

3.3.1 Synthesis of 2-methylene-4-phenyl-1,3-dioxolane (MDPL)

For the synthesis of MPDL, a slightly adapted literature procedure was used which is described in detail in paragraph 6.3.[27] A scheme for the synthesis is also given Figure 3.1.

Like with any CKA synthesis, it is a two-step procedure consisting of transacetalization followed by a dehydrohalogenation. While the transacetalization is straightforward, the dehydrohalogenation gives rise to some issues regarding degradation of the product. This can either happen by hydrolysis (as was seen with BMDO in Chapter 2) or by autopolymerization through the presence of cations. This can be prevented by adding a small amount of dry pyridine as a cation scavenger, though small portions of hydrolysis still occur as is shown in Figure 3.2. In this figure the ^{1}H-NMR (measured in deuterated chloroform) for freshly distilled MPDL is compared with a sample that has been left standing for a week in the freezer (at -18°C). It nicely shows the presence of MPDL. In addition, protons B give a split up due to the position of the protons caused by a shielding effect of the phenyl ring. Also note that even though a small amount (5 wt%) of dry pyridine is added, it can be observed in the spectrum as signals between 8 and 9 ppm.

When the freshly distilled MPDL was left undisturbed in a regular glass vial in the freezer a small amount of degradation through hydrolysis is observed (red graph in Figure 3.2). The same mechanism is at play which was already discussed under

Paragraph 2.3.1. Several peaks stemming from the hydrolyzed MPDL (left structure in Figure 3.2) are observed. Note that protons A for the right structure are not shown in the figure but are observed as signal at 2.1 ppm. While it may concern an impurity of only a few percent it can have a significant influence on the kinetics of the polymerization and therefore MPDL was distilled prior to use.

3.3.2 Copolymer evaluation of MPDL and selected comonomers under free-radical conditions

As already mentioned in the introduction, MPDL has only recently become more attractive as a CKA for the synthesis of degradable polymers but detailed studies in the copolymerization behavior under free-radical conditions are lacking. The aim is to screen several monomers from different classes to get an idea of which class would be compatible and suitable for further application. In this thesis it was already shown that using online IR measurements and the Mayo-Lewis equation one could construct the *f* vs. *F* plot and calculate the reactivity ratios. However, this method requires separate experiments for each composition and conversion needs to be kept low systematically. A better and more efficient alternative can be found in the Skeist-equation which is an integrated from of the Mayo_lewis equation. It was already shown in Paragraph 2.3 that both methods gave comparable values for the reactivity ratios that fit in the expected range ($r_{mon} < 1 < r_{CKA}$). An advantage of using the Skeist equation is the ability to perform the necessary reaction in a single experiment, significantly reducing the effort.

As mentioned before, the idea is to use this method for screening different monomer (classes). Therefore, five monomers were selected based on availability, popularity in RROP research and on the known literature on reactivity ratios in RROP. Based on these criteria, methyl methacrylate (MMA), methyl acrylate (MA),

n-butyl acrylate (BA) diethylene glycol ethylether acrylate (DEGA) and styrene were selected.

In order to perform the experiment, a more optimized procedure was applied as was described under Paragraph 2.3.2. Rather than mixing all components prior to degassing, here only the two monomers were mixed with a small amount of toluene. The initiator was dissolved in toluene in a separate vial. Both mixtures were degassed separately. First the monomer mixture was transferred to the reaction flask. The mixture was left to heat-up to reaction temperature T=100°C and was left to stir until a stable IR-signal was observed which was in practice around 15 minutes. The reaction is started by adding the initiator mixture to the reaction flask. Several IR-spectra were recorded after different time-steps, which are combined in Figure 3.3.

This graph shows a representative result for the copolymerization of MPDL and MMA with a molar feed ratio of 1:1. Only the section between 1700 and 1620 cm^{-1} is given, showing the signals for the stretch vibration for carbon-carbon double bonds for MPDL (left) and MMA (right). The signal for the stretch vibration of other vinylic monomers is typically located at the same wavenumber as MMA. For both MPDL and MMA a decline in peak height is observed over time. After 365 minutes almost of all MMA appears to be consumed while MPDL is still present. This behavior matches the behavior observed in Paragraph 2.3.2 for BMDO and MMA. This already gives an indication that the reactivity ratios are possibly on the expected range.

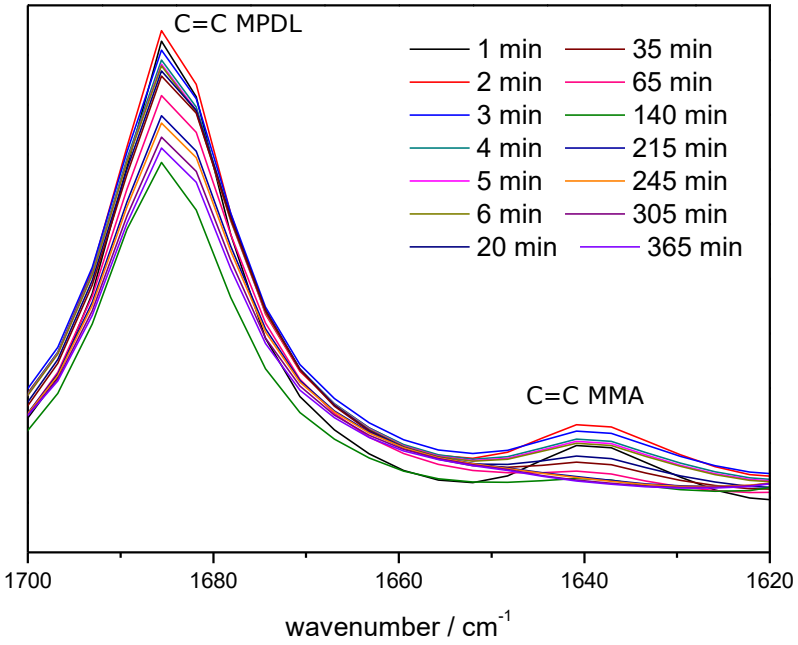

Figure 3.3 overlay of time resolved IR-spectra for the copolymerization of MPDL and MMA ranging from 1 minute to 365 minutes reaction time. The different vibrations are given in the graph.

By using the peak area as a measure for the conversion, the concentration for each monomer can be calculated individually for each point in time. Dividing the concentration of MPDL by the concentration of MMA and plotting it against the reaction time gives an indication of the more reactive monomer. This result is shown in Figure 3.4.

In case of an equal reactivity, the concentration remains constant with a value of 1 in case of a 1:1 molar feed ratio. Any deviation from this behavior indicates a superior reactivity for one of the monomers. This is exactly the behavior as observed in Figure 3.4. Herein, for the all aforementioned monomers the time resolved change in concentration ratio is shown and for all monomers an increase

is observed. Meaning that for all cases more monomer is consumed w.r.t. MPDL which in turn means that a higher reactivity for these monomers is to be expected. An interesting observation is that this effect appears to be more pronounced for certain monomers than for others. The smallest increase is observed for BA while MMA seems to have the highest increase

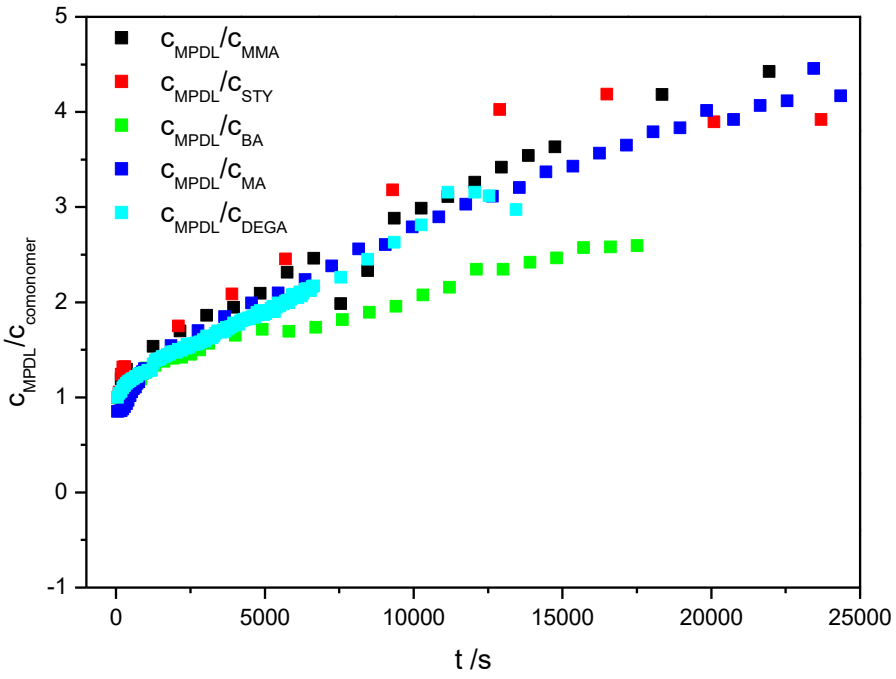

Figure 3.4 overlay for the change in the ratio of MPDL over the concentration for different monomers. These results are obtained from the IR spectra as shown in Figure 3.3 by integration of the shown peaks.

To calculate the composition at any given moment, the amount of MPDL is divided by the total amount of monomer at each specific moment. This data is then plotted against the total monomer conversion to construct the Skeist-plot as shown in Figure 3.5.

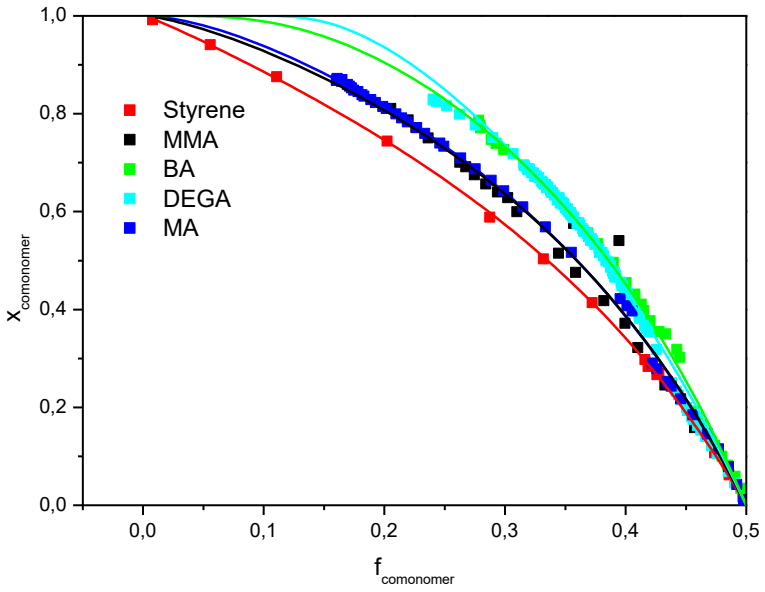

Figure 3.5 overlay for the monomer fraction in the feed ($f_{monomer}$) versus the total monomer conversion ($x_{comonomer}$) indicated by the square dots. The solid lines represent the fit for the Skeist equation (Equation 3.4) for the respective monomers. The calculated reactivity ratios (r) are given in Table 3.1.

Table 3.1 summary of the results for the determination of reactivity ratios for MPDL and various comonomers. The copolymer composition (F_{mon}) was determined using ^{1}H-NMR in $CDCl_3$. The comonomer conversion (x_{comon}) was determined by IR and were calculated after 8 hours reaction time. The values for the reactivity ratios r were calculated by fitting the Skeist equation (Equation 3.4) to the data in Figure 3.5.

CKA	monomer	f_{mon}	F_{mon}	X_{comon}	r_{MPDL}	r_{mon}
MPDL	Styrene	0,5	0,951	0,99	0,54 ± 0,12	3,31 ± 0,79
MPDL	MMA	0,5	0,772	0,81	0,59 ± 0,13	2,78 ± 0,68
MPDL	MA	0,5	0,785	0,87	0,65 ± 0,14	2,96 ± 0,71
MPDL	DEGA	0,5	0,898	0,82	1,31 ± 0,29	4,13 ± 0,99
MPDL	BA	0,5	0,815	0,79	0,89 ± 0,20	2,89 ± 0,69

This graph shows the dependence of the total monomer conversion ($x_{comonomer}$) on the fraction of specified monomer ($f_{comonomer}$) for styrene (red squares), MMA (black squares), BA (green squares), DEGA (light blue squares) and MA (dark blue squares). It nicely shows different behavior in regards to the copolymerization with MPDL of the different monomers. In the ideal case, where the reactivity ratios both have a value of 1, the ratio would have a constant value. However, any deviation would show as a curvature towards the side of the more reactive monomer. For all the monomers shown in Figure 3.5 the composition of the monomer is decreasing with increasing conversion. This confirms the already observed behavior that more monomer is consumed then MPDL, leading to the expectation that the reactivity ratios for all monomers will be higher than that of MPDL. Based on this data, the Skeist-equation is fitted (solid lines in Figure 3.5) whereby the reactivity ratios can be derived. These values are tabulated in Table 3.1. Besides the reactivity ratios, this table also shows the copolymer composition (F_{mon}) calculated by ^{1}H-NMR (in $CDCl_3$) and monomer conversion (x_{mon}) determined by IR. Please note that, due to the high monomer conversion, the reported copolymer compositions are cumulative. The starting point for all reactions was always a feed ratio of 1:1 for MPDL w.r.t. the specified monomer and all reactions were terminated after 8 hours.

Looking at the copolymer composition after 8 hours, there's significant difference among the selected monomers. In the case of styrene, a copolymer composition of 0.95 is reached while in the case of MA the copolymer only contains 0.75 of MA. Another interesting observation is that already after 8 hours most monomers have already been consumed for 80% or more with the extreme again being styrene with close to 100% of conversion. These values combined again indicate

a significant difference in reactivity for MPDL and comonomers. The calculated values for reactivity ratios confirm this indication as in all cases (with the exception of DEGA) the values for r_{MPDL} are smaller than 1 while for r_{mon} the values exceed 1 by a significant amount. In the case of MA, BA, MMA and styrene this leads to a mixture of homopolymers and copolymers with random structure due to the increased consumption monomer of the respective in the initial minutes of the polymerization, moreover the bigger the difference in *r*, the greater the fraction of homopolymer in the mixture.

This however does not directly apply to DEGA which is somewhat of an outlier for the aforementioned trend where r_{MPDL} is above 1 and the value for r_{DEGA} is above 4. While there is no direct explanation on hand it might have something to do with the polarity of DEGA and its polymer in comparison with the other monomers. The polymer of DEGA shows significantly higher hydrophilic behavior than all other polymers in this study. This can slightly reduce the solubility of the polymer in apolar solvents such as anisole in this case and it also is capable of repelling the more hydrophobic MPDL leading to a change in reactivity where DEGA is more prone to reacting with itself and MPDL also preferring to react with itself. This leads to a random copolymer with alternating longer segments of DEGA and shorter segments of MPDL. A repeat of this experiment gave similar results though the reactivity for MPDL was closer to 1 (r=1.11).

In conclusion, a novel fast method was introduced to calculate reactivity ratios for different comonomer systems. The results show that these values are in accordance with earlier mentioned ratios for BMDO/MMA in this thesis and with values found in literature. The follow-up will mainly focus on exploring the limits

of this method and ideally to set-up a database for reactivity ratios for all most-used CKA/monomer systems.

3.3.3 Exploring the RAFT-copolymerization of MPDL and several comonomers

The next step to exploring the possibilities of MPDL is to test the compatibility with polymerization under RAFT conditions. It was already shown in this thesis that RAFT can be helpful to control the molecular weight of copolymers of BMDO and MMA. A similar study on the (co)polymerization of MPDL was not yet reported in literature. However, by the group of J. Nicolas *et al.* the successful synthesis of different copolymers of MPDL and various monomers with defined molecular weight and composition was shown by using nitroxide mediated polymerization (NMP).[27-31] The choice of using RAFT instead of ATRP or NMP is that it is fairly straightforward to implement to an already existing procedure for free radical polymerization without the need for an elaborate optimization. Simply adding a suitable RAFT-agent and reducing the amount of initiator should be sufficient.

To show this easy implementation, the conditions from Paragraph 3.2.2 were directly used. Practically this means that MPDL was reacted at T=100°C with MMA, styrene, BA and NiPAM in the presence of the RAFT-agent RA-1 (synthesis in paragraph 6.2) and dicumyl peroxide in the following molar ratios; MPDL:Mon:RA-1:DCP, 25:25:1:0.1. A small amount (20 vol%) of toluene is added to avoid high viscosities. In Table 3.2 the copolymer composition, apparent molecular weights (Mn and Mw based on PS standards) and polydispersities are given.

According to the calculated values for the reactivity ratios, the resulting polymer should contain an increased amount of comonomer w.r.t MPDL. This trend is

reflected in the values for F_{mon} as calculated by ^{1}H-NMR (in $CDCl_3$). With the exception of styrene, all values are in a similar range as the values for free-radical polymerization.

Table 3.2 summary of result for the copolymerization of MPDL and different comonomers under RAFT-conditions; MPDL:Mon:RAFT:DCP 25:25:1:0.1. The copolymer composition (F_{mon}) was determined by ^{1}H-NMR in $CDCl_3$ and the M_n, M_w and Đ were determined by GPC in THF (apparent values based on PS standards)

CKA	monomer	f_{mon}	F_{mon}	M_n /10^3 g·mol^{-1}	M_W /10^3 g·mol^{-1}	Đ
MPDL	BA	0,5	0,79	2.92	4.33	1.48
MPDL	MMA	0,5	0,84	3.37	5.76	1.71
MPDL	styrene	0,5	0,78	2.26	2.72	1.20

A significant deviation with styrene is observed in comparison to the data reported in Table 3.1 (F_{mon} = 0.95 in table 3.1 w.r.t F_{mon} = 0.78 in table 3.2). The value in table 3.1 is considered too high to be valid.

A good indication for controlled behavior is the polydispersity (*Đ*), which typically has a value in the range 1 ≤ Đ ≤ 1.5 for controlled polymerization techniques. Although the values for MMA and NiPAM exceed this range, controlled behavior might still be at play.

In order to further proof the controlled behavior, the combination of BA and MPDL was further explored by looking at the effect of different feed ratios on the molecular weight of polymer. This result is given in Table 3.3.

We have already seen that in the case of BMDO and MMA (Paragraph 2.3.3) increasing amounts of MMA in the feed give polymers with a higher molecular weight. This was ascribed to the very different kinetics of the two monomers with

MMA being much faster the BMDO. A similar trend is expected for MPDL and BA as well. Looking at the data in Table 3.3, it is immediately obvious that this trend is indeed present with the molecular weight increasing going from 25 to 100% of BA in the feed.

Table 3.3 overview of results for the RAFT copolymerization of MPDL and BA under different feed compositions. The copolymer composition was determined by ^{1}H-NMR in $CDCl_3$ and the M_n, M_w and $Đ$ were determined by GPC in THF.

f_{BA}	F_{BA}	M_n / 10^3 g·mol^{-1}	M_W /·10^3 g·mol^{-1}	$Đ$
0	0	3,84	6,56	1,71
0,25	0,60	2,09	3,36	1,60
0,5	0,79	2,93	4,33	1,48
0,75	0,94	3,99	5,38	1,35
1	1	6,08	7,34	1,21

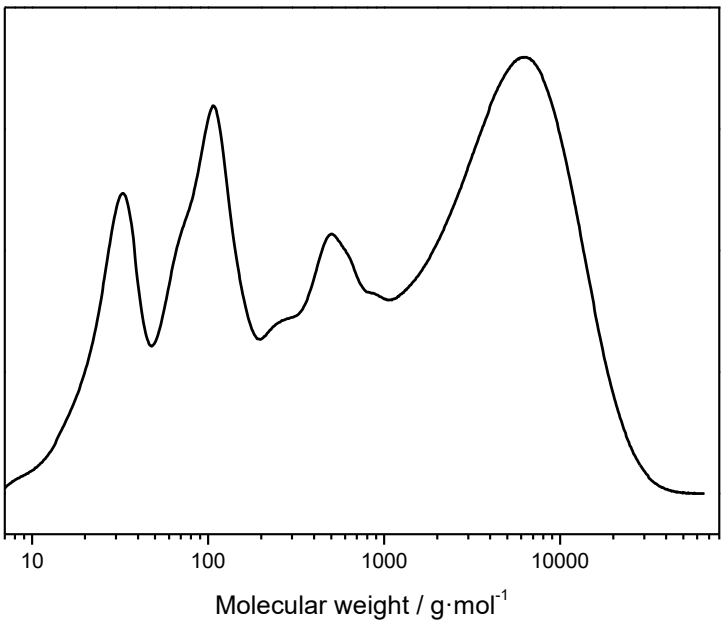

Figure 3.6 Full GPC trace for *poly(*phenyl butyrolactone) with $DP_{n,theo}$ = 50.

Another interesting factor is the decrease in polydispersity in the same range due to the fact the trithiocarbonate RAFT-agent is highly compatible with BA. This means that the more BA present the bigger the contribution of BA to the RAFT-equilibrium. While it is not said that the polymerization of MPDL is uncontrolled, one must note that a large amount of low molecular weight sideproducts occurred during the RAFT-homopolymerization of MPDL (as seen in Figure 3.6). Since these sideproducts are not as pronounced in the copolymerization of MPDL with BA, it is thought BA assists in suppressing the side reactions and improving control greatly.

Another way to show this controlled behavior is to check whether polymers with different degrees of polymerization (*DP*) can be achieved. For MPDL and BA, with a starting feed ratio of 1:1, polymers with a theoretical DP of 10, 20, 50, 100 and 200 were prepared. An overlay for the molecular weight distribution (MWD) for these polymers is shown in Figure 3.7.

This overlay shows a nice shift to higher molecular weight with increasing degree of polymerization. Please note that at lower DP the GPC chromatogram is cut-off due to an overlap with residual monomer and a small amount of hydrolyzed MPDL. To prove that BA was actually assisting in controlling the polymerization, the same test was performed on MPDL homopolymerization, which showed no shift in molecular weight upon increasing the degree of polymerization. This further proves that MPDL by itself has limited compatibility with RA-1 RAFT-agent while adding BA drastically improves the control over polymerization. Overall, we've shown that RAFT is a suitable method to produce copolymers with defined molecular weight and composition consisting of MPDL and several comonomers.

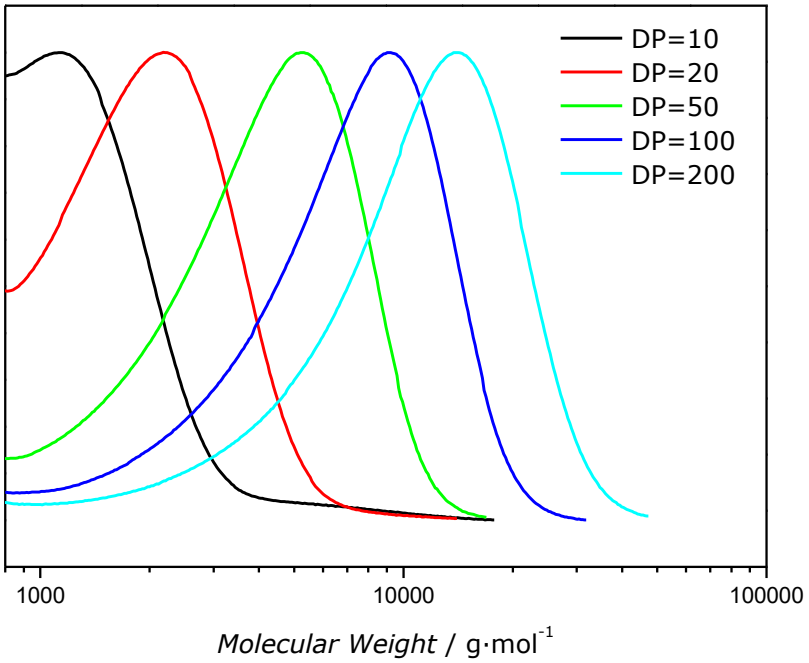

Figure 3.7 Evolution of molecular weight distributions with theoretical degree of polymerization (*DP*) for a RAFT copolymerization of MPDL and BA. The degree of polymerization was predetermined by changing the concentration of RAFT-agent and DCP w.r.t. the monomer concentration (which was kept constant). All reactions were polymerized at T=100°C for 24 hours. The molecular weights were determined by GPC in THF.

3.4 Conclusion and outlook

In this chapter, an optimized method was introduced to calculate reactivity ratios for basically any system by using a combination of online IR-measurements with the Skeist-method. This was given by the successful calculations of the reactivity ratios for MPDL and several common comonomers which proved to be nicely in range of what was already reported or expected.

Based on these results, a first attempt was made to introduce RAFT as a method for the controlled synthesis of polymers with defined molecular weights and composition. Several monomers were tested and the case of BA with MPDL was analyzed in more detail, proving the controlled behavior during the copolymerization by showing that polymers with different DP can be prepared.

While some optimization is still necessary, especially in the area of reproducibility, this versatile fast model can be easily implemented into an existing system. Further research should focus on setting-up a library/database for different combinations of CKAs and monomers.

3.5 References

1. Moad, G.; Rizzardo, E.; Thang, S. H., Living Radical Polymerization by the RAFT Process. *Australian Journal of Chemistry* **2005,** *58* (6), 379-410.
2. Nicolas, J.; Guillaneuf, Y.; Lefay, C.; Bertin, D.; Gigmes, D.; Charleux, B., Nitroxide-mediated polymerization. *Progress in Polymer Science* **2013,** *38* (1), 63-235.
3. Matyjaszewski, K., Atom Transfer Radical Polymerization (ATRP): Current Status and Future Perspectives. *Macromolecules* **2012,** *45* (10), 4015-4039.
4. Bailey, W. J.; Chen, P. Y.; Chiao, W.-B.; Endo, T.; Sidney, L.; Yamamoto, N.; Yamazaki, N.; Yonezawa, K., Free-Radical Ring-Opening Polymerization. In *Contemporary Topics in Polymer Science: Volume 3*, Shen, M., Ed. Springer US: Boston, MA, 1979; pp 29-53.
5. Bailey, W. J.; Ni, Z.; Wu, S.-R., Synthesis of poly-ϵ-caprolactone via a free radical mechanism. Free radical ring-opening polymerization of 2-methylene-1,3-dioxepane. *Journal of Polymer Science: Polymer Chemistry Edition* **1982,** *20* (11), 3021-3030.
6. Bailey, W. J.; Ni, Z.; Wu, S. R., Free radical ring-opening polymerization of 4,7-dimethyl-2-methylene-1,3-dioxepane and 5,6-benzo-2-methylene-1,3-dioxepane. *Macromolecules* **1982,** *15* (3), 711-714.
7. Bailey, W. J.; Wu, S.-R.; Ni, Z., Synthesis and free radical ring-opening polymerization of 2-methylene-4-phenyl-1,3-dioxolane. *Die Makromolekulare Chemie* **1982,** *183* (8), 1913-1920.
8. Kobben, S.; Ethirajan, A.; Junkers, T., Synthesis of degradable poly(methyl methacrylate) star polymers via RAFT copolymerization with cyclic ketene acetals. *Journal of Polymer Science Part A: Polymer Chemistry* **2014,** *52* (11), 1633-1641.
9. Maji, S.; Zheng, M.; Agarwal, S., Functional Degradable Polymers via Radical Ring-Opening Polymerization and Click Chemistry. *Macromolecular Chemistry and Physics* **2011,** *212* (23), 2573-2582.
10. Agarwal, S., Chemistry, chances and limitations of the radical ring-opening polymerization of cyclic ketene acetals for the synthesis of degradable polyesters. *Polymer Chemistry* **2010,** *1* (7), 953-964.
11. Agarwal, S., Microstructural characterisation and properties evaluation of poly (methyl methacrylate-co-ester)s. *Polymer Journal* **2007,** *39* (2), 163-174.
12. Agarwal, S., Radical Ring Opening and Vinyl Copolymerization of 2,3,4,5,6-pentafluorostyrene with 5,6-Benzo-2-methylene-1,3-dioxepane: Synthesis and Structural Characterization Using 1D and 2D NMR Techniques. *Journal of Polymer Research* **2006,** *13* (5), 403-412.
13. Wickel, H.; Agarwal, S.; Greiner, A., Homopolymers and Random Copolymers of 5,6-Benzo-2-methylene-1,3-dioxepane and Methyl Methacrylate:

Structural Characterization Using 1D and 2D NMR. *Macromolecules* **2003,** *36* (7), 2397-2403.
14. Wickel, H.; Agarwal, S., Synthesis and Characterization of Copolymers of 5,6-Benzo-2-methylene-1,3-dioxepane and Styrene. *Macromolecules* **2003,** *36* (16), 6152-6159.
15. Deb, P. C., Determination of penultimate model reactivity ratios and their non-uniqueness. *Polymer* **2007,** *48* (2), 432-436.
16. Ono, K.; Teramachi, S., Penultimate Unit Effects in Free-Radical Copolymerization. Number-Average Degree of Polymerization and Copolymerization Rate in Styrene/Methyl Methacrylate/Toluene System. *Polym J* **1995,** *27* (8), 790-796.
17. Schweer, J., Penultimate model description of the propagation kinetics for the free radical copolymerization of styrene and methyl methacrylate. *Macromolecular Theory and Simulations* **1993,** *2* (3), 485-502.
18. Roberts, G. E.; Coote, M. L.; Heuts, J. P. A.; Morris, L. M.; Davis, T. P., Radical Ring-Opening Copolymerization of 2-Methylene-1,3-Dioxepane and Methyl Methacrylate: Experiments Originally Designed To Probe the Origin of the Penultimate Unit Effect. *Macromolecules* **1999,** *32* (5), 1332-1340.
19. Mayo, F. R.; Lewis, F. M., Copolymerization. I. A Basis for Comparing the Behavior of Monomers in Copolymerization; The Copolymerization of Styrene and Methyl Methacrylate. *Journal of the American Chemical Society* **1944,** *66* (9), 1594-1601.
20. Fineman, M.; Ross, S. D., Linear method for determining monomer reactivity ratios in copolymerization. *Journal of Polymer Science* **1950,** *5* (2), 259-262.
21. Huang, J.; Gil, R.; Matyjaszewski, K., Synthesis and characterization of copolymers of 5,6-benzo-2-methylene-1,3-dioxepane and n-butyl acrylate. *Polymer* **2005,** *46* (25), 11698-11706.
22. Ren, L.; Agarwal, S., Synthesis, characterization, and properties evaluation of poly[(N-isopropylacrylamide)-co-ester]s. *Macromol. Chem. Phys.* **2007,** *208* (3), 245-253.
23. Zhang, Y.; Chu, D.; Zheng, M.; Kissel, T.; Agarwal, S., Biocompatible and degradable poly(2-hydroxyethyl methacrylate) based polymers for biomedical applications. *Polymer Chemistry* **2012,** *3* (10), 2752-2759.
24. Agarwal, S., Microstructural Characterisation and Properties Evaluation of Poly (methyl methacrylate-co-ester)s. *Polym. J* **2006,** *39* (2), 163-174.
25. Agarwal, S.; Kumar, R.; Kissel, T.; Reul, R., Synthesis of Degradable Materials Based on Caprolactone and Vinyl Acetate Units Using Radical Chemistry. *Polym. J* **2009,** *41* (8), 650-660.

26. Shi, Y.; Schmalz, H.; Agarwal, S., Designed enzymatically degradable amphiphilic conetworks by radical ring-opening polymerization. *Polymer Chemistry* **2015,** *6* (35), 6409-6415.
27. Delplace, V.; Guegain, E.; Harrisson, S.; Gigmes, D.; Guillaneuf, Y.; Nicolas, J., A ring to rule them all: a cyclic ketene acetal comonomer controls the nitroxide-mediated polymerization of methacrylates and confers tunable degradability. *Chemical Communications* **2015,** *51* (64), 12847-12850.
28. Delplace, V.; Tardy, A.; Harrisson, S.; Mura, S.; Gigmes, D.; Guillaneuf, Y.; Nicolas, J., Degradable and Comb-Like PEG-Based Copolymers by Nitroxide-Mediated Radical Ring-Opening Polymerization. *Biomacromolecules* **2013,** *14* (10), 3769-3779.
29. Tardy, A.; Delplace, V.; Siri, D.; Lefay, C.; Harrisson, S.; de Fatima Albergaria Pereira, B.; Charles, L.; Gigmes, D.; Nicolas, J.; Guillaneuf, Y., Scope and limitations of the nitroxide-mediated radical ring-opening polymerization of cyclic ketene acetals. *Polymer Chemistry* **2013,** *4* (17), 4776-4787.
30. Delplace, V.; Harrisson, S.; Tardy, A.; Gigmes, D.; Guillaneuf, Y.; Nicolas, J., Nitroxide-Mediated Radical Ring-Opening Copolymerization: Chain-End Investigation and Block Copolymer Synthesis. *Macromolecular Rapid Communications* **2014,** *35* (4), 484-491.
31. Tran, J.; Guegain, E.; Ibrahim, N.; Harrisson, S.; Nicolas, J., Efficient synthesis of 2-methylene-4-phenyl-1,3-dioxolane, a cyclic ketene acetal for controlling the NMP of methyl methacrylate and conferring tunable degradability. *Polym. Chem.* **2016,** *7* (26), 4427-4435.

Chapter 4

The synthesis of functionalized polyesters through a combination of RROP and click chemistry

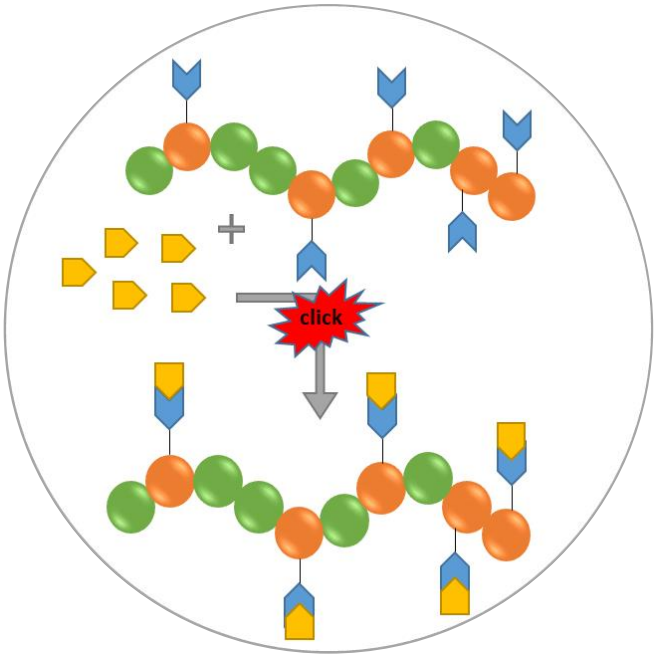

4.1 Abstract

Two approaches for the synthesis of functionalized degradable polyesters were tested. In the first approach, the copolymerization of 2-methylene-1,3-dioxepane (MDO) and propargyl acrylate (trimethylsilyl (TMS) protected) (PATMS) was tested. To prevent any reaction on the alkyne-group, a TMS protecting group was added prior to polymerization. The copolymerization behavior was studied using the online-IR method as described in Chapter 3 leading to the reactivity ratios r_{PATMS}= 1,112 ± 0,01 and r_{MDO} = 0,357 ± 0,004. Based on these results, copolymers of MDO and PATMS with different compositions were prepared. The successful deprotection of the alkyne groups by tetrabutyl ammonium fluoride (TBAF) was confirmed by ^{1}H-NMR. These copolymers were subsequently functionalized by 1-azido-2-(2-methoxyethoxy)ethane (DEGAzide) using the copper catalyzed 1,3-dipolar cycloaddition (CuAAC). The completion of this reaction was evidenced by ATR-IR showing no alkyne or azide related signals and showing the presence of signals related to the triazole formation. In a second approach, a novel way of employing alkyne functionalized CKAs for the preparation of functionalized degradable polymers was researched. To that extent, this alkyne containing CKA had to be designed from scratch. A four-step synthesis pathway was employed to synthesize this CKA. The last step (dehydrohalogenation) probed problematic by the formation of numerous side-products. In addition, purification lead to degradation of the product through hydrolysis leading to more loss of product.

4.2 Introduction

Polymer drug delivery is one of the hot topics of science nowadays with new papers in this area being published every day[1]. As the name already suggests, the idea is to deliver the medication to specific parts of the body where treatment is requirement. Using drug delivery, the efficiency of medicine can be greatly improved due to the lower amounts of required medication. In addition, the side-effects are also reduced owing to the drug only being present where it needs to be. There are numerous different ways to prepare materials for drug delivery purposes involving i.e. the synthesis of amphiphilic polymers for micelle formation[2-4] or the use of biodegradable polymers for nanoparticles synthesis[5-6]. The latter will be the focus in this chapter.

In order to use biodegradable polymers for drug delivery, simply using the bare polymer will not work as they are not accepted into the various biochemical pathways. To facilitate the recognition of the polymer particles into the biochemical systems the bare polymers must undergo post-functionalization. A common way to do this is to use click-chemistry. Introduced and developed by Sharpless, click-chemistry has become an important tool for polymer functionization[7]. The concept consists of several chemical reactions with straightforward reaction conditions reaching full conversion within a reasonable time without the formation of side products. Common reactions include the traditional copper catalyzed azide-alkyne reaction (CuAAC)[8-9] or the more recent thiol-ene[10] and thiol-yne[11-12] reactions. A schematic overview of both reactions is given in Figure 4.1.

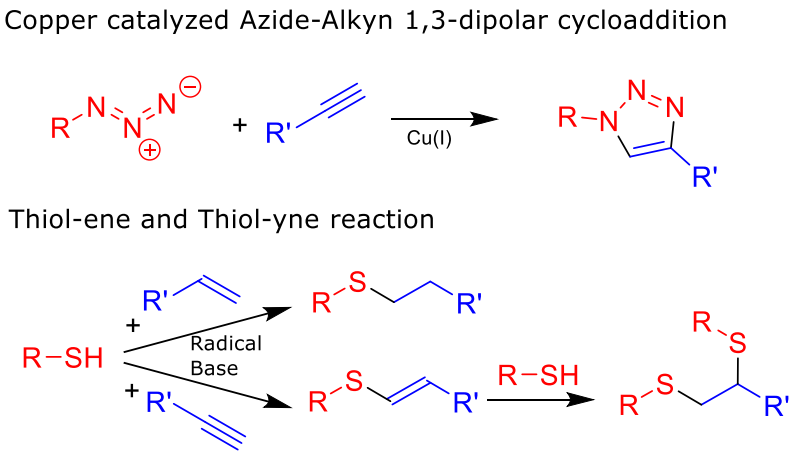

Figure 4.1 Schematic representation of the copper catalyzed azide alkyne 1,3-dipolar cycloaddition (CuAAC) and the thiol-ene and thiol-yne click reactions.

The combination of click-chemistry and radical ring-opening polymerization (RROP) has already been explored in literature[13-16]. Herein, the combination of MDO with propargyl acrylate is explored towards the preparation of functional materials for self-assembly towards micelle formation. It was shown that this combination follows known behavior, whereby the reactivity ratio for the acrylate is greater than 1 and the reactivity ratio for MDO is smaller than 1 (as discussed in Chapter 3). While no values for the reactivity ratios were given, this behavior was observed by analyzing the polymers. Simple CuAAC reactions were performed on these polymers with *poly*ethyleneglycol (PEG) containing azide to yield PEG functionalized polymers which in turn show hydrophilic properties. This work forms the basis of research performed in this chapter.

In extension of the published work, a detailed study on the copolymerization of MDO and trimethylsilyl (TMS)-protected propargyl acrylate (PATMS) is performed. The protecting agent (TMS) was added to the alkyne to prevent unwanted side reactions at the C≡H terminus. After polymerization, the TMS-group can be

cleaved in order to obtain alkyne functionalized degradable copolymers. The idea is to explore different azide containing molecules to prepare for future applications in nanoparticle synthesis and drug delivery.

Aside from this approach, a novel method will be explored for the first time where the alkyne is introduced on a CKA rather than on the acrylate. This kind of study has not yet been performed and allows for the copolymerization of such CKA with any comonomer of choice. The introduction of the alkyne can happen by introducing said group on the diol in CKA formation (Paragraph 1.6.1). The synthesis pathway will be discussed as well as a preliminary study on the copolymerization with butyl acrylate.

4.3 Results and discussion

Two approaches towards degradable polymers with clickable groups in the main chain were tested. In the first approach, the copolymerization of MDO with propargyl acrylate was tested. A second approach is based on a novel way of using an alkyne containing CKA in the copolymerization of MDO.

4.3.1 Click conjugation of *poly*(propargyl acrylate)

To prepare the polymers, the procedure as published by Agarwal et al. was slightly adapted whereby the standard two-step procedure involving a transacetalization and a dehydrohalogenation is used (details can be found in Paragraph 6.4). Based on previous results in this work, a different initiator was selected in dicumyl peroxide (DCP) in combination with a higher polymerization temperature (T=100°C).

Prior to the synthesis of different copolymers, a study on the copolymerization behavior was performed whereby the reactivity ratios are calculated. In a comparative study as mentioned under Paragraph 3.2.2, the change in composition was mapped with increasing conversion. A typical plot can be found in Figure 4.2. which shows the change in conversion of PATMS upon increasing the fraction of PATMS in the feed. The observed trend is in line with results found in earlier studies where the conversion increases at lower feed ratios of PATMS. This behavior already suggests that the reactivity ratios for PATMS will have a value greater than 1,0 while the value for MDO will probably lie below 1,0. To that extent, a fit for the Skeist equation was made to the data leading to values for the reactivity ratios $r_{PropAcr}$ = 1,112 ± 0,27 and r_{MDO} = 0,357 ± 0,09.

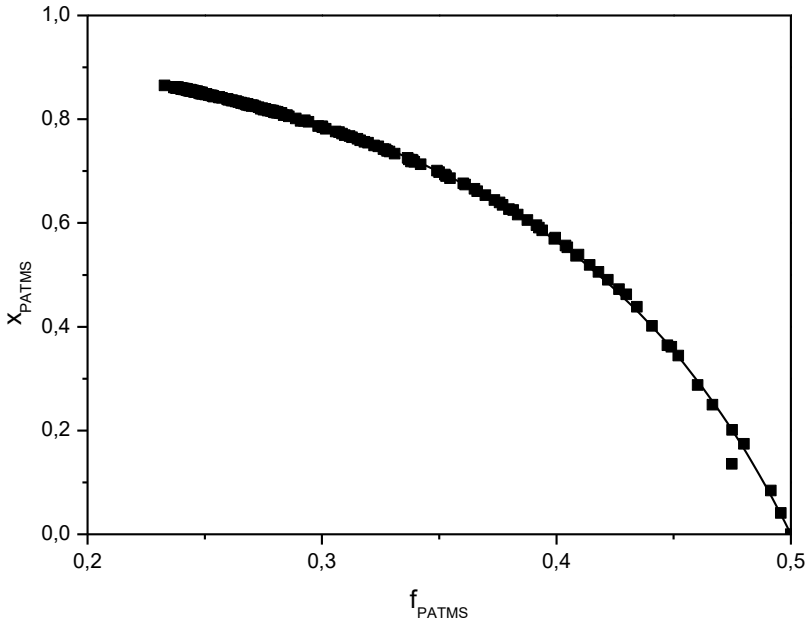

Figure 4.2 Evolution of conversion with the fraction of propargyl acrylate in the copolymerization with MDO. The fit for the Skeist equation (equation 3.4) is given as the solid line resulting in the reactivity $r_{PropAcr}$ = 1,112 ± 0,27 and r_{MDO} = 0,357 ± 0,09.

In comparison to values from previous studies, the value for MDO is in line with those results while on the other hand the value for PATMS is closer to 1,0. This means that the formed polymer is likely to contain more MDO with respect to other similar comonomer systems.

With this in mind, copolymers with varying amounts of MDO and PATMS were prepared. The copolymer composition was determined by using ^{1}H-NMR and the molecular weight was analyzed using THF-GPC. A summary of these results is given in Table 4.1

Table 4.1 Result for the copolymerization of MDO and PATMS with varying feed ratios (*f*). The copolymer composition (*F*) was determined by ^{1}H-NMR in $CDCl_3$ and the molecular weight data was obtained through GPC measurements in THF.

f_{MDO}	f_{PATMS}	F_{MDO}	F_{PATMS}	M_n /10^4 g·mol^{-1}	M_W /10^5 g·mol^{-1}	Đ
0,25	0,75	0,15	0,85	2,38	1,00	4,19
0,5	0,5	0,46	0,54	3,67	0,95	2,59
0,75	0,25	0,54	0,46	2,44	2,41	9,86

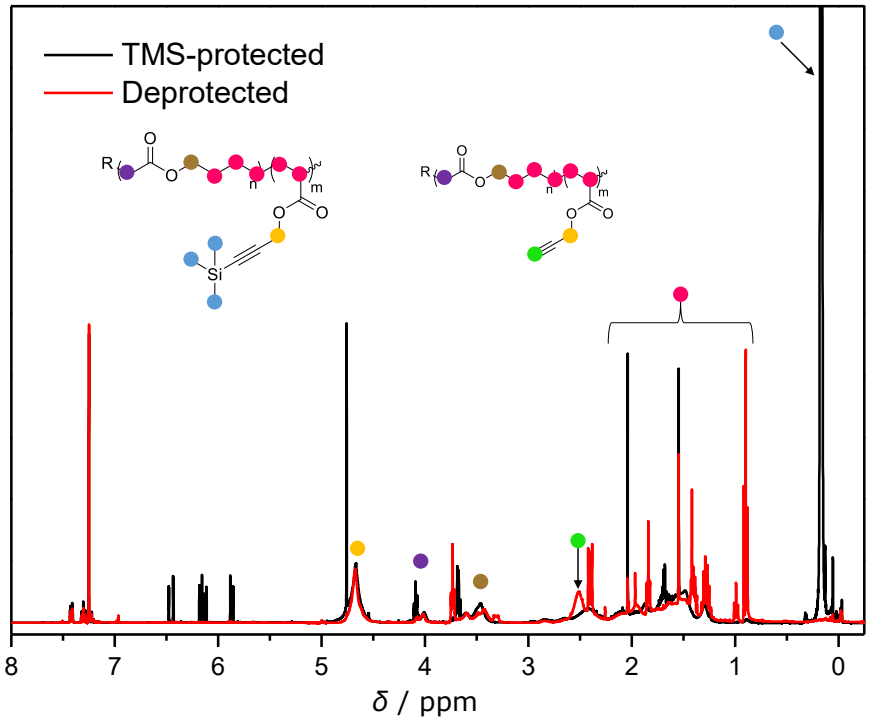

Figure 4.3 Comparison of the ^{1}H-NMR of *poly*(CL-*r*-PropAcr) with a copolymer composition of 85/15 PA/MDO both before (black graph) and after deprotection (red graph) (measured in $CDCl_3$). All relevant peaks are assigned according to the colored labels shown in both given structures.

The data in Table 4.1 shows that the copolymers indeed show increased amounts of build-in PATMS in comparison to the feed. For the molecular weights, the M_n values for all copolymers are in the same range. However, the M_w shows a decent increase going from $1 \cdot 10^5$ g·mol^{-1} at 85% PATMS to $2{,}5 \cdot 10^5$ g·mol^{-1} at 46% PATMS. Consequently, an increase in dispersity was also observed. These values are of course inherent to the free radical process and - although not as pronounced – the effect of increasing Mw with at lower CKA content was also observed in the case of BMDO and MMA as described under Paragraph 2.2.2. Therefore, these polymers are suitable for further modification. To that extent, the copolymers first have to undergo deprotection reaction in order to remove the TMS protecting group. This is done by using a common procedure from literature involving tetrabutylammonium fluoride (TBAF).[17] To confirm the successful deprotection the polymers were analyzed by ^{1}H-NMR in $CDCl_3$, both before and after deprotection. A typical result is shown in Figure 4.3 which shows an overlay for the ^{1}H-NMR for *poly*(PA-*r*-Cl) before (black graph) and after deprotection (red graph). A clear decrease in the signal at 0,1 ppm (blue dot) corresponding to the methyl groups from the TMS protecting group is observed. Simultaneously, a new signal is observed at 2,5 ppm (green dot) corresponding to the C-H proton at the newly formed (deprotected) alkyne. This proves the successful deprotection of the PATMS to form deprotected propargyl acrylate (PA).

The final step towards a functionalized polymer is to attempt the attachment of an azide functionalized diethyleneglycol monomethylether (DEGAzide). This was done by using the CuAAC reaction with conditions as described by Vandenbergh et al.[18] To confirm the successful attachment of DEGAzide to the polymer backbone, attenuated total reflection infrared (ATR-IR) spectroscopy was used.

Due to the low solubility in various organic solvents and the high molecular weight no GPC or ^{1}H-NMR in the liquid state could be recorded. Figure 4.4 shows an overlay for the ATR-IR spectrum for both DEGAzide as well as *poly*(PA-*r*-CL) containing 75% PA.

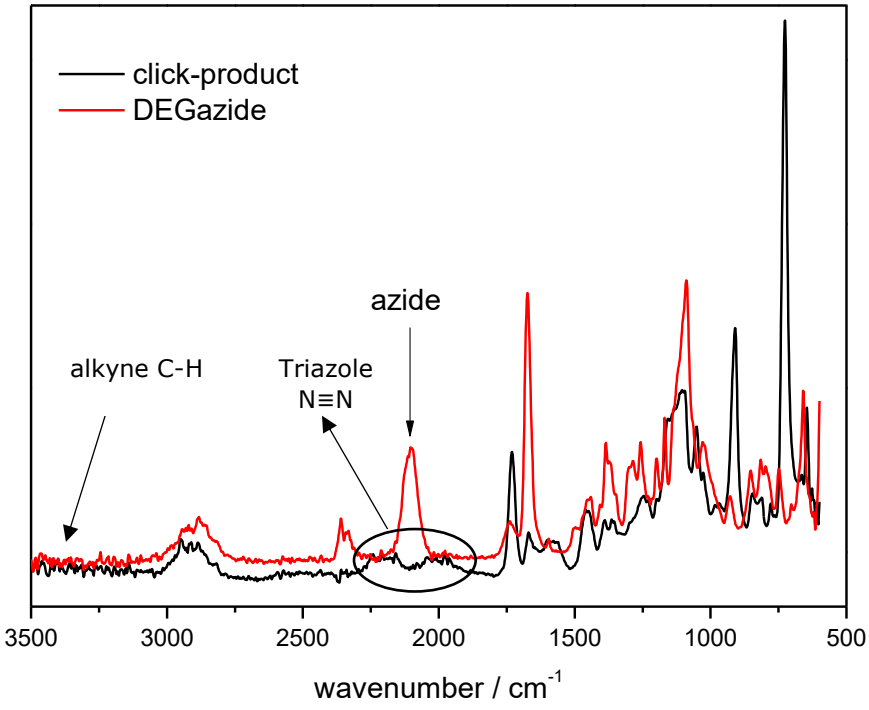

Figure 4.4 Overlay for the IR-spectrum of diethylene glycol monomethyl ether azide (DEGazide) and *poly*(Propagryl acrylate-*r*-caprolactone) with a copolymer composition of 85/15 of PA/CL.

An important signal to check for first is the presence of residual alkyne or azide in the copolymer spectrum. Specific signals for the stretch vibrations for alkyne can be found around 3300 cm^{-1} while the azide signal can be found at 2100 cm^{-1} (as observed in the red DEGAzide spectrum). Neither of the two signals are present in copolymer spectrum. To check whether the click reaction was successful, the

signals for the triazole need to be present. They should appear around the same position as the azide signal. Looking at the copolymer spectrum, two small broad bands can be seen around the azide location (as given by the black circle in Figure 4.4), thus hinting towards a successful click-reaction.

To confirm the successful click-reaction, independent analyses need to be performed. To this extent, GPC and ^{1}H-NMR were opted first. However, dissolving the copolymers in appropriate solvents proved to be troublesome resulting in bad spectra/chromatograms in both cases. Most likely this is caused by the dramatically increased molecular weight and the polarity-change due to attachment of the DEGA molecules. One solution might be to perform solid state NMR to circumvent the use of solvents. A different approach might be to aim for lower molecular weight copolymers. Since this is not possible with free radical polymerization, controlled radical polymerization techniques can be used. However, due to time constraints this was not performed during the work for this thesis.

In conclusion, the synthesis of copolymers of MDO and PA with varying amounts of both monomers was successful. Copolymerization parameters were determined using the Skeist method and found be $r_{PropAcr}$ = 1,112 ± 0,27 and r_{MDO} = 0,357 ± 0,09. Successful coupling of DEGAzide to the polymer backbone through the CuAAC reaction is given, though data from other independent measurements is necessary to confirm this.

4.3.2 Synthesis of alkyne functionalized cyclic ketene acetal

Rather than copolymerizing with functionalized acrylates, which is typically the way to go due to the abundance of these acrylates, one can also go for

functionalized CKAs instead. While a lot of different CKAs have been synthesized through the years, no record of alkyne or azide functionalized CKAs could be found. Synthesis of CKAs is very straightforward and always a transacetalization of a diol and with a halogen functionalized acetal. Introduction of the desired functionality should be feasible by incorporating it in the diol. For the case of an alkyne this is done through a three step procedure which is shown in Figure 4.5.

In the first step, solketal is reacted with propargyl bromide in the presence of sodium hydride according a literature procedure.[19] Work-up was easily done by vacuum distillation to give product (1) in 78% yield.

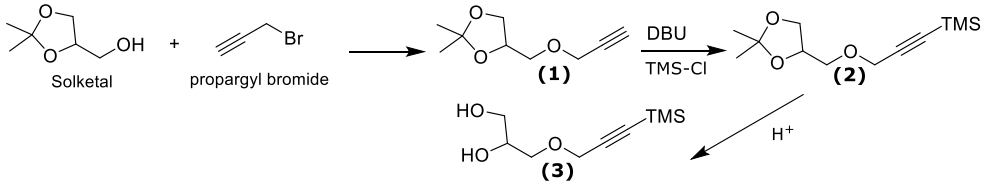

Figure 4.5 Schematic overview of the synthesis pathway towards alkyne functionalized diol (3).

The second step involves the protection of the alkyne and is key in order for the diol to withstand the treatments in the CKA synthesis. A slightly adapted literature procedure whereby TMS chloride was reacted with (1) in the presence of 1,8-Diazabicyclo[5.4.0]undec-7-ene (DBU) and silver chloride[20]. Also here, a simple vacuum distillation was enough to obtain pure product (2) in a yield of 65%. The final step is the acid catalyzed deprotection of the acetal to obtain the alkyne functionalized diol (3). This procedure was slightly adapted from literature whereby (2) was dissolved in methanol and Dowex 50 Ion-exchange resin was added. The progress of the reaction was followed by thin layer chromatography (TLC) until completion. After filtration, the alkyne functionalized diol (3) was

already pure with yield of 95+%. This product was readily used for the preparation of a functionalized CKA through the standard procedure (see Paragraphs 1.6.1 and 6.4) as given in Figure 4.6.

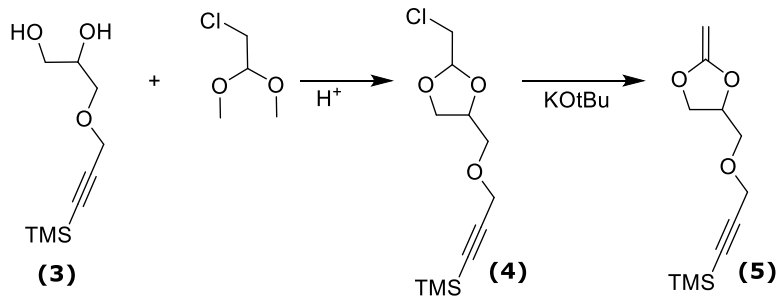

Figure 4.6 Schematic overview for the synthetic pathway towards alkyne functionalized cyclic ketene acetal (5).

In the transacetalization, the functionalized diol (4) is reacted with chloroacetaldehyde dimethyleacetal in the presence of a small amount of Dowex 50 Ion-exchange resin. During the course of the reaction, methanol is removed in order to increase conversion to the 1,3-dioxolane formation. A mixture of isomers and enantiomers was obtained through vacuum distillation in 80% yield. In the final step, a dehydrohalogenation was performed using potassium *tertiary*-butoxide (KOtBu) as a base at elevated temperatures. In contrary to all other steps, the resulting product showed some major impurities and side-products impossible to separate through distillation. Even after several distillations, the desired product could still not be identified. Moreover, the material started to show signs of hydrolysis. Purification via other means such as column chromatography proved unsuccessful whereas the material degrades on the column.

In conclusion, the synthesis of alkyne functionalized 1,3-dioxolane CKA is in theory feasible, however in practice the critical dehydrohalogenation gave major

issues in side product formation and work-up proved problematic due to hydrolysis of the material.

One problem with the traditional dehydrohalogenation is the need for elevated temperatures. With sensitive materials, such as CKAs, this can lead to a range of different side reactions and even autopolymerization lowering the yield of the reaction. Recently, a new method of performing the dehydrohalogenation was developed by the group of Nicholas and coworkers where the reaction was performed at T=0°C in a solid state reaction.[21] Herein, a phase transfer catalyst (Aliquat® 336) was used to facilitate the reaction between the solid KOtBu and the liquid halo-1,3-dioxolane. They showed that the amount of side products for MPDL could be limited and the yields could be improved, especially if the chlorine was switched for a bromine or even iodine.

This method might be the solution for the issues as posted here concerning the synthesis of the alkyne functionalized 1,3-dioxolane. Further research must therefore be performed to test this new method. When successful, this newly synthesized CKA should open paths to new functionalized degradable polymers.

4.4 Conclusion and outlook

In summary, the synthesis of copolymers with different ratios of PATMS and MDO is shown. Analysis of the copolymerization behavior lead to values for the reactivity ratios $r_{PropAcr}$ = 1,112 ± 0,27 and r_{MDO} = 0,357 ± 0,09. Deprotection of the alkyne was successful as shown by ^{1}H-NMR. Subsequent coupling of DEGAzide to the polymer by CuAAC click reaction was given by ATR-IR. Due to the limited solubility of the polymers, no other measurements could be performed to confirm the ATR-IR result.

The synthesis of alkyne functionalized CKA was unsuccessful due to the numerous side-products formed during the dehydrohalogenation step. Purification of the material did not result in pure material due to hydrolysis during the purification.

In conclusion, these results show that it is possible to prepare functionalizable degradable polymers via the copolymerization of MDO and propargyl acrylate. In further research these copolymers can be used to synthesize nanoparticles with clickable pendant groups which enables functionalization with any desired structure as long as it contains an azide.

As far as the clickable CKA route is concerned, more research needs to focus on optimizing the synthesis procedure with focus on the dehydrohalogenation. The aforementioned method of performing this reaction at low temperatures should benefit the formation of the CKA. This requires, however, a slight adaptation of the synthesis procedure by switching the halogen from chlorine to bromine or possibly even iodine.

4.5 References

1. Allen, T. M.; Cullis, P. R., Drug Delivery Systems: Entering the Mainstream. *Science* **2004,** *303* (5665), 1818.
2. Blanazs, A.; Armes, S. P.; Ryan, A. J., Self-Assembled Block Copolymer Aggregates: From Micelles to Vesicles and their Biological Applications. *Macromolecular Rapid Communications* **2009,** *30* (4-5), 267-277.
3. Jones, M.-C.; Leroux, J.-C., Polymeric micelles – a new generation of colloidal drug carriers. *European Journal of Pharmaceutics and Biopharmaceutics* **1999,** *48* (2), 101-111.
4. Nishiyama, N.; Kataoka, K., Current state, achievements, and future prospects of polymeric micelles as nanocarriers for drug and gene delivery. *Pharmacology & Therapeutics* **2006,** *112* (3), 630-648.
5. Kumari, A.; Yadav, S. K.; Yadav, S. C., Biodegradable polymeric nanoparticles based drug delivery systems. *Colloids and Surfaces B: Biointerfaces* **2010,** *75* (1), 1-18.
6. Soppimath, K. S.; Aminabhavi, T. M.; Kulkarni, A. R.; Rudzinski, W. E., Biodegradable polymeric nanoparticles as drug delivery devices. *Journal of Controlled Release* **2001,** *70* (1–2), 1-20.
7. Kolb, H. C.; Finn, M. G.; Sharpless, K. B., Click Chemistry: Diverse Chemical Function from a Few Good Reactions. *Angewandte Chemie International Edition* **2001,** *40* (11), 2004-2021.
8. Bock, V. D.; Hiemstra, H.; van Maarseveen, J. H., CuI-Catalyzed Alkyne–Azide “Click” Cycloadditions from a Mechanistic and Synthetic Perspective. *European Journal of Organic Chemistry* **2006,** *2006* (1), 51-68.
9. Tron, G. C.; Pirali, T.; Billington, R. A.; Canonico, P. L.; Sorba, G.; Genazzani, A. A., Click chemistry reactions in medicinal chemistry: Applications of the 1,3-dipolar cycloaddition between azides and alkynes. *Medicinal Research Reviews* **2008,** *28* (2), 278-308.
10. Lowe, A. B., Thiol-ene "click" reactions and recent applications in polymer and materials synthesis. *Polymer Chemistry* **2010,** *1* (1), 17-36.
11. Lowe, A. B.; Hoyle, C. E.; Bowman, C. N., Thiol-yne click chemistry: A powerful and versatile methodology for materials synthesis. *Journal of Materials Chemistry* **2010,** *20* (23), 4745-4750.
12. Hoogenboom, R., Thiol–Yne Chemistry: A Powerful Tool for Creating Highly Functional Materials. *Angewandte Chemie International Edition* **2010,** *49* (20), 3415-3417.
13. Maji, S.; Zheng, M.; Agarwal, S., Functional Degradable Polymers via Radical Ring-Opening Polymerization and Click Chemistry. *Macromolecular Chemistry and Physics* **2011,** *212* (23), 2573-2582.

14. Maji, S.; Mitschang, F.; Chen, L.; Jin, Q.; Wang, Y.; Agarwal, S., Functional Poly(Dimethyl Aminoethyl Methacrylate) by Combination of Radical Ring-Opening Polymerization and Click Chemistry for Biomedical Applications. *Macromol. Chem. Phys.* **2012,** *213* (16), 1643-1654.
15. Cai, T.; Chen, Y.; Wang, Y.; Wang, H.; Liu, X.; Jin, Q.; Agarwal, S.; Ji, J., Functional 2-methylene-1,3-dioxepane terpolymer: a versatile platform to construct biodegradable polymeric prodrugs for intracellular drug delivery. *Polym. Chem.* **2014,** *5* (13), 4061-4068.
16. Carter, M. C. D.; Jennings, J.; Appadoo, V.; Lynn, D. M., Synthesis and Characterization of Backbone Degradable Azlactone-Functionalized Polymers. *Macromolecules (Washington, DC, U. S.)* **2016,** *49* (15), 5514-5526.
17. Lang, A. S.; Neubig, A.; Sommer, M.; Thelakkat, M., NMRP versus "Click" Chemistry for the Synthesis of Semiconductor Polymers Carrying Pendant Perylene Bisimides. *Macromolecules* **2010,** *43* (17), 7001-7010.
18. Vandenbergh, J.; Tura, T.; Baeten, E.; Junkers, T., Polymer end group modifications and polymer conjugations via "click" chemistry employing microreactor technology. *Journal of Polymer Science Part A: Polymer Chemistry* **2014,** *52* (9), 1263-1274.
19. Latxague, L.; Ziane, S.; Chassande, O.; Patwa, A.; Dalila, M.-J.; Barthelemy, P., Glycosylated nucleoside lipid promotes the liposome internalization in stem cells. *Chemical Communications* **2011,** *47* (47), 12598-12600.
20. Prasher, A.; Loynd, C. M.; Tuten, B. T.; Frank, P. G.; Chao, D.; Berda, E. B., Efficient fabrication of polymer nanoparticles via sonogashira cross-linking of linear polymers in dilute solution. *Journal of Polymer Science Part A: Polymer Chemistry* **2016,** *54* (1), 209-217.
21. Tran, J.; Guegain, E.; Ibrahim, N.; Harrisson, S.; Nicolas, J., Efficient synthesis of 2-methylene-4-phenyl-1,3-dioxolane, a cyclic ketene acetal for controlling the NMP of methyl methacrylate and conferring tunable degradability. *Polym. Chem.* **2016,** *7* (26), 4427-4435.

Chapter 5

Preparation of degradable nanoparticles through a combination of RROP and Miniemulsion

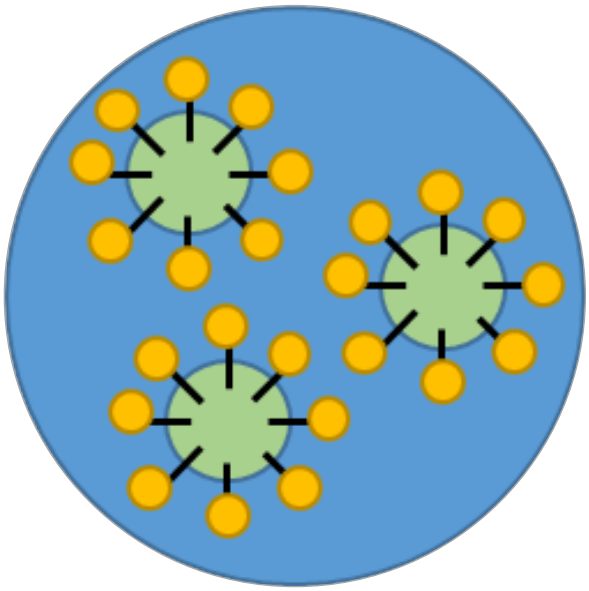

5.1 Abstract

An attempt was done to synthesize degradable nanoparticles in one pot by using a combination of miniemulsion with RROP. Therefore, a mixture of monomers, solvent, initiator and stabilizer was mixed with a water/SDS (sodium dodecyl sulfate) solution. After ultrasonication the monomer inside the nanodroplets were polymerized at T=90°C leading to nanoparticles. This effort proved, however, to be unsuccessful mainly due to degradation of the CKA through hydrolysis. Therefore, the method was changed to using preformed polymers with defined composition. The preparation of nanoparticles by using premade *p*(phenyl butyrolactone(PBL)-*r*-MMA) as well as *p*(PBL-*r*-Styrene) in miniemulsion was studied in combination with solvent evaporation. Herein, the premade polymer was first dissolved in a suitable solvent prior to mixing with a water/surfactant solution. After ultrasonication, the solvent was carefully evaporated under stirring to induce precipitation of the polymers leading to polymer nanoparticles. These particles have a size range of 80 to 120 nm and zeta-potential (ζ) in the range of -50 mV. Imaging techniques such as Atomic Force Microscopy (AFM) as well as Transmission Electron Microscopy (TEM) showed uniform particles for both polymers.

5.2 Introduction

The use of synthetic polymers in the biomedical world has become increasingly popular in the years, mainly due to their high mechanical strength and relatively low production cost. However, not all polymer classes are applicable for biomedical applications since they have to be biocompatible, biodegradable and non-cytotoxic. Polyesters are the most pronounced candidates for the creation of bioapplications due to their hydrolytically cleavable ester bonds in the backbone. Certain polyesters such as poly(L-lactide)[1], poly(hydroxybutyrate)[2] and poly(ε-caprolactone)[3] have already been successfully employed in tissue engineering, drug delivery and for implants. However, the synthesis of these materials is not straightforward, as high temperatures and removal of condensates are required to reach high molecular weights. In that sense, radical polymerization is much more suitable, while it can be performed under mild conditions.

While the synthesis of polyesters using radical polymerization was already described back in 1979[4], it remained largely unused for some time since its discovery. Through this technique, linear polyesters are created by exposing cyclic ketene acetals (CKAs) to a radical source. Under influence of the radicals the CKAs undergo a ring-opening reaction to form a linear ester. While the linear polyester is usually the main product, CKAs can also undergo regular vinyl addition. In practice this means that a linear polyester is formed with a small fraction of un-ring-opened segments.

With the current drive towards the synthesis of environmentally friendly and tailor-made materials, interest in radical ring-opening polymerization (RROP) of CKAs was renewed. This is also related to the development of controlled radical polymerization techniques such as ATRP[5-6] and RAFT[7-8] and 'click chemistry'[9-10].

Radical ring-opening polymerization also provides the opportunity to incorporate ester-bonds into the backbone of the classic vinyl polymers such as *poly*styrene and *poly*(methyl methacrylate) via copolymerization of CKAs with the respective vinyl monomers.

This can be highly beneficial, while it combines the inherent strength and stability of classical vinyl polymers with the degradability of polyesters. While in theory a lot of CKAs are accessible, only a handful of CKAs have proven to be suitable for (co)polymer synthesis of which 2-methylene-4-phenyl-1,3-dioxolane (MPDL)[11-20], 2-methylene-5,6-benzo-1,3-dioxepane (BMDO)[15-17, 21-42] and 2-methylene-1,3-dioxepane (MDO)[15, 17, 43-72] are the most used ones. Early work by Bailey et al. already showed that MPDL was much more suitable in copolymerization with styrene then MDO or BMDO.[11, 21, 73] In more recent work by Agarwal the combination of MDO with methyl methacrylate was explored and work by d'Ayala and coworkers showed the possibility to copolymerize BMDO with vinyl acetate.[39, 74] As was described in Chapter 2, the combination of BMDO and methyl methacrylate was explored.[40] Using online IR measurements during the copolymerization, we observed that both monomers are consumed simultaneously but at the different rates. By fitting the Mayo-Lewis equation to the compositional data, the following reactivity ratios were obtained: r_{BMDO}= 0.33 ± 0.06 and r_{MMA} = 6.0 ± 0.8. A simple degradation test was performed on these materials by exposing them to 1M sodium hydroxide solution. This showed a clear shift of the GPC trace to lower molecular weight, meaning that the materials can be considered degradable. These characteristics make this material especially suitable for use in the biomedical field, due to the degradability of the ester-bonds and the mechanical strength of the methyl methacrylate. With the current

research in the polymer/biomedical field mainly focused on drug delivery applications, one could immediately see the potential of these materials in this field. Some notable work has already been performed on the use of CKAs in drug delivery applications. Work by Agarwal and coworkers showed for the first time the use of the combination of RROP and radical polymerization to synthesize particles as possible drug carriers.[37, 58] In their reports, they used MDO in conjunction with functionalized acrylates to create amphiphilic copolymers, which were subsequently employed for the creation of micelles. Due to the build-in functionality, the micelles were allowed to crosslink in the presence of the anticancer drug doxorubicin (DOX). Hydrolytic as well as enzymatic degradation of the crosslinked micelles lead to controlled release of the DOX. A drawback of this method however is that several synthesis and purification steps have to be implemented in order to prepare the loaded micelles.

This can be circumvented by introducing the miniemulsion technique. This versatile technique allows for the preparation of nanoparticles/droplets with defined size and morphology for a whole range of different materials in a small amount of time.[75-77] Herein, two different approaches were opted: miniemulsion and postpolymerization as well as a combination of miniemulsion and solvent evaporation. In the first method, all components for the (co)polymerization are premixed and emulsified using an ultrasonication probe. Subsequent polymerization leads to polymer nanoparticles. In the latter approach, the hydrophobic polymers are dissolved in chloroform and mixed with a SDS solution in water to create a heterophase system (Figure 5.1). Using ultrasonication the large droplets are broken down in nanodroplets of roughly 150 nm in diameter. Subsequently, precipitation of the polymer in the nanodroplets is induced by

evaporating the chloroform resulting in polymer nanoparticle formulation with a size in the range of 80-120 nm.

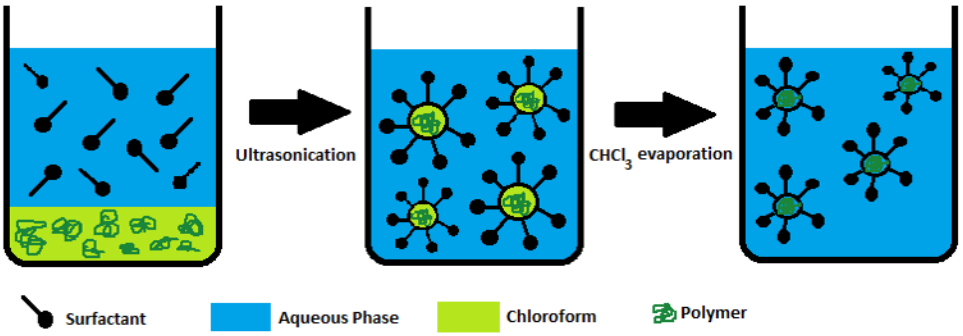

Figure 5.1 Combination of the miniemulsion technique and solvent evaporation method for the synthesis of polymer nanoparticles.

In this research, two different copolymers were opted for preparation of nanoparticles. MPDL was selected as CKA due its compatibility with a broad range of comonomers (as seen in Chapter 3). For the purpose of comonomer, styrene and MMA were selected due to the high glass transition temperature (T_g) and good mechanical strength that the respective polymers offer. The method for preparing these polymers under free-radical conditions was already described in Chapter 3. Several different ratios of both copolymers were synthesized leading to nanoparticles with varying amounts of degradable linkages. The size of the nanoparticles was determined by using dynamic light scattering (DLS). ζ-potential was measured by applying a voltage and measuring the mobility with DLS. A visualization of the particles was facilitated by atomic force microscopy (AFM) and transmission electron microscopy (TEM).

5.3 Results and discussion

As described in the introduction, there are in essence two approaches to synthesizing polymer nanoparticles via miniemulsion. The difference lies in the order of different aspects being polymerization and ultrasonication. One can first create nanodroplets of monomer and initiator and do post-polymerization inside the nanodroplets. The other involves then of course synthesizing the polymers in batch and making nanoparticles by applying a combination of miniemulsion and solvent evaporation. Both approaches were tested and the results are presented in the following paragraphs.

5.3.1 Synthesis of nanoparticles using a combination of miniemulsion and post-polymerization

So far, there has been one report on the use of miniemulsion in combination with RROP.[36] In this publication, they make use of the post-polymerization approach. Their results were considered a good starting point, however, based on the results described in Chapter 2, a few aspects were altered. One of the important factors is which CKA to choose. In the publication by Siebert *et al.* they opted for BMDO in combination with styrene, however as was shown in Paragraph 2.2.2. polymerization temperatures in excess of 100°C are necessary to yield quantitative ring-opening. Since water is used as continuous phase, polymerization is impossible at these temperatures. On the other hand, choosing a lower temperature prolongs the polymerization time, in addition to the limitations on the ring-opening. Another important factor is stability of the CKA towards water. Herein, BMDO lacks this stability as was shown in Paragraph 2.2.1. Based on these considerations, MDO was found to be much more suitable as it requires lower temperatures for quantitative ring-opening and the susceptibility

to hydrolysis is negligible. As a consequence, the comonomer in this study had to be changed as well due to compatibility issues of MDO with styrene. For MDO, acrylates are known to be the most suitable candidates. With future analysis in mind, benzyl acrylate was opted because of the improved contrast the phenyl ring has in electron microscopy techniques w.r.t. for example the alkyl chain in n-butyl acrylate. The complete procedure for the preparation of the nanoparticles can be found in Paragraph 6.5 and will be briefly discussed here.

To make the nanodroplets, the two phases were first prepared separately. The continuous phase consists of water and sodium dodecyl sulfate (SDS) as surfactant while the dispersed phase consists of equimolar amounts of MDO and benzyl acrylate, azobisisobutyronitrile (AIBN) (initiator) and hexadecane as stabilizing agent. After mixing the two phases, the emulsion was left to stir for one hour at high rpm where the mixture turned slightly opaque. The premixed emulsion was then exposed to ultrasound whereby the mixture turns milk like. Post-polymerization was performed immediately after the ultrasonication by immersing the miniemulsion in an oil bath at T=90°C and stirring it overnight. The resulting emulsion was filtered over a paper filter leaving behind a small amount of solid residue which was found to be pure *poly*(benzyl acrylate). The filtered miniemulsion was found to contain 5 wt% of particles. The particle size distribution was measured by dynamic light scattering resulting in a size of 320 ± 30 nm with dispersity of 0.17. Although these results may not look decent, the size is acceptable for this approach and with a dispersity of 0.17 the particles can also be considered fairly uniform in size. The most important factor, however, for these materials is the composition of the formed polymer. For this purpose, a

small amount of material was dried under vacuum and ^{1}H-NMR was measured in deuturated chloroform. The resulting spectrum is shown in Figure 5.2.

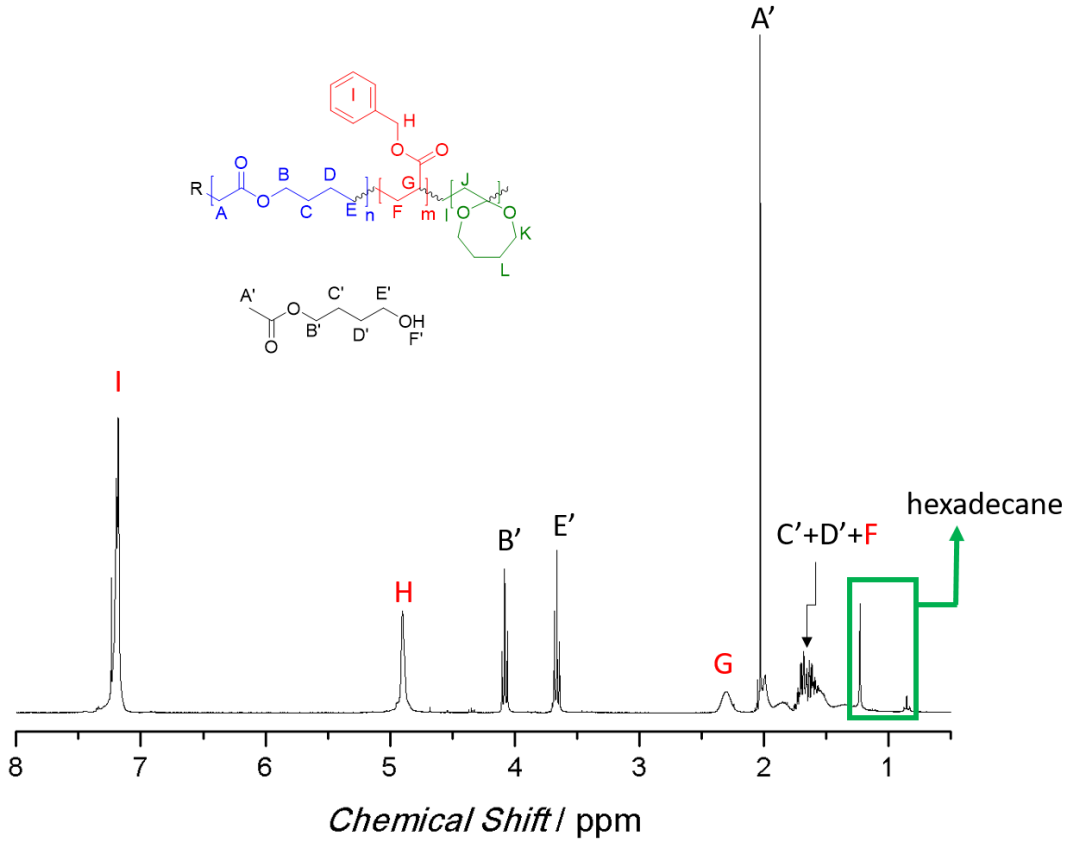

Figure 5.2 ^{1}H-NMR spectrum and peak assignment for the nanoparticle copolymerization of MDO and Benzyl Acrylate with a feed monomer ratio of 50:50 [MDO]:[BzAcr] (measured in $CDCl_3$).

In this spectrum the chemical structure of the copolymer and other important structures are depicted. Peak assignments are also given for all relevant components. At first glance, the spectrum appears relatively clean compared to other polymerization products (see earlier Chapters 2,3 and 4). When comparing the different signals to the amount of different protons in the polymer structure

(the top structure in the figure) several signals seem to be missing. For benzyl acrylate (marked in red) all signals are present, however this is different for MDO. Typical signals for polycaprolactone (PCL) include broad peaks at 1.5 ppm, 2.2 ppm and 4.1 ppm. While these signals appear to be present at first a closer inspection reveals that the corresponding signals are too sharp to be able to be related to a polymer. As mentioned before, CKAs are prone to hydrolysis (though some more than others) leading to an unreactive linear molecule which in this case results in the structure depicted in black (lower structure) in Figure 5.2. Not only do the positions of the signals match up but also the patterns match with the respective protons (depicted as the black numbers with apostrophes in Figure 5.2). This means that, rather than being incorporated in the polymer, MDO is consumed through hydrolysis leading to nanoparticles consisting of near pure *poly*(benzyl acrylate) which is non-degradable. This result is confirmed by comparing the results found for experiments performed with different feed ratios for MDO and Benzyl acrylate. While MDO should not be prone to hydrolysis when exposed to water under atmospheric conditions, different conditions apply when contained in particles on nanometer scale. Things such as the presence of ionic surfactants or the increased surface area possibly facilitate the acceleration of the hydrolysis reaction. There are several options to work around these issues, for instance using non-ionic surfactants or using other continuous phases (i.e. ethylene glycol or formamide) but after some quick tests other problems regarding stability and shelf-life of the miniemulsion occurred after which it was decided to put further research into this approach on hold.

In conclusion, while the synthesis of particles was successful the resulting structure was not as expected given by the large amount of hydrolyzed MDO and

lack of PCL signals. Further research into different compositions confirmed the result. Several tests using other surfactants or continuous phases did not reduce the hydrolysis but in fact lead to more problems regarding the stability.

The next step in the synthesis of degradable nanoparticles would be to reverse the order of action and test the other approach as mentioned in the beginning of Paragraph 5.3. These results will be discussed in the next paragraph.

5.3.2 Preparation of nanoparticles by using batch-synthesized polymers and miniemulsion.

For this approach, batch polymers based on MPDL and MMA and styrene were synthesized according to the procedure described under Paragraph 6.3 and a schematic overview is shown in Figure 5.3. In short, both MPDL and MMA or styrene respectively in different feed ratios were added to a solution of dicumyl peroxide (DCP, 2 wt% w.r.t total monomer weight) in anisole.

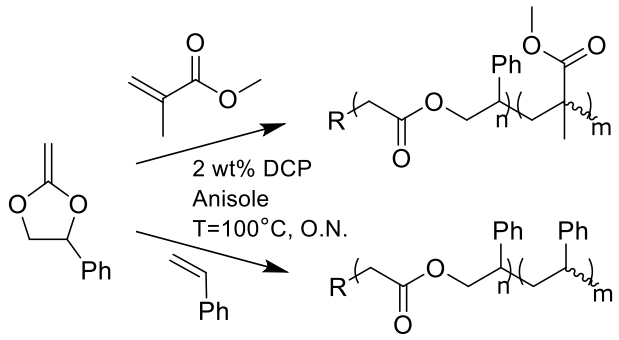

Figure 5.3 schematic overview of copolymers with either MMA (top) or styrene (bottom).

The mixture was polymerized overnight at T=100°C and the obtained polymers were precipated in hexane and thoroughly dried before use in miniemulsions. A major advantage of using this approach w.r.t. using the post-polymerization

method is the freedom of choice for CKA because of the limited exposure to water causing hydrolysis. Taking this into consideration, MPDL was selected based on the inherent presence of a phenyl ring (yielding high contrast in electron microscopy imaging) and the lower polymerization temperature for quantitative ring-opening (in comparison with BMDO). Also, extensive studies have been performed in this work in Chapter 3.

The procedure to produce the miniemulsion is written in detail in Paragraph 6.5. Herein, the polymer was dissolved in an easy to evaporate hydrophobic solvent for which chloroform was selected. For the continuous phase, SDS was dissolved in water and after adding the phases together the emulsion was stirred vigorously for one hour before being exposed to ultrasonication. The chloroform was evaporated on a hot plate at a temperature of T=40°C under mild stirring for a few hours. During this evaporation the emulsion changed from milk-like to almost translucent. The resulting dispersion was filtered and the size distribution and ζ-potential were measured using DLS. An overview of the results is given in Table 5.1 and Table 5.2.

As was already seen in Paragraph 3.2.2, MMA and styrene both show slightly different behavior in combination with MPDL – reactivity ratio for styrene is higher than for MMA -. This behavior is also reflected nicely in this dataset where at the same value for monomer fraction in the feed (f_{mon}) a higher value for copolymer composition (F_{mon}) is found for styrene, meaning that more styrene is built in in the same time compared to MMA (0.68 for styrene compared to 0.34 for MMA). This observation is recurring for all feed ratios for both monomers.

Table 5.1 Overview of results for synthesis of *poly*(MPDL-*r*-styrene) and *poly*(MPDL-*r*-MMA). The values for F_{mon} were determined using ^{1}H-NMR in $CDCl_3$. M_n, M_w and $Đ$ were determined by GPC in THF.

CKA	***Monomer***	f_{mon}	F_{mon}	M_n /10^4 g·mol^{-1}	M_w /10^5 g·mol^{-1}	$Đ$
MPDL	Sty	0.25	0.68	4.57	2.13	4.66
MPDL	Sty	0.50	0.81	2.54	3.40	13.3
MPDL	Sty	0.75	0.95	7.89	4.04	5.12
MPDL	MMA	0.25	0.34	1.36	1.89	13.9
MPDL	MMA	0.50	0.67	2.13	5.91	25.2
MPDL	MMA	0.75	0.81	3.08	6.45	20.9

Table 5.2 The number average size (washed) and ζ (pre- and post-washing) were determined using Dynamic Light Scattering (DLS).

CKA	***Monomer***	***Size* / nm**	***PDI***	***ζ* / mV**	***ζ$_{washing}$* / mV**
MPDL	Sty	67	0.22	-56	-51
MPDL	Sty	84	0.35	-51	-58
MPDL	Sty	82	0.26	-51	-32
MPDL	MMA	85	0.15	-48	-31
MPDL	MMA	82	0.24	-56	-51
MPDL	MMA	82	0.23	-53	-52

For all entries, the size of the particles seems similar being in range of 80-85 nm with the exception of entry 1. The same can be said about the ζ-potential values which all seem to be between -50 and -55 mV. The negative charge on the particle surface stems from the presence of the ionic surfactant SDS of which all the negatively charged sulfate ions on the alkyl chain are sticking out. This value is also a measure for the stability of the system as higher values (either negative or positive) show higher stability due to the increased repulsion. In addition, all systems have a dispersity between 0.1 and 0.4 indicating a slight polydisperse behavior. The solid content was measured by taking a small amount of dispersion, evaporating the solvent and weighing the leftover material. For these materials, values are typical in the range of 0.9 and 1.6 depending on the amount of polymer used in the formulation.

In order to prepare the particles for future applications and surface measurements, the particles underwent several washing steps with water in an attempt to remove most of the surfactant. To check whether the washing was successful, the ζ-potential was measured once again as the value should become more positive the more surfactant is removed. These values are also tabulated in Table 5.2. In comparison with the values for ζ-potential prior to washing some entries indeed show a decrease in negativity (entry 3 and 4) but in most cases, no change is observed. This may indicate that the removal of the surfactant was unsuccessful and may be firmly attached to the particles by the strong forces at play at such small sizes (Van der Waals forces but also osmotic pressure). While these data give an indication for the successful preparation of nanoparticles, other techniques are necessary to confirm the morphology of the particles.

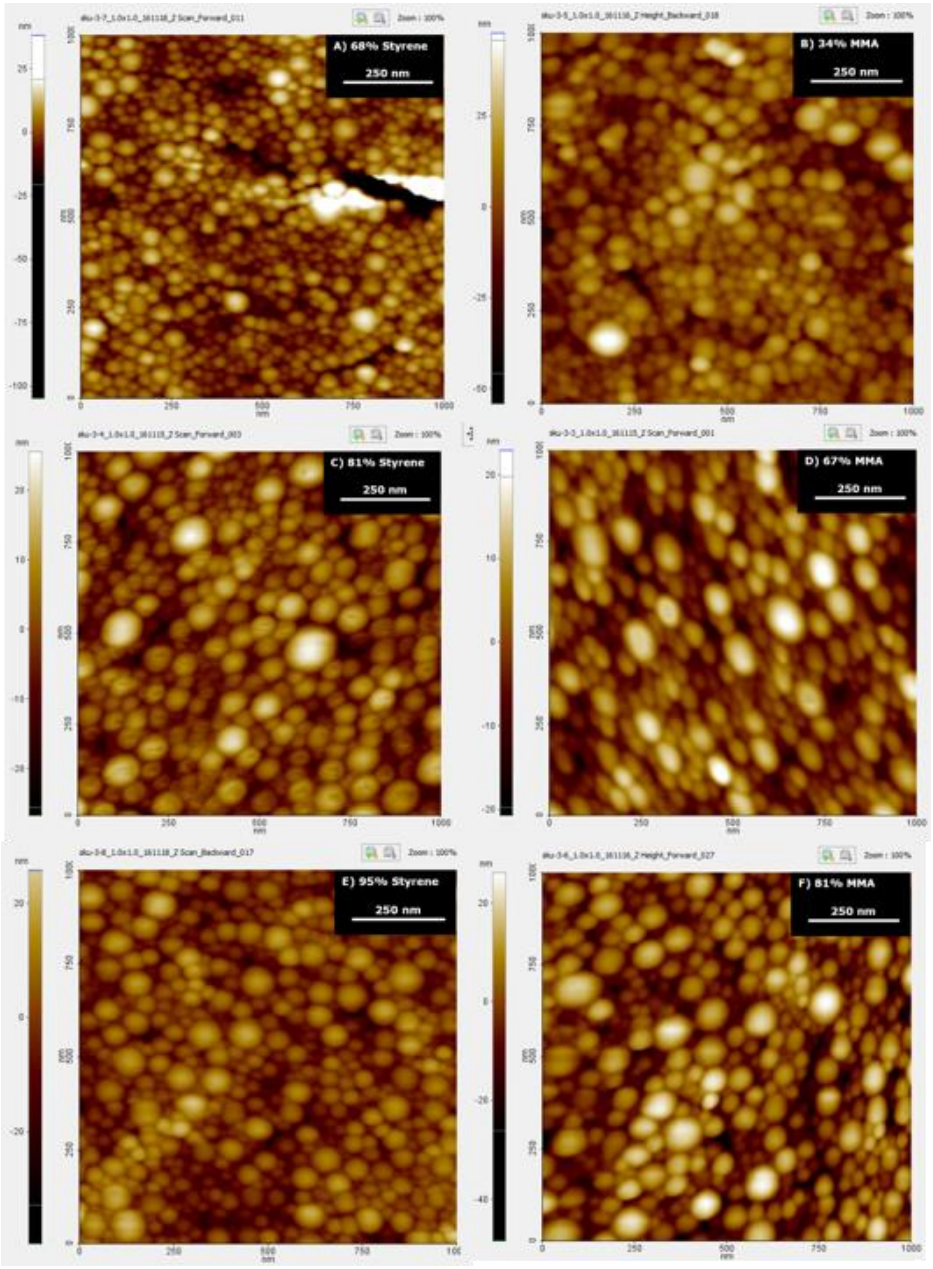

Figure 5.5 Collection of AFM-images for different copolymers of MPDL with either MMA or styrene in different compositions; A) 68% styrene, B) 34% MMA, C) 81% styrene, D) 67% MMA, E) 95% styrene and F) 81% MMA.

To get an idea of the shape and morphology of the particles, atomic force microscopy is utilized. To facilitate the measurement, the particles were deposited on a silicon substrate. This was done for all polymers given in Table 5.1 and 5.2. An overview of recorded images is shown in Figure 5.5.

A collection of images for all different copolymers of MPDL with either styrene (AFM images on the left side A, C and E) or MMA (AFM images on the right side B, D and F) with different compositions. Height bars are added to each individual picture to get an idea of the size.

While the images are not always very clear, overall, the particles look uniform in size with a decent spherical appearance. Thanks to high contribution of MMA and styrene in the respective copolymers, the particles retain their shape during film formation owing to the relative high glass transition temperature (T_g) for PMMA (T_g = 85°C) and PS (T_g = 90°C).[78] Comparing styrene to MMA, the styrene particles seem to have a slightly smaller size and height differential. An explanation for this effect with styrene is not readily available but it might be related to the copolymer composition: Due to the large difference in reactivity ratios for MPDL and styrene, there will be more styrene homopolymers and less random copolymers with respect to MMA. This can lead to a difference in solubility and might have an influence on the size. To this extent, phase images were recorded but unfortunately no clear phase separation could be observed.

To further investigate this effect and to get a better idea of the composition of the particles, Transmission Electron Microscopy (TEM) images were taken. Not all copolymers would be compatible with this technique as this technique requires good scattering due to a high electron density to be able to get decent contrast.

Therefore, styrene is much more suitable due to the high electron density in the aromatic ring. In addition, MMA is considered beam sensitive making it even less suitable. With that in mind, the MPDL/MMA copolymer with 67% of MMA (entry 5 table 5.1) was selected. In addition, the copolymer with the highest styrene content (95%, entry 3 Table 5.1) was selected. The TEM pictures for the aforementioned copolymers are shown in Figure 5.6 whereby the MMA copolymer is shown on the left side and the styrene copolymer is shown on the right side.

Both pictures nicely show spherical particles. In both cases, a collection of large particles (80 nm) and a lot of smaller particles is observed reflecting the large PDI values as seen with DLS. The size of the large (almost black) particles is approximately 80 nm nicely matches up to the values given in Table 5.2.

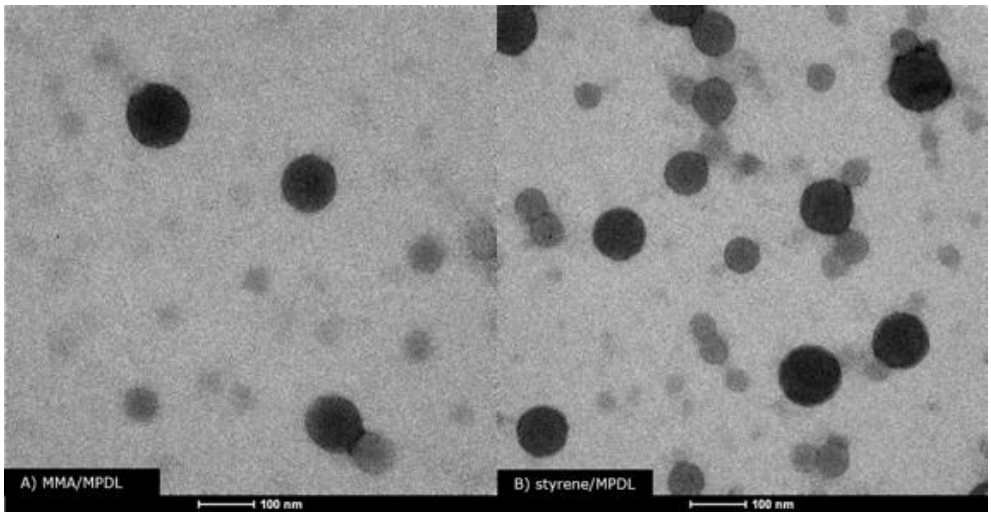

Figure 5.6 TEM images for nanoparticles consisting of A) *poly*(MPDL-*r*-MMA) with a composition MPDL:MMA of 33:67 and B) *poly*(MPDL-*r*-styrene) with a composition MPDL:styrene of 5:95.

In conclusion, the preparation of *poly*(MPDL-*r*-MMA) and *poly*(MPDL-*r*-styrene) nanoparticles was successful. The particles are spherical the size is in the expected

range for these formulations (between 80-85nm). To test for degradability, more tests will need to be performed on these particles.

5.4 Conclusion and outlook

For nanoparticle preparation, two approaches were tested in this study. In the first approach consisting of ultrasonication with subsequent post-polymerization, nanoparticles were synthesized. Clarification of the copolymer composition by ^{1}H-NMR showed that practically all MDO was hydrolyzed during the process, resulting in almost pure *poly*(benzyl acrylate) particles caused by a combination of water, ionic surfactant and the increased surface area. Several tests with non-ionic surfactants and different continuous phases proved problematic with respect to the stability of the miniemulsion.

For the second approach, batch polymers of MPDL and MMA as well as styrene were synthesized using a batch procedure followed by ultrasonication and solvent evaporation. The resulting nanoparticles proved uniform in size and shape. Since the polymers are known to contain degradable parts, there is no doubt that the particles will show degradation. Further research will need to be performed by exposing the particles to mild basic or mild acidic conditions to prove the hydrolytic degradation of the ester bonds. To check whether these nanoparticles are also suitable for drug delivery, the degradation test may be combined with controlled release studies whereby a (fluorescent) dye is encapsulated in the particles and the release can then be studied with UV/Vis or Fluorescence spectroscopy.

In conclusion, nanoparticles with defined copolymer structures were successfully prepared. These particles are expected to show degradation due to the confirmed presence of degradable ester bonds.

5.5 References

1. Hu, F. X.; Neoh, K. G.; Kang, E. T., Synthesis and in vitro anti-cancer evaluation of tamoxifen-loaded magnetite/PLLA composite nanoparticles. *Biomaterials* **2006,** *27* (33), 5725-5733.
2. Martin, D. P.; Williams, S. F., Medical applications of poly-4-hydroxybutyrate: a strong flexible absorbable biomaterial. *Biochemical Engineering Journal* **2003,** *16* (2), 97-105.
3. Dash, T. K.; Konkimalla, V. B., Poly-ϵ-caprolactone based formulations for drug delivery and tissue engineering: A review. *Journal of Controlled Release* **2012,** *158* (1), 15-33.
4. Bailey, W. J.; Chen, P. Y.; Chiao, W.-B.; Endo, T.; Sidney, L.; Yamamoto, N.; Yamazaki, N.; Yonezawa, K., Free-Radical Ring-Opening Polymerization. In *Contemporary Topics in Polymer Science: Volume 3*, Shen, M., Ed. Springer US: Boston, MA, 1979; pp 29-53.
5. Matyjaszewski, K.; Xia, J., Atom Transfer Radical Polymerization. *Chemical Reviews* **2001,** *101* (9), 2921-2990.
6. Matyjaszewski, K., Atom Transfer Radical Polymerization (ATRP): Current Status and Future Perspectives. *Macromolecules* **2012,** *45* (10), 4015-4039.
7. Moad, G.; Rizzardo, E.; Thang, S. H., Living Radical Polymerization by the RAFT Process. *Australian Journal of Chemistry* **2005,** *58* (6), 379-410.
8. Moad, G.; Rizzardo, E.; Thang, S. H., Radical addition–fragmentation chemistry in polymer synthesis. *Polymer* **2008,** *49* (5), 1079-1131.
9. Kolb, H. C.; Finn, M. G.; Sharpless, K. B., Click Chemistry: Diverse Chemical Function from a Few Good Reactions. *Angewandte Chemie International Edition* **2001,** *40* (11), 2004-2021.
10. Sumerlin, B. S.; Vogt, A. P., Macromolecular Engineering through Click Chemistry and Other Efficient Transformations. *Macromolecules* **2010,** *43* (1), 1-13.
11. Bailey, W. J.; Wu, S.-R.; Ni, Z., Synthesis and free radical ring-opening polymerization of 2-methylene-4-phenyl-1,3-dioxolane. *Die Makromolekulare Chemie* **1982,** *183* (8), 1913-1920.
12. Endo, T.; Yako, N.; Azuma, K.; Nate, K., Ring-opening polymerization of 2-methylene-4-phenyl-1,3-dioxolane. *Die Makromolekulare Chemie* **1985,** *186* (8), 1543-1548.
13. Bailey William, J.; Kuruganti Vijaya, K.; Angle Jay, S., Biodegradable Polymers Produced by Free-Radical Ring-Opening Polymerization. In *Agricultural and Synthetic Polymers*, American Chemical Society: 1990; Vol. 433, pp 149-160.
14. Pan, C.-Y.; Lou, X.-D., "Living" free radical ring-opening polymerization of 2-methylene-4-phenyl-1,3-dioxolane by atom transfer radical polymerization. *Macromolecular Chemistry and Physics* **2000,** *201* (11), 1115-1120.

15. Delplace, V.; Tardy, A.; Harrisson, S.; Mura, S.; Gigmes, D.; Guillaneuf, Y.; Nicolas, J., Degradable and Comb-Like PEG-Based Copolymers by Nitroxide-Mediated Radical Ring-Opening Polymerization. *Biomacromolecules* **2013,** *14* (10), 3769-3779.
16. Tardy, A.; Delplace, V.; Siri, D.; Lefay, C.; Harrisson, S.; de Fatima Albergaria Pereira, B.; Charles, L.; Gigmes, D.; Nicolas, J.; Guillaneuf, Y., Scope and limitations of the nitroxide-mediated radical ring-opening polymerization of cyclic ketene acetals. *Polymer Chemistry* **2013,** *4* (17), 4776-4787.
17. Delplace, V.; Harrisson, S.; Tardy, A.; Gigmes, D.; Guillaneuf, Y.; Nicolas, J., Nitroxide-Mediated Radical Ring-Opening Copolymerization: Chain-End Investigation and Block Copolymer Synthesis. *Macromolecular Rapid Communications* **2014,** *35* (4), 484-491.
18. Delplace, V.; Guegain, E.; Harrisson, S.; Gigmes, D.; Guillaneuf, Y.; Nicolas, J., A ring to rule them all: a cyclic ketene acetal comonomer controls the nitroxide-mediated polymerization of methacrylates and confers tunable degradability. *Chemical Communications* **2015,** *51* (64), 12847-12850.
19. Shi, Y.; Schmalz, H.; Agarwal, S., Designed enzymatically degradable amphiphilic conetworks by radical ring-opening polymerization. *Polymer Chemistry* **2015,** *6* (35), 6409-6415.
20. Tran, J.; Guegain, E.; Ibrahim, N.; Harrisson, S.; Nicolas, J., Efficient synthesis of 2-methylene-4-phenyl-1,3-dioxolane, a cyclic ketene acetal for controlling the NMP of methyl methacrylate and conferring tunable degradability. *Polym. Chem.* **2016,** *7* (26), 4427-4435.
21. Bailey, W. J.; Ni, Z.; Wu, S. R., Free radical ring-opening polymerization of 4,7-dimethyl-2-methylene-1,3-dioxepane and 5,6-benzo-2-methylene-1,3-dioxepane. *Macromolecules* **1982,** *15* (3), 711-714.
22. Yuan, J.-Y.; Pan, C.-Y.; Tang, B. Z., “Living” Free Radical Ring-Opening Polymerization of 5,6-Benzo-2-methylene-1,3-dioxepane Using the Atom Transfer Radical Polymerization Method. *Macromolecules* **2000,** *34* (2), 211-214.
23. He, T.; Zou, Y.-F.; Pan, C.-Y., Controlled/“Living” Radical Ring-Opening Polymerization of 5,6-Benzo-2-Methylene-1,3-Dioxepane Based on Reversible Addition-Fragmentation Chain Transfer Mechanism. *Polymer Journal* **2002,** *34* (3), 138-138.
24. Yuan, J. Y.; Pan, C. Y., Block copolymerization of 5,6-benzo-2-methylene-1,3-dioxepane with conventional vinyl monomers by ATRP method. *European Polymer Journal* **2002,** *38* (8), 1565-1571.
25. Yuan, J.-y.; Pan, C.-y., The effects of monomer structure of cyclic ketene acetals on the behavior of controlled radical ring-opening polymerization. *Chin. J. Polym. Sci.* **2002,** *20* (1), 9-14.

26. Wickel, H.; Agarwal, S., Synthesis and Characterization of Copolymers of 5,6-Benzo-2-methylene-1,3-dioxepane and Styrene. *Macromolecules* **2003,** *36* (16), 6152-6159.
27. Wickel, H.; Agarwal, S.; Greiner, A., Homopolymers and Random Copolymers of 5,6-Benzo-2-methylene-1,3-dioxepane and Methyl Methacrylate: Structural Characterization Using 1D and 2D NMR. *Macromolecules* **2003,** *36* (7), 2397-2403.
28. Huang, J.; Gil, R.; Matyjaszewski, K., Synthesis and characterization of copolymers of 5,6-benzo-2-methylene-1,3-dioxepane and n-butyl acrylate. *Polymer* **2005,** *46* (25), 11698-11706.
29. Huang, J.; Gil, R.; Matyjaszewski, K., Atom transfer radical copolymerization of 5,6-benzo-2-methylene-1,3-dioxepane and n-butyl acrylate. *Polym. Prepr. (Am. Chem. Soc., Div. Polym. Chem.)* **2005,** *46* (2), 150-151.
30. Agarwal, S., Radical Ring Opening and Vinyl Copolymerization of 2,3,4,5,6-pentafluorostyrene with 5,6-Benzo-2-methylene-1,3-dioxepane: Synthesis and Structural Characterization Using 1D and 2D NMR Techniques. *Journal of Polymer Research* **2006,** *13* (5), 403-412.
31. Lutz, J. F.; Andrieu, J.; Uzgun, S.; Rudolph, C.; Agarwal, S., Biocompatible, thermoresponsive, and biodegradable: Simple preparation of "all-in-one" biorelevant polymers. *Macromolecules* **2007,** *40* (24), 8540-8543.
32. Ren, L.; Agarwal, S., Synthesis, characterization, and properties evaluation of poly[(N-isopropylacrylamide)-co-ester]s. *Macromol. Chem. Phys.* **2007,** *208* (3), 245-253.
33. Ren, L.; Speyerer, C.; Agarwal, S., Free-Radical Copolymerization Behavior of 5,6-Benzo-2-methylene-1,3-dioxepane and Methacrylic Acid via the in Situ Generation of 3-Methyl-1,5-dihydrobenzo[e][1,3]dioxepin-3-yl Methacrylate and 2-(Acetoxymethyl)benzyl Methacrylate. *Macromolecules* **2007,** *40* (22), 7834-7841.
34. Agarwal, S.; Ren, L., Unexpected new route to free radical copolymerisation of 5,6-benzo-2-methylene-1,3-dioxepane with methacrylic acid as proved by 1D and 2D NMR techniques. *Polym. Prepr. (Am. Chem. Soc., Div. Polym. Chem.)* **2008,** *49* (1), 743-744.
35. Siegwart, D. J.; Bencherif, S. A.; Srinivasan, A.; Hollinger, J. O.; Matyjaszewski, K., Synthesis, characterization, and in vitro cell culture viability of degradable poly(N-isopropylacrylamide-co-5,6-benzo-2-methylene-1,3-dioxepane)-based polymers and crosslinked gels. *Journal of Biomedical Materials Research Part A* **2008,** *87A* (2), 345-358.
36. Siebert, J. M.; Baumann, D.; Zeller, A.; Mailänder, V.; Landfester, K., Synthesis of Polyester Nanoparticles in Miniemulsion Obtained by Radical Ring-Opening of BMDO and Their Potential as Biodegradable Drug Carriers. *Macromolecular Bioscience* **2012,** *12* (2), 165-175.

37. Zhang, Y.; Chu, D.; Zheng, M.; Kissel, T.; Agarwal, S., Biocompatible and degradable poly(2-hydroxyethyl methacrylate) based polymers for biomedical applications. *Polymer Chemistry* **2012,** *3* (10), 2752-2759.
38. Zhang, Y.; Zheng, M.; Kissel, T.; Agarwal, S., Design and Biophysical Characterization of Bioresponsive Degradable Poly(dimethylaminoethyl methacrylate) Based Polymers for In Vitro DNA Transfection. *Biomacromolecules* **2012,** *13* (2), 313-322.
39. d'Ayala, G. G.; Malinconico, M.; Laurienzo, P.; Tardy, A.; Guillaneuf, Y.; Lansalot, M.; D'Agosto, F.; Charleux, B., RAFT/MADIX Copolymerization of Vinyl Acetate and 5,6-Benzo-2-methylene-1,3-dioxepane. *Journal of Polymer Science Part a-Polymer Chemistry* **2014,** *52* (1), 104-111.
40. Kobben, S.; Ethirajan, A.; Junkers, T., Synthesis of degradable poly(methyl methacrylate) star polymers via RAFT copolymerization with cyclic ketene acetals. *Journal of Polymer Science Part A: Polymer Chemistry* **2014,** *52* (11), 1633-1641.
41. Decker, C. G.; Maynard, H. D., Degradable PEGylated protein conjugates utilizing RAFT polymerization. *Eur. Polym. J.* **2015,** *65*, 305-312.
42. Ganda, S.; Jiang, Y.; Thomas, D. S.; Eliezar, J.; Stenzel, M. H., Biodegradable Glycopolymeric Micelles Obtained by RAFT-controlled Radical Ring-Opening Polymerization. *Macromolecules (Washington, DC, U. S.)* **2016,** *49* (11), 4136-4146.
43. Wei, Y.; Connors, E. J.; Jia, X.; Wang, B., First Example of Free Radical Ring-Opening Polymerization with Some Characteristics of a Living Polymerization. *Chemistry of Materials* **1996,** *8* (3), 604-606.
44. Jin, S.; Gonsalves, K. E., A study of the mechanism of the free-radical ring-opening polymerization of 2-methylene-1,3-dioxepane. *Macromolecules* **1997,** *30* (10), 3104-3106.
45. Zhu, P. C.; Wu, Z.; Pittman, C. U., Jr., Ring opening during the cationic polymerization of 2-methylene-1,3-dioxepane: cyclic ketene acetal initiation with sulfuric acid supported on carbon. *J. Polym. Sci., Part A: Polym. Chem.* **1997,** *35* (3), 485-491.
46. Jin, S.; Gonsalves, K. E., Synthesis and Characterization of Functionalized Poly(ε-caprolactone) Copolymers by Free-Radical Polymerization. *Macromolecules* **1998,** *31* (4), 1010-1015.
47. Wei, Y.; Connors, E. J.; Jia, X.; Wang, C., Controlled free radical ring-opening polymerization and chain extension of the "living" polymer. *J. Polym. Sci., Part A: Polym. Chem.* **1998,** *36* (5), 761-771.
48. Roberts, G. E.; Coote, M. L.; Heuts, J. P. A.; Morris, L. M.; Davis, T. P., Radical Ring-Opening Copolymerization of 2-Methylene-1,3-Dioxepane and Methyl Methacrylate: Experiments Originally Designed To Probe the Origin of the Penultimate Unit Effect. *Macromolecules* **1999,** *32* (5), 1332-1340.

49. Morris, L. M.; Davis, T. P.; Chaplin, R. P., An assessment of the copolymerization reaction between styrene and 2-methylene-1,3-dioxepane. *Polymer* **2000,** *42* (2), 495-500.
50. Sun, L. F.; Zhuo, R. X.; Liu, Z. L., Synthesis and enzymatic degradation of 2-methylene-1,3-dioxepane and methyl acrylate copolymers. *J. Polym. Sci., Part A: Polym. Chem.* **2003,** *41* (18), 2898-2904.
51. Agarwal, S., Microstructural Characterisation and Properties Evaluation of Poly (methyl methacrylate-co-ester)s. *Polym. J* **2006,** *39* (2), 163-174.
52. Xu, J.; Liu, Z.-L.; Zhuo, R.-X., Synthesis and biodegradability evaluation of 2-methylene-1,3-dioxepane and styrene copolymers. *Journal of Applied Polymer Science* **2007,** *103* (2), 1146-1151.
53. Kwon, S.; Lee, K.; Bae, W.; Kim, H., Precipitation polymerization of 2-methylene-1,3-dioxepane in supercritical carbon dioxide. *Polym. J. (Tokyo, Jpn.)* **2008,** *40* (4), 332-338.
54. Agarwal, S.; Kumar, R.; Kissel, T.; Reul, R., Synthesis of Degradable Materials Based on Caprolactone and Vinyl Acetate Units Using Radical Chemistry. *Polym. J* **2009,** *41* (8), 650-660.
55. Seema, A.; Liqun, R., Polycaprolactone-Based Novel Degradable Ionomers by Radical Ring-Opening Polymerization of 2-Methylene-1,3-dioxepane. *Macromolecules* **2009,** *42* (5), 1574-1579.
56. Maji, S.; Zheng, M.; Agarwal, S., Functional Degradable Polymers via Radical Ring-Opening Polymerization and Click Chemistry. *Macromolecular Chemistry and Physics* **2011,** *212* (23), 2573-2582.
57. Guo, J.-w.; Ma, Q.; Cui, Y.-h.; Liu, S.; Peng, J.-p., Synthesis and characterization of biodegradable copolymers as non-phosphorous detergent builders. *Gaofenzi Xuebao* **2012,** (9), 958-964.
58. Jin, Q.; Maji, S.; Agarwal, S., Novel amphiphilic, biodegradable, biocompatible, cross-linkable copolymers: synthesis, characterization and drug delivery applications. *Polym. Chem.* **2012,** *3* (10), 2785-2793.
59. Maji, S.; Mitschang, F.; Chen, L.; Jin, Q.; Wang, Y.; Agarwal, S., Functional Poly(Dimethyl Aminoethyl Methacrylate) by Combination of Radical Ring-Opening Polymerization and Click Chemistry for Biomedical Applications. *Macromol. Chem. Phys.* **2012,** *213* (16), 1643-1654.
60. Undin, J.; Illanes, T.; Finne-Wistrand, A.; Albertsson, A.-C., Random introduction of degradable linkages into functional vinyl polymers by radical ring-opening polymerization, tailored for soft tissue engineering. *Polym. Chem.* **2012,** *3* (5), 1260-1266.
61. Undin, J.; Finne-Wistrand, A.; Albertsson, A.-C., Copolymerization of 2-Methylene-1,3-dioxepane and Glycidyl Methacrylate, a Well-Defined and Efficient Process for Achieving Functionalized Polyesters for Covalent Binding of Bioactive Molecules. *Biomacromolecules* **2013,** *14* (6), 2095-2102.

62. Zhang, Y.; Aigner, A.; Agarwal, S., Degradable and Biocompatible Poly(N,N-dimethylaminoethyl Methacrylate-co-caprolactone)s as DNA Transfection Agents. *Macromol. Biosci.* **2013,** *13* (9), 1267-1275.
63. Cai, T.; Chen, Y.; Wang, Y.; Wang, H.; Liu, X.; Jin, Q.; Agarwal, S.; Ji, J., Functional 2-methylene-1,3-dioxepane terpolymer: a versatile platform to construct biodegradable polymeric prodrugs for intracellular drug delivery. *Polym. Chem.* **2014,** *5* (13), 4061-4068.
64. Hedir, G. G.; Bell, C. A.; Ieong, N. S.; Chapman, E.; Collins, I. R.; O'Reilly, R. K.; Dove, A. P., Functional Degradable Polymers by Xanthate-Mediated Polymerization. *Macromolecules* **2014,** *47* (9), 2847-2852.
65. Louguet, S.; Verret, V.; Bedouet, L.; Servais, E.; Pascale, F.; Wassef, M.; Labarre, D.; Laurent, A.; Moine, L., Poly(ethylene glycol) methacrylate hydrolyzable microspheres for transient vascular embolization. *Acta Biomater.* **2014,** *10* (3), 1194-1205.
66. Undin, J.; Finne-Wistrand, A.; Albertsson, A.-C., Adjustable Degradation Properties and Biocompatibility of Amorphous and Functional Poly(ester-acrylate)-Based Materials. *Biomacromolecules* **2014,** *15* (7), 2800-2807.
67. Asoh, T.-A.; Nakajima, T.; Matsuyama, T.; Kikuchi, A., Surface-Functionalized Biodegradable Nanoparticles Consisting of Amphiphilic Graft Polymers Prepared by Radical Copolymerization of 2-Methylene-1,3-Dioxepane and Macromonomers. *Langmuir* **2015,** *31* (24), 6879-6885.
68. Bell, C. A.; Hedir, G. G.; O'Reilly, R. K.; Dove, A. P., Controlling the synthesis of degradable vinyl polymers by xanthate-mediated polymerization. *Polym. Chem.* **2015,** *6* (42), 7447-7454.
69. Chen, T.; Cai, T.; Jin, Q.; Ji, J., Design and fabrication of functional polycaprolactone. *e-Polym.* **2015,** *15* (1), 3-13.
70. Shi, Y.; Agarwal, S., Thermally stable optically transparent copolymers of 2-methylene-1,3-dioxepane and N-phenyl maleimide with degradable ester linkages. *e-Polym.* **2015,** *15* (4), 217-226.
71. Shi, Y.; Zhou, P.; Jérôme, V.; Freitag, R.; Agarwal, S., Enzymatically Degradable Polyester-Based Adhesives. *ACS Biomaterials Science & Engineering* **2015**.
72. Carter, M. C. D.; Jennings, J.; Appadoo, V.; Lynn, D. M., Synthesis and Characterization of Backbone Degradable Azlactone-Functionalized Polymers. *Macromolecules (Washington, DC, U. S.)* **2016,** *49* (15), 5514-5526.
73. Bailey, W. J.; Ni, Z.; Wu, S.-R., Synthesis of poly-ϵ-caprolactone via a free radical mechanism. Free radical ring-opening polymerization of 2-methylene-1,3-dioxepane. *Journal of Polymer Science: Polymer Chemistry Edition* **1982,** *20* (11), 3021-3030.
74. Agarwal, S., Microstructural characterisation and properties evaluation of poly (methyl methacrylate-co-ester)s. *Polymer Journal* **2007,** *39* (2), 163-174.

75. Landfester, K., The Generation of Nanoparticles in Miniemulsions. *Advanced Materials* **2001,** *13* (10), 765-768.
76. Landfester, K., Miniemulsion Polymerization and the Structure of Polymer and Hybrid Nanoparticles. *Angewandte Chemie International Edition* **2009,** *48* (25), 4488-4507.
77. Peters, M.; Zaquen, N.; D'Olieslaeger, L.; Bové, H.; Vanderzande, D.; Hellings, N.; Junkers, T.; Ethirajan, A., PPV-Based Conjugated Polymer Nanoparticles as a Versatile Bioimaging Probe: A Closer Look at the Inherent Optical Properties and Nanoparticle–Cell Interactions. *Biomacromolecules* **2016,** *17* (8), 2562-2571.
78. Appendix A - Data for Engineering Materials A2 - Ashby, Michael F. In *Materials Selection in Mechanical Design (Fourth Edition)*, Butterworth-Heinemann: Oxford, 2011; pp 495-523.

Chapter 6

Materials and methods

6.1 Analytical Equipment

Liquid state NMR ^{1}H-NMR spectra were recorded in deuterated chloroform (unless otherwise mentioned) with two NMR-spectrometers (300 and 400 MHz) from Agilent (Varian) using a 5 mm-4-nucleus AutoSWPFG probe. For all polymer samples a 12 second pulse delay was applied

Size exclusion chromatography Analysis of the MWDs of the polymer samples were performed on a Tosoh EcoSEC System, comprising an autosampler, a PSS guard column SDV (50 × 7.5 mm), followed by three PSS SDV analytical linear XL columns (5 µm, 300 × 7.5 mm) and a differential refractive index detector (Tosoh EcoSEC RI) using THF as the eluent at 40 °C with a flow rate of 1 $mL \cdot min^{-1}$. The SEC system was calibrated using linear narrow polystyrene standards ranging from 474 to 7.5 x 10^{6} $g \cdot mol^{-1}$ (PS (K = 14.1 x 10^{-5} $dL \cdot g^{-1}$ and α = 0.70)). Polymer concentrations were in the range of 3–5 $mg \cdot mL^{-1}$. Since Mark-Houwink parameters for CKA-polymers are not reported, only apparent values for these samples are discussed.

In-Situ InfraRed Spectroscopy In-situ Infrared measurements were performed on a Metter Toledo ReactIR 15 machine equipped with a AgX 6.3 Di-comp probe.

Attenuated Total Reflectance InfraRed spectroscopy ATR-IR was measured on a Brucker Tensor 27 FT-IR spectrophotometer (nominal resolution 4 cm^{-1}).

Ultrasonication Ultrasonication was performed on a Branson 450 W digital sonifier (1/4” tip) with 65% amplitude in a pulse regime (20 s sonication, 20 s pause) for 2 minutes under ice cooling.

Dynamic light scattering and Zeta-potential Dynamic light scattering and Zeta-potential were performed on a Brookhaven Instruments ZetaPALS system.

Transmission Electron Microscopy The study of both size and morphology of the conjugated nanoparticles was performed with TEM on a Tecnai G2 spirit twin, FEI, at an accelerating voltage of 120 keV.

Atomic Force Microscopy The topographic (height) and phase images of the films were investigated by an AFM (NX-10, Park systems) in non-contact mode. The AFM tip was n-type silicon probe and has a spring constant and radius of 13-77 N/m and <10 nm, respectively. The image of a 1 um x 1 um sample area was recorded with a 256 x 256 pixel resolution at a scanning rate of 1 Hz.

6.2 Experimental part for Chapter 2 -, Synthesis of Degradable Poly(Methyl Methacrylate) Star Polymers via RAFT Copolymerization with Cyclic Ketene Acetals

Materials $LiAlH_4$ (95%), dimethyl phthalate (99%), anhydrous $MgSO_4$ (99+%), anhydrous NaOH (99+%), Na_2HCO_3 (99+%), potassium *tert*-butoxide (98+%), dicumyl peroxide (99%), anhydrous Na_2SO_4 (99+%), cyclohexane (99+%), celite® 545, 1-octanethiol (97%), triethylamine (99+%), CS_2 (99,9%) and methyl-2-bromopropionate (MBP) (99%), ordered from Acros were used as received. Methyl methacrylate (MMA) stabilized (99%) ordered from Acros was passed over a basic alumina column prior to use. *tert*-Butyl alcohol extra pure (99,5%) ordered from Acros was distilled over CaH_2 prior to use. Anisole ordered from Acros was stored on mol sieves. Bromoacetaldehyde diethyl acetal (97%), *p*-toluenesulfonic acid mono hydrate (≥98,5%) and pentaerythritol *tetrakis*(3-mercaptopropionate) (>95%) ordered from Sigma Aldrich were used as received. Sulfuric acid (AR), chloroform (AR), n-hexane, ethyl acetate (AR), n-pentane (AR) and hydrochloric acid 37% (AR) ordered from VWR were used as received. Toluene (AR) and diethyl ether (AR) were distilled using MBraun SPS-5580 solvent purification system.

5,6-benzo-2-methylene-1,3-dioxepane (BMDO) was synthesized using the route as published by Wickel *et al.* with some adaptations and the tetra-functional RAFT agent was prepared using a method as published by Boschman *et al.*

Synthesis of 1,2-benzene dimethanol

In a one liter three neck flask equipped with a reflux condenser and dripping funnel, 28 grams (0.74 mol) of $LiAlH_4$ was weighed. The set-up was put under

inert atmosphere. 500 ml of dry THF was slowly added to the three neck flask. A mixture of 100 ml (0.61 mol) of dimethyl phthalate in 150 ml of dry THF was added to the dripping funnel and was added dropwise to the three neck flask. The reaction was cooled by ice during the addition. After the completion of the addition the temperature was raised 80°C to maintain a gentle reflux. The reaction was left to run overnight. The mixture was hydrolyzed by gently pouring it into a mixture of 200 ml concentrated sulfuric acid in 750 ml of water. The product was extracted three times with 500 ml of chloroform and the organic phase was washed with 250 ml saturated Na_2HCO_3 solution and 250 ml of water. The organic phase was then dried over $MgSO_4$. After filtering off the solid, the solvents were removed under vacuum, resulting in a white residue. The product was recrystallized in 500 ml of a 50:50 mixture of chloroform and n-hexane resulting in 72 grams (85%) of white crystals. ^{1}H-NMR (300 MHz; $CDCl_3$): chemical shift (ppm) 2.93 (s, 2H), 4.71 (s, 4H) and 7.31 (s, 4H).

Synthesis of 5,6-benzo-2-(bromomethyl)-1,3-dioxepane

To a 250 ml round bottom flask, 72.02 gram (0.52 mol) of 1,2-benzene dimethanol, 78.4 ml (0.52 mol) of bromoacetaldehyde diethyl acetal and 720 mg of *p*-toluenesulfonic acid mono hydrate were added. The flask was equipped with a Claisen condenser and the set-up was put under inert atmosphere. The reaction was heated to 120°C and was left to run until most of the expected ethanol (60.7 ml (1.04 mol)) was collected. Afterwards, de reaction was left to cool down to room temperature in which the mixture solidified. The solid was dissolved in 250 ml of chloroform and was washed with 250 ml of saturated Na_2HCO_3 solution and 250 ml of water. The organic phase was dried over Na_2SO_4. The solvent was removed under vacuum leaving a slightly brown solid in the flask. The solid was

recrystallized in 500 ml cyclohexane, resulting in 94.62 (75%) of white fluffy crystals. ^{1}H-NMR (300 MHz; $CDCl_3$): chemical shift (ppm) 3.43 (d, 2H), 4.92 (s, 4H), 5.11 (t, 1H) and 7.18-7.24 (m, 4H).

Synthesis of 5,6-benzo-2-methylene-1,3-dioxepane (BMDO)

To a one liter round bottom flask equipped with a reflux condenser, 90 gram (0.37 mol) of 5,6-benzo-2-(bromomethyl)-1,3-dioxepane, 41.52 (0,37 mol) potassium *tert*-butoxide and 500 ml dry *tert*-butyl alcohol were added. The reaction was put under inert atmosphere and was heated to 80°C to maintain a gentle reflux. The reaction was left to run for 15 hours. After letting the reaction cool down, 500 ml of dry diethyl ether was added. The solid was filtered of over a small celite column and solvent was removed under vacuum. The resulting product was purified by distillation under vacuum (typically at T=80°C and p=0,3 mbar). The liquid solidified on standing and resulted in 50 gram (83%) of white crystals. Due to the possibility of degradation at atmospheric conditions, the product was stored under nitrogen atmosphere at -20°C. ^{1}H-NMR (300 MHz; $CDCl_3$): chemical shift (ppm) 3.71 (s, 2H), 5.06 (s, 4H), 7.06-7.09 (m, 2H) and 7.22-7.25 (m, 2H).

Synthesis of methyl-2-(((octylthio)carbonothioyl)thio)propanoate (RA-1)

In a 100 ml three neck flask equipped with a reflux condenser and dripping funnel, 1,2 ml (6,84 mmol) of octanethiol and 50 ml of chloroform were added. 1,14 ml (8,20 mmol) of triethylamine was added and the mixture was left to stir for one hour. Subsequently, 0,92 ml (8,20 mmol) of methyl-2-bromopropionate in 5 ml of CS_2 were added dropwise to the reaction. During the addition, the mixture turned yellow to slightly orange. After the addition was completed, the reaction

was left to stir overnight at room temperature. The mixture was quenched 56 ml of a 10 % HCl solution. The layers were separated and the organic layer was washed twice with 50 ml of water. The organic layer was dried over Na_2SO_4. After filtering off the solid, solvents were removed under vacuum, resulting in 1,835 gr (87 %) yellow/orange slightly viscous liquid. ^{1}H-NMR (300 MHz; $CDCl_3$): chemical shift (ppm) 0.85 (t, 3H), 1.25-1.32 (m, 10H), 1.57 (d, 3H, 1.66 (m, 2H), 3.32 (t, 2H), 3.71 (s, 3H) and 4.82 (q, 1H).

Synthesis of pentaerythritol-tetrakis-(3-(S-methyl-2-propanoato-trithiocarbonyl)propanoate) (RA-4)

The four functional Z-star RAFT agent was synthesized using the procedure from Boschman *et al.*.

A 500 ml three neck flask was charged with 1.42 gr (5.89 mmol) of pentaerythritol-*tetrakis*(3-mercaptopropionate and 200 ml of chloroform. Under stirring, 6.57 ml (47.1 mmol, 8 eq) triethylamine was slowly added to the flask. The reaction was left to stir for an hour at room temperature. Subsequently, 20 ml of CS_2 and 5.26 ml (47.1 mmol, 8 eq) of methyl-2-bromopropionate were added dropwise to the reaction after which the reaction as left to stir overnight. The reaction was then quenched by adding 200 ml of a 10 % HCl solution. Afterwards, the layers were separated and the organic layer was washed three times with 200 ml of water. The organic layer was dried over $MgSO_4$. After removing the drying agent by filtration, the solvents were evaporated under vacuum. The residue, an orange/yellow viscous liquid, was purified by column chromatography using a 3:1 mixture of n-pentane/ethyl acetate as eluent. The product (4 gr (60%)) was obtained as an orange, highly viscous liquid. ^{1}H-NMR

(300 MHz; $CDCl_3$): chemical shift (ppm) 1.57 (d, 12H), 2.77 (t, 8H), 3.57 (t, 12H), 4.10 (s, 8H) and 4.80 (q, 4H).

Free-radical (co)polymerization of BMDO and MMA

The composition of the polymer was set by changing the monomer concentrations in the feed. In a typical run, a schlenk flask was charged with 125 mg (0.77 mmol) BMDO, 77.5 µl (0.77 mmol) MMA, 6.9 mg DCP (0.026 mmol) and 250 µl of anisole. The mixture was degassed by bubbling with nitrogen gas. Subsequently, the flask was immersed in an oil bath at a temperature of 120°C and was left to run for 24 hours. To achieve low conversions, the IR-probe was inserted in the flask and the conversion was estimated from the in-situ IR-spectra. After acquiring the desired conversion, the reaction mixture was poured into an aluminum bowl with known weight. All solvents and reactants were removed in a vacuum oven at 40°C and the conversion was determined gravimetrically. M_n, M_w and PDI were determined by SEC in THF.

(Co)polymerization of BMDO and MMA under RAFT conditions

In a typical run, 250 mg (1.54 mmol) BMDO, 164 µl (1.54 mmol) MMA, 9.5 mg (0.031 mmol) RA-1, 0.83 mg ($3.1 \cdot 10^{-3}$ mmol) DCP and 500 µl were put into a schlenk flask. The flask was degassed by three freeze-pump-thaw cycles and was subsequently put under a nitrogen atmosphere. The flask was immersed in an oil bath at 100°C. The reaction was left to run for 24 hours after which the content of flask was transferred to an aluminum bowl with known weight. The solvents/reactants were removed in a vacuum oven at 40°C. The conversion was determined gravimetrically by weighing the dry polymer. M_n, M_w and PDI were determined by SEC in THF.

Preparation of tetra-functional (co)polymers of BMDO and MMA using a Z-star RAFT approach

A similar procedure as the mono-functional polymer was used, the only difference being an increased amount of initiator (four times higher). In a typical run, 250 mg (1.54 mmol) BMDO, 164 µl (1.54 mmol) MMA, 35.1 mg (0,031 mmol) RA-4, 3.32 mg (0.012 mmol) DCP and 500 µl toluene were weighed into a schlenk flask. The flask was degassed by three freeze-pump-thaw cycles. The flask was put under a nitrogen atmosphere and the reaction was started by putting the flask in an oil bath with a temperature of 90°C. The reaction was left to run for 24 hours and was subsequently poured into an aluminum bowl with known weight. The solvent/reactants were removed in a vacuum oven at 40°C. The conversion was gravimetrically by weighing the dry polymer. M_n, M_w and PDI were determined by SEC in THF.

Degradation of (co)polymers of BMDO and MMA

In a typical experiment, 200 mg of polymer was weighed into a glass vial. A minimal amount of THF was added until the polymer as completely dissolved. Subsequently, 5 ml of a 1M NaOH solution was added and the reaction was left stir at room temperature. Samples were taken at several time intervals to check for a decline in molecular weight.

6.3 Experimental part for Chapter 3-, Copolymer evaluation of MPDL and various vinyl monomers.

Materials Methyl methacrylate (MMA, Acros, 99%), Methyl acrylate (MA, Acros, 99%), n-butyl acrylate (nBA, Acros, 99 %), Styrene (Sigma Aldrich, 99%) and di(ethylene glycol) ethyl ether acrylate (DEGA, Acros, 99%) were deinhibited over columns of activated basic alumina, prior to use. styrene glycol (97%), dicumyl peroxide (DCP, 99%), Potassium *tertiary*-butoxide (tert-BuOK, 99+%), *tertiary*-Butyl Alcohol (*tert*-BuOH, 99+%) Dowex® 50WX8 were ordered from Acros and used as received.

RAFT-agent RA-1 was synthesized as described in chapter 6.2. 2-methylene-4-phenyl-1,3-dioxolane (MPDL) was synthesized according to the procedure reported by Delplace *et al*. [1]

Synthesis of 2-chloromethyl-4-phenyl-1,3-dioxolane A 200 mL round-bottom flask fitted with a magnetic bar and equipped with a claisen condensor (to collect methanol), was charged with chloroacetaldehyde dimethyl acetal (25 g, 2.01 × 10-1 mol, 1 eq.), styrene glycol (27.75 g, 2.01 × 10-1 mol, 1 eq.) and Dowex 50 (H^+) resin (250 mg) and was subsequently heated to 120 °C. This reaction was left to stir until no methanol was collected anymore. The reaction was left to cool down to ambient temperature and was subsequently filtered over a paper filter to remove the resin. The residual methanol was then removed under reduce pressure and the crude product was purified by vacuum distillation at T=90°C at a pressure of $p=3\cdot10^{-2}$ mbar. Yield: 70 % (28 g, 1.4 × 10-1 mol) of a mixture of two diastereoisomers (a white solid and a colorless liquid). ^{1}H-NMR (300 MHz; $CDCl_3$): chemical shift (ppm) 3,46-3,56 (m, 2H), 3,74-4,48 (m, 2H), 5,06-5,19 (m, 1H), 5,32-5,50 (m, 1H), 7,28-7,43 (m, 5H).

Synthesis of 2-methylene-4-phenyl-1,3-dioxolane (MPDL) A 250 mL three-neck round bottom flask, equiped with a reflux condenser and a dropping funnel, was charged with *tert*-BuOK (10.1 g, $9{,}02 \cdot 10^{-2}$ mol, 1.2 eq.) and 110 mL *tert*-BuOH. The mixture was put under an inert atmosphere and was heated to 80 °C. 2-chloromethyl-4-phenyl-1,3-dioxolane (15 g, $7.54 \cdot 10^{-2}$ mol, 1 eq.) in 40 mL of *tert*-BuOH were loaded in the dropping funnel and dropwise added to the reaction. After the addition was completed, the temperature was raised to 100 °C to maintain a gentle reflux overnight. After the reaction mixture was cooled down to ambient temperature, 200 mL of cold diethyl ether were added and the resulting precipitate was removed by filtration over a paper filter. After the solvents were removed under reduced pressure, the residue was purified by vacuum distillation at T=75°C at a pressure of $p=3 \cdot 10^{-2}$ mbar. A small amount (± 2 wt%) of dry pyridine was added to stabilize the material. Note that pyridine was not removed prior to any of the polymerizations. Yield: 45% (5.5 g, $3.4 \cdot 10^{-2}$ mol) of a colorless liquid. ^{1}H-NMR (300 MHz; $CDCl_3$): chemical shift (ppm) 3.33-3.37 (dd, 2H), 4.02 (t, 1H), 4.50 (t, 1H), 5.35 (t, 1H) and 7.26-7.44 (m, broad, 5H).

General method for free radical (co)polymerization of MPDL and vinyl monomers using the In-Situ IR probe In a typical run, a 50 ml three neck flask was equipped with a magnetic stir bar and the IR-probe. The set-up was preheated in an oil bath at T=100°C. In a separate flask, 2.53 g ($1.56 \cdot 10^{-2}$ mol) MPDL, 1.47 g ($1.56 \cdot 10^{-2}$ mol) MMA and 0.8 ml of dry toluene were weighed. In another flask, a stock solution of 300 mg of DCP in 1 ml of dry toluene was prepared. Both flasks were degassed by purging with Argon for 15 minutes. The content of flask containing the monomers was transferred to the preheated reaction flask using an argon flushed syringe and was left to warm-up for 10 minutes. To initiate the reaction, 0.2 ml of stock solution (containing 2 wt% of

DCP) was added to the reaction using an argon flushed syringe. When the reaction was completed (or at any desired point) the polymerization mixture was poured in an aluminium pan with known weight which was subsequently left to dry overnight. Further drying was done in a vacuum oven at T=70°C until constant weight. The polymer was analyzed by ^{1}H-NMR and SEC in THF.

General method for RAFT (co)polymerization of MPDL and vinyl monomers using the In-Situ IR probe In a typical run, a 50 ml three neck flask was equipped with a magnetic stir bar and the IR-probe. The set-up was preheated in an oil bath at T=100°C. In a separate flask, 1.12 g ($6.91 \cdot 10^{-3}$ mol, 50 eq) MPDL, 0.59 g ($6.91 \cdot 10^{-3}$ mol, 50 eq) MA, 42.6 mg ($1.38 \cdot 10^{-4}$ mol, 1 eq) of RA-1 and 0.8 ml of dry toluene were weighed. In another flask, a stock solution of 3.72 mg ($6.91 \cdot 10^{-5}$, 5 times 0.1 eq) of DCP in 1 ml of dry toluene was prepared. Both flasks were degassed by purging with Argon for 15 minutes. The content of flask containing the monomers was transferred to the preheated reaction flask using an argon flushed syringe and was left to warm-up for 10 minutes. To initiate the reaction, 0.2 ml of stock solution (containing 0.1 eq of DCP) was added to the reaction using an argon flushed syringe. When the reaction was completed (or at any desired point) the polymerization mixture was poured in an aluminium pan with known weight which was subsequently left to dry overnight. Further drying was done in a vacuum oven at T=70°C until constant weight. The polymer was analyzed by ^{1}H-NMR and SEC in THF.

General method for RAFT (co)polymerization of MPDL and vinyl monomers In a typical run, a 10 ml vial was charged with 280 mg ($1.72 \cdot 10^{-3}$ mol, 5 eq) MPDL, 220 mg ($1.72 \cdot 10^{-3}$ mol, 5 eq) BA, 106 mg ($3.44 \cdot 10^{-4}$ mol, 1 eq), 9.31 mg ($3.44 \cdot 10^{-5}$ mol, 0.1 eq) DCP and 1 ml of dry toluene. After adding a magnetic stir bar, the vial was closed with a septum and some metal wire and was

subsequently purged with Argon for 15 minutes. The flas was then transferred to a preheated copper heat block at T=100°C and was left to stir overnight. The contents of the flask were poured in an aluminium pan with known weight which was subsequently left to dry overnight. Further drying was done in a vacuum oven at T=70°C until constant weight. The polymer was analyzed by ^{1}H-NMR and SEC in THF.

6.4 Experimental part for Chapter 4 -, Synthesis of functional degradable copolymers using RROP and click-chemistry

Materials Propargyl alcohol, Acryloyl chloride, triethyl amine, DCM, silver nitrate, DBU, TMS-Cl, 1,4-butanediol, chloroacetaldehyde dimethyl acetal, dowex 50, hexadecane, KOH, solketal, propargyl bromide, toluene, sodium hydride 60%, anhydrous MgSO4, methanol, tert-BuOK, tert-BuOH, diethylene glycol monomethyl ether

Synthesis of propargyl acrylate A 250 ml three neck flask equipped with a stir bar was charged with 10.1 ml (0.17 mol) propargyl alcohol, 22.1 ml (0.16 mol) trimethylamine and 90 ml of dry dichloromethane. The mixture was put under inert atmosphere and cooled down to 0°C in an ice/water bath. Subsequently, 11.7 ml (0.144 mol) of acryloyl chloride was added dropwise using an argon flushed syringe. After the addition was completed, the reaction was left to stir overnight at ambient temperature. The reaction was quenched with 100 ml of water and the contents of the flash were transferred to an extraction funnel. The layers were separated and the water layer was washed 3 times with dichloromethane (100 ml). Combined organic layer was washed with brine and was dried over $MgSO_4$. After concentration under reduced pressure, the product was distilled under vacuum yielding a slightly yellow liquid. Yield 15.06g (95%), ^{1}H NMR (300 MHz, CHCl3): chemical shift (ppm) 2.48 (t, 1H), 5.13 (d, 2H) 5.80 (dd, 1H), 6.1 (dd, 1H), 6.5 (dd, 1H).

Synthesis of trimethylsilyl propargyl acrylate (PA-TMS) A 250 ml three neck flask, equipped with a condenser and dropping funnel, was charged with 573 mg

(6 mmol) Silver Nitrate and 75 ml of dry dichloromethane. The suspension was left to stir for 30 minutes. Subsequently, 7.5 g (68 mmol) Propargyl acrylate and 10.7 ml (71.3 mmol) of DBU were added to the suspension. The reaction was heated to T=40°C after which 14.1 ml (95.2 mmol) trimethylsilyl chloride was added dropwise to the reaction. The reaction was left to stir overnight at T=40°C. The reaction was left to cool down to ambient temperature and concentrated under reduced pressure. The product was isolated by distillation under high vacuum resulting in 4.94 g (62%) of a slightly yellow liquid. ^{1}H NMR (300 MHz, CHCl3): chemical shift (ppm) 0.19 (s, 9H), 4.77 (s, 2H), 5.85 (dd, 1H), 6.16 (dd, 1H), 6.43 (dd, 1H)

Synthesis 2-chloromethyl-1,3-dioxepane 114 ml (1 mol) of chloroacetaldehyde dimethyl acetal, 89 ml (1 mol) of butanediol and 125 mg of Dowex 50 (H^{+}) resin were put in a 250 ml round bottom flask. The flask was equipped with a small vigreux column, a cooler and stir bar. The flask was immersed in an oil bath set to 115°C. The reaction was left to run until nearly all methanol (81 ml, 2 mol) was collected, approximately 5 hours. The reaction was left to cool down and the mixture was passed over a paper filter to remove the resin. The product was obtained by distillation from the reaction mixture (T=75-80°C at p=5 mbar), resulting in 107 ml (71%) of a clear viscous liquid. ^{1}H-NMR (300 MHz; CDCl3): chemical shift (ppm) 1.72 (m, 4H), 3.44 (d, 2H), 3.64-3.68 and 3.91-3.95 (m, 4H), 4.84 (t, 1H).

Synthesis of 2-methylene-1,3-dioxepane (MDO) A 500 ml round bottom flask was charged with a magnetic stir bar, 55,05 gram (0,37 mol) of 2-chloromethyl-1,3-dioxepane, 137,7 gram (3,7 mol) of potassium hydroxide and 500 ml of hexadecane. The flask was equipped with a condenser and was

immersed in an oil bath thermostated at 130°C. The reaction was left to reflux overnight. The insoluble material was removed by filtering over a celite column. The MDO was readily distilled from the mixture (T=30-40°C at p=5 mbar) resulting in 21.7 g (52%) of a colorless liquid, ^{1}H-NMR (300 MHz; $CDCl_3$): chemical shift (ppm) 1.72 (m, 4H), 3.45 (s, 2H), 3.91-3.94 (m, 4H).

Synthesis of 2,2-dimethyl-4-((prop-2-yn-1-yloxy)methyl)-1,3-dioxolane (1) To a solution of 4.8 g (36.5 mmol) solketal in 75 ml toluene at T=0°C was added 1.6 g (40 mmol) 60% sodium hydride over a period of 30 minutes followed by 6.9 ml (40 mmol) propargyl bromide (80% in toluene). The reaction was left to run overnight under inert atmosphere at room temperature. The reaction was quenched by adding 50 ml of water. The layers were extracted and the water layer was washed three times with 50 ml of dichloromethane. The organic extracts were combined and were dried over $MgSO_4$. After filtration, the solvents were removed under reduced pressure and the product was further purified by distillation under high vacuum (T=50°C at p=$2\cdot10^{-2}$ mbar) yielding 4.8 g (78%) of a colorless liquid. ^{1}H-NMR (300 MHz; $CDCl_3$): chemical shift (ppm) 1.35 (s, 3H), 1.42 (s, 3H), 2.45 (t, 1H), 3.58 (dd, 2H), 3.71-3.76 (m, 1H), 4.04-4.09 (m, 1H), 4.20 (t, 2H), 4.29 (tt, 1H).

Synthesis of (3-((2,2-dimethyl-1,3-dioxolan-4-yl)methoxy)prop-1-yn-1-yl)trimethylsilane (2) A 250 ml three neck flask, equipped with a condenser and dropping funnel, was charged with 573 mg (6 mmol) Silver Nitrate and 75 ml of dry dichloromethane. The suspension was left to stir for 30 minutes. Subsequently, 11.6 g (68 mmol) of (1) and 10.7 ml (71.3 mmol) DBU were added to the suspension. The reaction was heated to T=40°C after which 14.1 ml (95.2 mmol) trimethylsilyl chloride was added dropwise to the reaction. The reaction

was left to stir overnight at T=40°C. The reaction was left to cool down to ambient temperature and concentrated under reduced pressure. The product was isolated by distillation under high vacuum resulting in 16.4 g (65%) of a colorless oil. ^{1}H NMR (300 MHz, CHCl3): chemical shift (ppm) 0.15 (s, 9H), 1.35 (s, 3H), 1.42 (s, 3H), 3.58 (dd, 2H), 3.71-3.76 (m, 1H), 4.04-4.09 (m, 1H), 4.20 (s, 2H), 4.29 (tt, 1H).

Synthesis of 3-((3-(trimethylsilyl)prop-2-yn-1-yl)oxy)propane-1,2-diol (3) A 100 ml round bottom flask was charged with 2 g (8.4 mmol) of (2), 4.5 g of Dowex 50 (H^+) resin and 50 ml of methanol. The reaction was left to stir at ambient temperature until completion – this was checked by TLC (pentane:AcOEt 1:1)-. After completion, the reaction was poured over a paper filter to remove the resin. The solvent was removed under reduced pressure yielding 2.9 g (95%) of an orange/red oil which was used without further purification. ^{1}H-NMR (300 MHz, $CHCl_3$): chemical shift (ppm) 0.15 (s, 9H), 4.20 (s, 2H), 4.29 (m, 1H), 3.71-4.09 (m, 4H).

Synthesis of (3-((2-(chloromethyl)-1,3-dioxolan-4-yl)methoxy)prop-1-yn-1-yl)trimethylsilane (4) 2.5 g (12.3 mmol) of (3), 1.4 ml (12.3 mmol) of chloroacetaldehyde dimethyl acetal and 20 mg of Dowex 50 (H^+) resin were put in a 50 ml round bottom flask. The flask was equipped with a small vigreux column, a cooler and stir bar. The flask was immersed in an oil bath set to 115°C. The reaction was left to run until nearly all methanol was collected, approximately 5 hours. The reaction was left to cool down and the mixture was passed over a paper filter to remove the resin. The product was obtained by distillation from the reaction mixture (T=75-80°C at $p=2\cdot10^{-2}$ mbar), resulting in 2.59 g (80%) of a clear viscous liquid. ^{1}H-NMR (300 MHz; CDCl3): chemical shift (ppm) 0.15 (s, 9H),

3.46-3.56 (m, 2H) 3.58 (dd, 2H), 3.71-3.76 (m, 1H), 4.04-4.09 (m, 1H), 4.20 (s, 2H), 4.29 (tt, 1H).

Synthesis of trimethyl(3-((2-methylene-1,3-dioxolan-4-yl)methoxy) prop-1-yn-1-yl)silane (CKA-Alkyn) A 100 mL three-neck round bottom flask, equipped with a reflux condenser, was charged with *tert*-BuOK (1.28 g, 11.4 mmol, 1.2 eq.) and 15 mL *tert*-BuOH. The mixture was put under an inert atmosphere and was heated to 80 °C. (4) (2.5 g, 9.5 mmol, 1 eq.) in 5 mL of *tert*-BuOH was added slowly to the reaction using a syringe. After the addition was completed, the temperature was raised to 100 °C to maintain a gentle reflux overnight. After the reaction mixture was cooled down to ambient temperature, 20 mL of cold diethyl ether were added and the resulting precipitate was removed by filtration over a paper filter. After the solvents were removed under reduced pressure, the residue was purified by vacuum distillation at T=90°C at a pressure of $p=2\cdot10^{-2}$ mbar. A small amount (± 2 wt%) of dry pyridine was added to stabilize the material. Note that pyridine was not removed prior to any of the polymerizations. Yield: 25% (540 mg) of a colorless liquid. ^{1}H-NMR (300 MHz; $CDCl_3$): chemical shift (ppm) 0.15 (s, 9H), 3.46-3.56 (m, 2H) 3.58 (dd, 2H), 3.71-3.76 (m, 1H), 4.04-4.09 (m, 1H), 3.33-3.37 (dd, 2H), 4.29 (tt, 1H).

Free-radical (co)polymerization MDO and PA-TMS In a typical run, 507 mg (4.46 mmol) MDO, 1.47 g (13.4 mmol) PA-TMS, 40 mg DCP (2 wt%) and 1 ml of toluene were weighed into a 10 ml vial. The reaction mixture was purged with nitrogen for 15 minutes. The vial was subsequently transferred to a preheated copper heat block thermostated at T=100°C. The reaction was left to react for 24 hours. The content of the vial was poured into an aluminium pan with known weight and was left to dry overnight at ambient conditions. The product was dried

further in a vacuum over at T=70°C until constant weight. The polymer was analyzed with ^{1}H-NMR and SEC in THF.

Deprotection of *poly*(caprolactone-*r*-PATMS) In a typical experiment, 500 mg of *poly*(caprolactone-*r*-PATMS) is dissolved in 30 ml of THF. Subsequently, 1.2 molar equivalents of acetic acid (with respect to alkyn units) is added to the polymer solution. The mixture was degassed by purging with nitrogen gas for 30 minutes. Afterwards, the mixture was cooled to T=-20°C in a sodium chloride:ice bath (1:3 by weight) followed by the slow addition of 1.2 molar equivalents (with respect to alkyn units) of TBAF (1M in THF). The reaction was allowed to warm up to ambient temperature and was left to stir overnight. The reaction mixture was passed over a short basic alumina column. Evaporation of solvents yielded a colorless solid. The polymer was analyzed by ^{1}H-NMR and SEC in THF.

Click reaction of *poly*(caprolactone-*r*-PA) with DEGAz In a typical experiment, 500 mg of *poly*(caprolactone-*r*-PA) was dissolved in 25 ml of DMF (100 mg per 5 ml). To this solution was added 1 molar equivalent (with respect to alkyn units) PMDETA and 1 molar equivalent (with respect to alkyn units) DEGAz. In a separate flask was weighed in 1 molar equivalent (with respect to alkyn units) CuBr. The polymer solution was purged with nitrogen for 30 minutes. The polymer solution was transferred to the CuBr loaded flask using a nitrogen flushed syringe. The reaction was left to stir for 24 hours at ambient temperature. The copper salts were removed over a basic alumina column and the solvents were removed under reduced pressure. The slightly green polymer was analyzed by ATR-IR, ^{1}H-NMR and SEC in THF.

Copolymers for MDO and CKA-Alkyn were prepared in analogous way as for MDO and PATMS.

6.5 Experimental part for Chapter 5-, The synthesis of degradable nanoparticles through a combination of radical ring-opening polymerization and miniemulsion.

Materials SDS, MilliQ water, chloroform, MPDL, Styrene, MMA, Dicumyl peroxide, toluene.

Copolymers of MPDL and styrene or MPDL and MMA were prepared according to the procedure described in chapter 6.3.

Preparation of *poly*(caprolactone-*r*-Benzyl acrylate) using a combination of miniemulsion and post-polymerization In a typical run, the continuous phase was prepared by dissolving 40 mg of SDS in 15 g of MilliQ water. In a separate vial, 3.42 g of benzyl acrylate, 270 mg MDO, 50 mg AIBN and 150 mg hexadecane were weighed. The continuous phase was subsequently added to the monomer (dispersed) phase and the mixture was left to pre-emulsify at 1000 rpm for 1 hour under stirring with a magnetic stirrer. The emulsion was ultrasonicated (for details see paragraph 6.1). Prior to polymerization, the miniemulsion was degassed by purging with nitrogen gas for 15 minutes under stirring. Post-polymerization was performed by immersing the miniemulsion in an oil bath thermostated at 90°C and was left to run overnight. The emulsion was filtered and solid content was determined by taking 300 mg of emulsion and evaporating all solvents. The particle size and ζ-potential were determined by DLS.

Preparation of *poly*(phenyl-butyrolactone-*r*-MMA) and *poly*(phenyl-butyrolactone-*r*-styrene) nanoparticles For the dispersed phase, 100 mg of polymer was dissolved in 3 g of chloroform. In a separate flask, 35 mg of SDS was dissolved in 12 g of MilliQ water. Both solutions were mixed and left to stir at 1000 rpm for 1 hour. Subsequently, the emulsion was ultrasonicated (for details

see chapter 6.1). After ultrasonication, the chloroform was evaporated at T=40°C for 6 hours under stirring. The emulsion was filtered and solid content was determined by taking 300 mg of emulsion and evaporating all solvents. The particle size and ζ-potential were determined by DLS.

6.6 References

1. Delplace, V.; Guegain, E.; Harrisson, S.; Gigmes, D.; Guillaneuf, Y.; Nicolas, J., A ring to rule them all: a cyclic ketene acetal comonomer controls the nitroxide-mediated polymerization of methacrylates and confers tunable degradability. *Chemical Communications* **2015,** *51* (64), 12847-12850.

Chapter 7

Summary and outlook

7.1 Summary

The use of radical ring-opening polymerization has expanded in recent years. Many examples have shown the versatility of this technique in the world of biomedical applications. The work presented in this thesis gives valuable (new) insights to the field of radical ring-opening polymerization and opens up paths for future applications in the biomedical field. Several aspects are presented here which, when combined, form a solid base for future use in preparing degradable nanoparticles with defined properties and the ability to allow post-functionalization in pursuit of preparing nanoparticles for drug delivery purposes.

Initial research focused on the synthesis of copolymers containing varying amounts of 5,6-benzo-2-methylene-1,3-dioxepane (BMDO) and methylmetacrylate (MMA). The copolymerization behavior was studied using an optimized way involving online IR-measurements during the polymerization. By fitting the Mayo-Lewis equation to the dataset, the reactivity ratios for both BMDO were calculated; r_{BMDO} = 0.33 ± 0.06 and r_{MMA} = 6.0 ± 0.8. This result was compared with data obtained by fitting the Skeist-equation to the same dataset resulting in somewhat similar value for r_{BMDO} = 0.7 and r_{MMA} = 3.88. Follow-up research on this combination was done by showing for the first time the synthesis of copolymers of BMDO and MMA with defined size, composition and architecture by using reversible addition/fragmentation transfer (RAFT)-conditions. The successful synthesis of linear as well as 4-arm star copolymers was shown with regards to composition. A hydrolytic degradation showed on these respective copolymers was performed and successful degradation in terms of molecular weight was observed.

Knowing the copolymerization of any system tremendously helps in predicting the outcome of the copolymer structure. To that extent, the procedure to determine reactivity ratios was optimized to allow for fast and easy screening. Based on the methods described before, the combination of online IR measurements and the Skeist equation was optimized and tested for several different combinations surrounding 2-methylene-4-phenyl-1,3-dioxolane (MPDL). I've shown that by using this method, reactivity ratios could be determined in a single experiment. A collection of reactivity ratios for MPDL and several typical vinyl monomers were determined as showing the versatility of this techniques (Table 7.1).

Table 7.1 Summary of the results for the determination of reactivity ratios for MPDL and various comonomers.

CKA	monomer	r_{MPDL}	r_{mon}
MPDL	Styrene	0,54 ± 0,02	3,31 ± 0,08
MPDL	MMA	0,59 ± 0,19	2,78 ± 0,68
MPDL	MA	0,65 ± 0,02	2,96 ± 0,10
MPDL	DEGA	1,31 ± 0,09	4,13 ± 0,25
MPDL	BA	0,89 ± 0,09	2,89 ± 0,25

Like in the previous chapter, these monomer pairs were exposed to RAFT conditions. The resulting copolymers showed controlled molecular weights and low dispersities. Important to note is that better control occurs at higher amounts of vinyl monomer w.r.t. MPDL.

In preparation of nanoparticles synthesis of and future application to drug delivery systems the possibility of introducing side chain functionality in RROP was explored by using the click chemistry in the form of the copper catalyzed

azide/alkyne 1,3-dipolar cycloaddition (CuAAC) reaction. Two approaches were tested where the first approach employed the copolymerization of the cyclic ketene acetal (CKA) 2-methylene-1,3-dioxepane (MDO) and propargyl acrylate. The copolymers were shown to nicely contain side chain functionality in the form of an alkyn. Subsequent attachment of azide terminate diethylene glycol resulted in proof of functionalization through attenuated total reflectance (ATR)-IR measurements. In the second approach, the idea was to synthesize a CKA containing a pendant alkyne group to allow the synthesis of functionalized polymers by readily copolymerizing with any other non-functionalized CKA. Synthesis, however, proved to be quite tedious where the isolation of pure functionalized CKA was not possible. Optimization of the synthetic procedure is therefore required in future research.

In the final stage of the research presented in this thesis, preformed MPDL-based copolymers were used in the preparation of nanoparticles through a combination of miniemulsion and solvent evaporation. Both copolymers of styrene and MMA with MPDL were synthesized in batch. The resulting particles were approximately 80-120 nm in size and showed nice uniform mixing throughout the particle.

7.2 Nederlandse Samenvatting

In de laatste jaren is het gebruik van radicalaire ring-opening polymerizatie (RROP) steeds belangrijker geworden. De veelzijdigheid van deze techniek wordt gedemonstreerd door de vele toepassingen in de biomedische wereld. De resultaten van het werk in dit proefschrift zorgen voor waardevolle (nieuwe) inzichten in het veld van RROP and openen nieuwe wegen voor biomedische toepassingen. Hierbij worden verschillende aspecten belicht die samen een solide basis vormen voor het produceren van degradeerbare nanodeeltjes met gekende

eigenschappen. Hierbij bestaat ook de mogelijkheid tot het post-functionaliseren van deze nanodeeltjes voor gebruik in 'drug-delivery'.

Het initiële onderzoek richtte zich op het synthetiseren van 5,6-benzo-2-methyleen-1,3-dioxepaan (BMDO)- en methyl methacrylaat (MMA)-gebaseerde copolymeren. Het gedrag van de copolymerisatie werd onderzocht door gebruik te maken van een geoptimaliseerde techniek waarbij 'online' IR-metingen werden verricht gedurende de polymerisatie. Door de Mayo-Lewis vergelijking te fitten aan de verkregen data werden de reactiviteitsverhoudingen van de betreffende monomeren verkregen: r_{BMDO} = 0.33 ± 0.06 en r_{MMA} = 6.0 ± 0.8. Dit resultaat werd vervolgens vergeleken met reactiviteitsverhoudingen waarbij gebruik werd gemaakt van de Skeist vergelijking. Dit resulteerde in vergelijkbare waardes r_{BMDO} = 0.7 en r_{MMA} = 3.88. Dit comonomeer paar werd verder gebruikt voor het produceren van copolymeren met goed gedefinieerde eigenschappen zoals ketenlengte, samenstelling en architectuur door gebruik te maken van reversibele additie/fragmentatie transfer (RAFT)-condities. De succesvolle synthese van lineaire en 4-armen stercopolymeren werd aangetoond op basis van verschillende samenstellingen. Degradatie door middel van hydrolyse werd uitgevoerd op deze copolymeren. Dit resulteerde in een afname van het molecuulgewicht waarmee de degradatie werd bevestigd.

Het begrijpen van het copolymerisatiegedrag van elk systeem is van groot belang voor het kunnen voorspellen van de copolymeerstructuur. Hiervoor werd de procedure voor het bepalen van de reactiviteitsverhoudingen geoptimaliseerd om op een snelle en efficiënte manier de reactiviteitsverhoudingen te kunnen bepalen. Gebaseerd op de eerder beschreven methode werd ervoor gekozen om de Skeist vergelijking in combinatie met 'online' IR-metingen te optimaliseren. Hiertoe

werden verschillende systemen onderzocht uitgaande van 2-methyleen-4-phenyl-1,3-dioxolaan (MPDL) als cyclisch keteen acetaal (CKA). Hierin is aangetoond dat, door gebruik te maken van deze methode, het bepalen van reactiviteitsverhoudingen van elk systeem gedaan kan worden in één enkel experiment. In Tabel 7.2 is een overzicht gegeven van reactiviteitsverhoudingen voor verschillende combinaties van MPDL met standaardmonomeren.

Tabel 7.2 Overzicht van resultaten voor de bepaling van reactiviteitsverhoudingen voor MPDL en verschillende monomeren

CKA	**monomeer**	r_{MPDL}	r_{mon}
MPDL	Styrene	0,54 ± 0,02	3,31 ± 0,08
MPDL	MMA	0,59 ± 0,19	2,78 ± 0,68
MPDL	MA	0,65 ± 0,02	2,96 ± 0,10
MPDL	DEGA	1,31 ± 0,09	4,13 ± 0,25
MPDL	BA	0,89 ± 0,09	2,89 ± 0,25

Net zoals in hoofdstuk 2 is ook hier gebruikgemaakt van RAFT-condities voor de verschillende monomeerparen ten behoeve van het controleren van molecuulgewichtopbouw om zodoende polymeren te verkrijgen met gekende eigenschappen. Hierbij moet worden opgemerkt dat de controle beter is bij polymeren met een groter aandeel van het comonomeer ten opzichte van MPDL.

Ter voorbereiding op het maken van nanodeeltjes voor 'drug delivery'-toepassingen is het nodig om functionaliteiten in te bouwen in de zijketens van CKA copolymeren. Hierbij werd gebruikgemaakt van 'click'-chemie in de vorm van de koper gekatalyseerde azide/alkyn 1,3-dipolaire cyclo-additie (CuAAC) reactie. Twee methodes werden hierbij getest waarbij de eerste methode gebruikmaakt

van de copolymerizatie van 2-methyleen-1,3-dioxepaan (MDO) en propargyl acrylaat. Dit leidde tot copolymeren met alkyn-groepen in de zijketens. Met behulp van azide-gefunctionaliseerd diethyleenglycol werd de functionalisering getest. Het verkregen product werd geanalyseerd met behulp van 'attenuated total reflectance' (ATR)-IR die de functionalisering bevestigde. In de tweede methode werd gebruikgemaakt van een alkyn-gefunctionaliseerd CKA in combinatie met traditionele niet-gefunctionaliseerde CKAs om zodoende tot functionaliseerbare polymeren te komen. Hiertoe moest het alkyn-gefunctionaliseerd CKA eerst gesynthetiseerd worden. Dit bleek echter geen recht-toe-recht-aan procedure te zijn en vooral de laatste stap bleek lastig, resulterend in het niet verkrijgen van zuiver product. Hiertoe is optimalisatie van de procedure vereist.

In het laatste stadium van het werk voor dit proefschrift werd onderzoek gedaan naar de mogelijkheid tot het maken van nanodeeltjes van vooraf gesynthetiseerde copolymeren van MPDL met styreen en MMA. Hierbij werd gebruikgemaakt van de miniemulsie techniek in combinatie met 'solvent evaporation'. Dit resulteerde in nanodeeltjes met een grootte tussen de 80 en 120 nm die bestonden uit een uniforme mix van de copolymeren.

7.3 Outlook

During the 4 years for this thesis, the world of radical ring-opening has expanded tremendously. More and more people are using RROP in combination with a whole array of reactions to synthesize materials for biomedical applications. This research performed in this thesis forms a good starting point for the preparation of nanoparticles for use in drug delivery systems. To this extent, studies on the

(controlled) release of these particles have to be performed by means of using a (fluorescent) dye and studying the release through UV/Vis or Fluorescent spectrometry. In addition, the biocompatibility of these particles and their degradation products have to be tested. Decoration of these particles is readily accessible by using preformed copolymers of MDO and propargyl acrylate.

When going for larger amounts of these materials, limitations of batch chemistry are quickly reached. To assist in the synthesis of larger quantities, flow chemistry might prove a useful tool. More and more researchers are walking away from traditional batch chemistry and using flow chemistry instead thanks to some major advantages:

- ✓ Fast heat exchange
- ✓ Rapid mixing
- ✓ Extreme conditions (i.e. working above boiling point)
- ✓ Increased safety
- ✓ Good reproducibility
- ✓ Easy scalability

The use of flow chemistry in combination with RROP has not yet been reported. While it may not be suitable for CKA homopolymerization (due to the long reaction time), copolymerization as well as CKA synthesis may benefit from a transition to flow. This opens many opportunities for improving/optimizing the existing systems for several CKAs and any imaginable comonomer.

While the biomedical is the predominant area of choice for degradable materials, these materials also have good potential to be used in i.e. packaging industry. With only a few percent (5-15%) of added to CKA, these materials would maintain

the properties of the bulk material while adding a small amount of degradability to allow for a more environmentally friendly material.

List of Abbreviations

^{1}H-NMR	Proton Nuclear Magnetic Resonance
AIBN	Azobisisobutyronitrile
AFM	atomic force microscopy
ATRP	Atom Transfer Radical Polymerization
BA	n-Butyl acrylate
BMDO	5,6-benzo-2-methylene-1,3-dioxepane
c	concentration
C	carbon
^{13}C-NMR	Carbon-13 Nuclear Magnetic Resonance
CKA	cyclic ketene acetal
Co	copolymer
CRP	controlled radical polymerization
d	days
Đ	polydispersity
DBU	1,8-Diazabicyclo[5.4.0]undec-7-ene
DCM	dichloromethane
DCP	dicumylperoxide
DEGA	di(ethylene glycol) ethyl ether acrylate
DLS	dynamic light scattering
DP	degree of polymerization
Eq	equivalent
f	feed composition
F	copolymer composition
FRP	free radical polymerization
FT-IR	Fourier transformation infrared spectroscopy
GPC	gel permeation chromatography
H	hydrogen

h	hours
K	Kelvin
k_{11}	homopropagation rate coefficients
k_{12}	crosspropagation rate coefficients
M	molar
MA	methyl acrylate
MeOH	methanol
MDO	2-methylene-1,3-dioxepane
MMA	methyl methacrylate
M_n	number average molecular weight
M_p	molecular weight at peak maximum
MPDL	2-methylene-4-phenyl-1,3-dioxolane
M_w	weight average molecular weight
MWD	molecular weight distribution
mV	millivolt
NiPAM	N-isopropylacrylamide
nm	nanometer
NMP	nitroxide mediated polymerization
PBL	poly(phenyl butyrolactone)
PCL	polycaprolactone
PEG	poly(ethylene glycol)
PMMA	poly(methyl methacrylate)
PPM	parts per million
PS	polystyrene
r	random
R	radical
r_1	reactivity ratio monomer 1
r_2	reactivity ratio monomer 2

RA-1	trithiocarbonate methyl-2-(((octylthio)-carbonothioyl)thio)propanoate
RAFT	radical addition-fragmentation chain transfer
rpm	revolutions per minute
RROP	radical ring-opening polymerization
SDS	sodium dodecyl sulfate
SEC	size exclusion chromatography
t	time
T	temperature
TEA	trimethylamine
TEM	transmission electron microscopy
Tert	tertiary
tert-BuOK	potassium *tertiary*-butoxide
THF	tetrahydrofuran
VAc	vinyl acetate
vol%	volume percent
wt%	weight percent
w.r.t	with respect to
x	conversion
ζ	zeta potential

List of Publications

Kobben, S.; Ethirajan, A.; Junkers, T., *Synthesis of degradable poly(methyl methacrylate) star polymers via RAFT copolymerization with cyclic ketene acetals, J. Pol. Sci. A: Polym. Chem.* **2014,** *52* (11), 1633-1641.

- Article writing
- All synthetic work

Kobben, S.; Ethirajan, A.; Junkers, T. *Synthesis of Degradable PolyMMA via Copolymerization with Cyclic Ketene Acetals. In Proceedings of the 1st Int. Electron. Conf. Mater., 26 May–10 June 2014; Sciforum Electronic Conference Series*, Vol. 1, **2014**, d002

- Article writing
- Electronic presentation
- All synthetic work

M. Peeters, S. Kobben, K.L. Jimenez-Monroy, L. Modesto, M. Kraus, T. Vandenryt, A. Gaulke, B. van Grinsven, S. Ingebrandt, T. Junkers, P. Wagner, *Thermal detection of histamine with a graphene oxide based molecularly imprinted polymer platform prepared by reversible addition–fragmentation chain transfer polymerization*, *Sens. Actuators B: Chem*. **2014**, 203, 527-535.

- Grafting of RAFT-polymers on Graphene Oxide
- Not presented in this thesis

List of Conference Poster Presentations

Synthesis of biodegradable polyesters via radical polymerization processes, S. Kobben, A. Busza, A. Ethirajan, T. Junkers, 19th Annual meeting of the Belgian Polymer Group (BPG), May 16-17, **2013**, Houffalize

Synthesis of biodegradable polyesters via radical polymerization processes, S. Kobben, A. Ethirajan, T. Junkers, IAP FS2 7/05 Annual Network Meeting, September 18, **2013**, Gent

Synthesis of biodegradable polyesters via radical polymerization processes, S. Kobben, A. Ethirajan, T. Junkers, Precision Polymer Materials (P2M) Winter School, January 13-17, **2014**, Zakopane (Poland)

Synthesis of biodegradable polyesters via radical polymerization processes, S. Kobben, A. Ethirajan, T. Junkers, 1st Electronic Conference on Materials, May 26-June 10, **2014**

- Electronic Powerpoint presentation was used instead of Poster

Synthesis of biodegradable polyesters via radical polymerization processes, S. Kobben, A. Ethirajan, T. Junkers, 20th Annual meeting of the Belgian Polymer Group (BPG), May 19-20, **2014**, Gent

Synthesis of degradable nanoparticles through a combination of radical polymerization and miniemulsion, S. Kobben, T. Junkers, A. Ethirajan, 21st Annual meeting of the Belgian Polymer Group (BPG), May 18-19, **2015**, Houffalize

Synthesis of star-shaped degradable copolymers through a combination of RAFT and radical ring-opening polymerization (RROP), IAP FS2 P7/05 Annual Network Meeting S. Kobben, T. Junkers, A. Ethirajan, September, **2015**, Hasselt

Synthesis of degradable nanoparticles through a combination of radical polymerization and miniemulsion, S. Kobben, T. Junkers, A. Ethirajan, 21st Annual meeting of the Belgian Polymer Group (BPG), May 23-24, **2016**, Hasselt

Dankwoord

Hier ben ik dan. Vier jaar PhD zijn voorbij gevlogen. In die vier jaar heb ik veel geleerd en veel nieuwe mensen leren kennen. Het is een vreemde gedachte dat het nu allemaal voorbij is. Gedurende die vier jaar heb ik veel ups maar toch ook downs gekend. Dankzij de steun van een hele boel mensen heb ik dit allemaal toch tot een goed einde weten te brengen. Daarom wil ik deze laatste paar pagina's gebruiken om deze mensen te bedanken.

Allereerst wil ik de Uhasselt bedanken voor het financieren van mijn doctoraat. Zonder haar steun had ik überhaupt niet kunnen starten. Daarnaast wil ik uiteraard mijn promoter Tanja Junkers bedanken. Zij heeft ervoor gezorgd dat ik, na de vele afwijzingen, toch kon beginnen aan een PhD. Gedurende mijn doctoraat kon ik altijd bij haar terecht voor advies of hulp wanneer weer eens iets niet werkte. Furthermore, I would like to thank my copromoter Anitha Ethirajan for the help and knowledge I obtained through the many meetings about miniemulsions.

Ik wil ook alle collega's van OBPC bedanken die ik door de jaren heen allemaal heb leren kennen. Neomy en Evelien, jullie hebben me door redelijk wat moeilijke situaties geholpen. Als ik weer eens in zak en as zat, hielpen jullie me er weer doorheen. Pieter en Rafaël, bedankt voor jullie hulp als ik weer eens een probleem had met mijn synthesestappen. Brecht, David en Rebekka van de BDG groep, bedankt dat ik gebruik heb mogen maken van jullie centrifuge en shaker en jullie hulp als ik weer eens bio-gerelateerde vragen had. Lien en Evelien K. van het IMO, dank voor jullie hulp bij het uitvoeren van de miniemulsies. Derese en Martijn, thanks for your help with AFM measurements. Gunther, Peter en Koen, dank dat jullie altijd netjes op tijd mijn NMR-metingen hebben gedaan en dat jullie

altijd wel wat tijd konden vinden om me te helpen als ik weer eens niet uit mijn NMR-spectrum kwam. Joris, Gijs en Neomy, dank voor jullie hulp bij de GPC. Jullie hebben er al die jaren voor gezorgd dat het apparaat bleef draaien en ik altijd bij jullie terecht kon met mijn vragen. Voor de rest wil ik nog Joachim bedanken voor de goede samenwerking tijdens ons gezamenlijke project. Dries G., ook jou wil ik bedanken voor de goede samenwerking in al die jaren. Jouw onderzoek heeft mij ook waardevolle inzichten opgeleverd. Alle studenten die ik gedurende de vier jaar heb mogen begeleiden (Agnieszka, Pieter L., Jorgo en Melvin). Jullie werk heeft mij op nieuwe ideeën gebracht en heeft uiteindelijk een groot aandeel gehad in mijn thesis. Huguette, bedankt voor je hulp bij de vele UV-Vis en FT-IR metingen. Hilde, Eugene en Iris van didactiek, ook jullie wil ik bedanken voor het lenen van materiaal en de hulp bij het geven van de labo's.

Verder wil ik alle bewoners van G61 (Joke, Jeroen D, Evelien, Jeroen B., Dries D., Geert, Veronique, Nok, Julija, Ruben, Benjamin, Jeroen V. Maarten en alle studenten) bedanken voor de gezellige werksfeer en vele leuke, grappige maar toch ook serieuze gesprekken die ik met jullie heb gevoerd. Jurgen en Jorne met wie ik het laatste half jaar regelmatig op pad ben geweest om een 'wandeling' te maken over het universiteitsterrein of in het centrum van Hasselt;). Alle PRD-leden door de jaren heen (Linny, Inge, Joke, Luk, Kayte, Matthias C., Benjamin, Evelien, Neomy, Svitlana, Joris, Joachim, Martijn, Nok, Ya-mi, Jeroen V., Jeroen D., Lowie, Kirsten, Erika, Maarten en Veronique) voor hun hulp gedurende mijn PhD. Alle overige collega's van OBPC wil ik bedanken voor de vele tripjes en team buildings die we gemaakt hebben. Ik ben altijd met veel plezier meegegaan.

Als laatste wil ik nog mijn ouders, stiefouders, grootouders, stiefgrootouders en zus bedanken voor hun steun en hulp gedurende deze vier jaar. Ze hebben al die tijd al mijn leuke maar ook minder leuke momenten aangehoord en ik voelde me gedurende deze vier jaar altijd gesteund. Ook alle andere familieleden en kennissen wil ik bedanken voor de interesse die zij altijd hebben getoond in mijn onderzoek. Ik wil verder nog Antoine bedanken voor zijn hulp en steun gedurende mijn doctoraat en Julien en Kevin met wie ik veel plezier heb gehad op IJsland. Ook de vrienden die ik niet zo vaak zag Louis en Mike wil ik bedanken voor hun steun op afstand.

Ik zie wel wat de toekomst mij zal brengen maar deze vier jaar neemt niemand mij meer af!